The Active Barrier:

A Role for Epithelial Cells in Chitin Induced Allergic Inflammation

By

René M. Roy

A dissertation submitted in partial fulfillment of

the requirements for the degree of

Doctor of Philosophy

(Cellular and Molecular Biology)

at the

UNIVERSITY OF WISCONSIN-MADISON

2012

Date of final oral examination: 08/13/12

The dissertation is approved by the following members of the Final Oral Committee:

Bruce Klein, Professor, Pediatrics
Anna Huttenlocher, Professor, Pediatrics
Charles Czuprynski, Professor, Pathobiological Sciences
Loren Denlinger, Associate Professor, Medicine
James Gern, Professor, Pediatrics

TABLE OF CONTENTS

ACKNOWLEDGEMENTS

When I look back at the incredible level of support given to me over my lifetime I am truly humbled. While I won't be able to thank everyone by name please know that your help earns you a portion of this accomplishment so I hope you celebrate it along with me.

Bruce Klein, my thesis advisor, is a wonderful role model for me. He took an optimistic and enthusiastic graduate student and molded me into a competent scientist who could set realistic goals. He also made sure I never lost sight of the bigger picture and encouraged me to reach for big ideas. I go forward with even more enthusiasm and optimism for the good that scientific discovery can provide for humanity. With luck, I might achieve some small portion of the success Bruce has had as a tribute to his expert mentorship and eager curiosity.

While Bruce was my most recent mentor others have also boosted me in my scientific journey. Jennifer Steele piqued my interest in research while in college instilling the initial spark of the joy of discovery that is still with me today. Ofer Levy gave me a chance to learn immunology and cemented my desire to pursue a career in immunology research. He remains a strong role model as a wonderful human being and passionate physician-scientist. Teresa Compton taught me to focus my efforts and to persevere through the inevitable difficulties in research. I also want to thank Teresa for encouraging me to meet with Bruce when I was considering research experiences.

My thesis committee provided me with support and encouragement and helped me to place my research project into a wider context. Anna Huttenlocher always reminded me of my place as an aspiring physician-scientist, Chuck Czuprynski was always first to respond to my pleas for help and brought his unique and varied experiences to bear on the project, Loren Denlinger centered the work in physiology and relevance to human disease, and Jim Gern selflessly rose to the occasion on short

notice for which I will always be thankful. I also want to thank Paul Bertics, who I first met when I was a research technician in Teresa Compton's lab, and who was a constant positive presence in my journey at the University of Wisconsin.

The members of the Klein lab always were ready to help and provided a nurturing environment for me to pursue my research and a social environment to forget about the stress of science everyone once in a while. In particular, John Carmen helped me explore the philosophical corners of life and the universe while Brad Tebbets joined me on numerous quests to discover new and exciting beverages, obscure facts, and *joie de vivre*.

In closing, I recognize those most responsible for who I am, my family. My grandfather, Waldemar Liefke, taught me that through hard work and humility, one can achieve great things in life. My parents, Serge and Karen Roy, never accepted good enough while equally encouraging honest effort and achievement. More importantly they loved and supported me unconditionally. My wife Carrie has been my rock for over ten years. Any achievements I have or may have in the future are because of the better person you make me want to be. Also, your patience and grace has allowed me to pursue discoveries even in the dead of night. To my daughter Tilda, you remind me of the joy of discovery every day and the reason that we must try to make tomorrow a little bit better.

I thought often of these words from Tennyson's Ulysses as I completed this work and I will mind them in the future: "To strive, to seek, to find, and not to yield."

DISSERTATION ABSTRACT

Chitin is a linear polysaccharide of N-acetylglucosamine that is absent in vertebrates but that forms the cell wall of fungi, the exoskeleton of insects, and the shell of crustaceans. Exposure to chitin and chitin-associated environmental allergens is associated with an increase in allergic disease and asthma yet little is known about how chitin is recognized by the immune system or the mechanism by which chitin can promote allergic disease. Previous studies have focused on the interaction of chitin with the macrophage to explore the immunological impact of chitin and have yielded conflicting results, namely that macrophages become alternatively activated in vivo but classically activated in vitro following chitin exposure. I hypothesized that, in vivo, chitin promoted the alternative activation of macrophages and allergic inflammation via interaction with another cell.

Airway epithelial cells represent the first point of contact for inhaled particles and are important mediators of allergic airway disease. This dissertation investigates the role of airway epithelial cells in mediating allergic inflammation following chitin exposure. Airway epithelial cells bind chitin and secrete CCL2 in vitro and in vivo. CCL2 is required for chitin induced alternative activation of macrophages in vitro and the CCL2 receptor – CCR2– is required for innate allergic inflammation in vivo.

Chitin also promotes adaptive allergic inflammation in a model of chitin-dependent sensitization to *Aspergillus* antigens. Chitin-dependent sensitization to *Aspergillus* antigens requires complement factor 3 and the anaphylatoxin receptor C3aR. In addition, chitin-dependent activation of airway epithelial cell NF-kB is required for the polarization of *Aspergillus*-specific T cells toward allergy associated Th2 and severe allergy associated Th17 phenotypes. Also, chitin-dependent sensitization to *Aspergillus* antigens results in pulmonary eosinophilia and elevated levels of IgE. Both eosinophilia and elevated IgE are dependent on the C3-C3aR axis and airway epithelial

cell NF-kB activation.

Thus, chitin exposure activates airway epithelial cells to promote innate and adaptive allergic inflammation. The interaction of airway epithelial cells with chitin could represent an early event in the development of allergic airway disease and asthma.

Chapter 1

Introduction, literature review, and specific aims.

Airway epithelial cells and the immune recognition of fungal cell wall carbohydrates in allergic airway disease

INTRODUCTION

Fungi exact a heavy toll on human health and society

Fungi are commonly encountered by humans yet humans don't commonly notice them. Humans have described approximately 10^5 fungal species to date although the actual number of fungal species may actually be 50-fold higher [1]. Some fungal genera are used for human benefit such as *Saccharomyces* in fermentation and *Penicillium* in antibiotic production, but other fungi exact a heavy toll on human society. *Cryphonectria* has devastated chestnut trees in North America [2], while *Magnaporthe* and *Puccinia* threaten rice and wheat crops [3] decreasing the world's food supply and leading to billions of dollars in lost economic activity.

Similarly, human fungal pathogens are a serious emerging infectious disease threat linked to the increase in immunocompromised patients, specifically, patients with AIDS, patients with cancer, and recipients of solid organ or hematopoietic stem cell transplants [4-6]. Furthermore, the endemic mycoses can cause lethal systemic infections in apparently healthy individuals and can reactivate in the setting of immune suppression [7-9]. Of great concern is the recent emergence of virulent *Cryptococcus gattii* in British Columbia, Washington, and Oregon [10,11] highlighting the ongoing threat of fungal pathogens. Set against a backdrop of a limited antifungal pharmacological armamentarium [12], emerging resistance to multiple antifungal compunds [13], poor diagnostic capabilities, and limited research investment compared to other infectious diseases [14], the rising incidence of fungal infections represents a daunting challenge to health care systems worldwide.

Adding to the fungal burden on health care systems is the prominent role of sensitization to fungi in the development, maintenance, and exacerbation of allergic airway disease. At least 20%, but possibly as high as 80%, of the 25 million Americans

with asthma have a positive skin test to at least one fungal allergen [15,16]. More than 50 genera from across the fungal kingdom are capable of sensitizing exposed individuals and most fungal species possess multiple allergens [17]. While many humans are exposed to millions of fungal spores daily with little effect [18], increases in atmospheric fungal spore levels are associated with increases in asthma exacerbations and hospital admissions in patients sensitized to fungi [19]. Ongoing climate change linked to increased temperature and atmospheric CO_2 levels further increases atmospheric fungal spore concentrations with a parallel increase in allergic airway disease [20,21]. When economic losses, infections, and allergy are considered together, the growing impact of fungi on the human condition cannot be overstated.

In this chapter I will review the mechanisms governing allergic sensitization to fungi focusing on immune recognition of the fungal cell wall and the role of airway epithelial cells in promoting allergic sensitization.

Determinants of fungal allergenicity

Fungi are well suited to promote airway disease due to their size, their ubiquitous airborne presence, and their particular repertoire of carbohydrates and proteins that interact with cells in the airways. In addition, the ability of fungi to colonize the human body ensures that pathologic allergic responses could be augmented by local production of allergens or toxins [22]. The size of fungal spores from so-called "allergenic" genera varies from 1μm to 100μm although most are smaller than 10μm [18]. Along with other particulates of this size range such as diesel exhaust particles, fungal spores can penetrate deeply into the airways depositing near the terminal bronchioles [23]. The composition of the outer shell of fungal spores also allows them to penetrate deeply into the airways. For example, the rodlet protein, RodA, coats *Aspergillus fumigatus* spores and renders the spore coat hydrophobic [24], which allows

for increased deposition in the small airways compared to hygroscopic particles which swell and deposit in larger airways [25].

The ubiquity of fungal spores in the environment ensures that the airway will be exposed to fungal spores with each breath. Upon germination, fungi secrete proteases, which have direct effects on the airway epithelial layer. First, the proteases act on and degrade proteins of the tight junctions between airway epithelial cells leading to dysregulated barrier function. The dysregulated barrier allows for the passage of antigen into the submucosal layer where antigen presenting cells reside and reduces the ability of airway eptihelial cells to maintain the appropriate chemical composition of the fluid layer lining the airways. Second, fungal proteases cleave and activate protease activated receptors (PAR), which are a family of G protein-coupled receptors activated when a portion of their extracellular domain is cleaved by a protease revealing a teathered ligand [26]. Acitvation of PAR is critical for the allergenicity of purified fungal allergens and activation can also exacerbate existing allergic inflammation and break inhalational tolerance to otherwise innocuous antigens in the airway [27,28].

While hundreds of protein fungal allergens have been characterized, little is known about the role of the fungal cell wall in mediating sensitization to fungi. Fungi are surrounded by a protective, rigid cell wall which undergoes constant modification in response to environmental cues [29]. Over 90% of the cell wall is comprised of polysaccharides that are linked together into a three dimensional matrix. The relative homogeneity of fungal polysaccharides and their absence in humans makes fungal polysaccharides a prime drug target. For example, the echinocandin drug class inhibits the activity of beta-glucan synthases [30] whereas, nikkomycin Z, an antifungal drug that inhibits chitin synthase, has demonstrated a favorable safety profile in a Phase I clinical trial [31]. In animal models, antibodies raised against laminarin (a β-1,3-glucan**:**β-1,6-glucan polysaccharide) were protective against fungal infection [32]

suggesting that recombinant antibody therapy against fungal wall polysaccharides may be useful clinically. Similarly, their absence in humans, yet near universal presence in fungi, makes fungal cell wall polysaccharides clear targets for immune recognition.

The recognition of fungal carbohydrates

Fungal carbohydrates represent a broad variety of pathogen associated molecular patterns (PAMP). Recognition of PAMP via pattern recognition receptors (PRR) is an evolutionarily conserved immunological strategy that allows for the rapid recognition of conserved molecular patterns by germ line encoded receptors [33]. While efforts over the past 25 years have resulted in great advances in understanding the diversity of receptors in mammals, matching receptors to fungal carbohydrate ligands has proceeded more slowly.

Beta glucan

The cell wall of fungi contains beta-1,3, beta-1,4, and beta-1,6 linked chains of D-glucose. The central core of the fungal cell wall is comprised of branched β-1,3-glucan cross-linked to chitin [34]. Recognition of beta-1,3-glucan is mediated by the C-type lectin dectin-1 [35], which is present primarily on myeloid cells. Beta glucans are also recognized by complement receptor 3 and the scavenger receptors SCARF1 and CD36 [36]. Recognition of beta-1,3-glucan via dectin-1 elicits phagocytosis and a strong inflammatory response from innate immune cells. Thus, fungi often mask beta1,3-glucan with other cell wall components to shield themselves from immune recognition . Dectin-1 requires at least 7 to 11 beta 1,3-linked glucose units and affinity is greatly enhanced by one beta1,6-linked unit [37]. Dectin-1 recognition of particulate, but not soluble, beta-glucans triggers the recruitment of the adapter Syk to the signaling

complex [38]. Syk, in turn, mediates the assembly the the CARD9-Bcl1-Malt10 complex, which is essential for subsequent NF-κB activation [39]. Dectin-1 is able to distinguish particulate beta-glucan from soluble beta-glucan through the formation of a "phagocytic synapse." Interactions of particulate beta-glucans with dectin-1 receptors allow for the clustering of receptors and the exclusion of the regulatory phosphatases CD45 and CD148 [40] from the synapse. Thus, dectin-1 is able to mediate inflammation in response to beta-glucan particles, like fungi, while ignoring soluble beta-glucans.

Alpha glucan

The interaction of α1,3-glucan with mammalian cells is poorly understood. Some evidence suggests that α1,3-glucan serves to hide the more immunogenic polysaccharides such as beta-glucan in *Histoplasma* [41] and can negatively impact TLR2 and TLR4 mediated cytokine production [42], while other evidence points to a role for α1,3-glucan in activating protective T cell responses against *Aspergillus* [43]. Since a recognition mechanism for α1,3-glucan has not yet been described, it is difficult to address the polysaccharide's role in fungal recognition or masking through indirect studies.

Mannans

Fungal mannans are primarily associated with cell wall proteins linked via the hydroxy oxygen of serine, threonine, tyrosine; hydroxy-modified amino acids (O-linked); or via the nitrogen of asparagine or arginine (N-linked). Many modifications in mannan structure also exist across the fungal kingdom [44]. While immunostimulatory in most cirucmstances, mannans also mask beta-glucans to limit immune recognition [45]. Mannans are recognized by a broad variety of receptors although some receptors demonstrate specificity for either O-linked mannans or N-linked mannans. The

eponymous mannose receptor (CD206) and DC-SIGN (CD209) recognize mannosylated proteins and augment uptake of these antigens by antigen presenting cells [46]. Dectin-2 also recognizes fungal mannan and appears to mediate the induction of robust anti-*Candida* Th17 mediated host defence [47]. The broad diversity of mannan structures and receptors that mediate their recognition, highlights the prominent role of mannans in the interaction between fungi and their human hosts.

The polysaccharide capsule of *Cryptococcus* deserves special mention as it is a unique structure that shields the fungal cell wall and mediates many of the immunological responses to this organism. Comprised chiefly of glucoronoxylomannan (GXM) and galactoxylomannan (GalXM)**,** the capsule is the organism's major virulence factor [48]. While antibody and complement opsonize the capsule and mediate recognition via complement receptors and Fc receptors, GXM may also be recognized via interactions with TLR2 and/or TLR4 [49]. However, interactions with GXM are generally thought to suppress immune responses rather than augment them [50,51].

Chitin

Chitin, a linear polysaccharide of beta-1,4 N-acetyl D-glucosamine (GlcNAc), forms part of the core structure of the fungal cell wall along with beta-1,3-glucan. While absent in almost all vertebrates, chitin also comprises the exoskeleton of insects, the shell of crustaceans, the egg shell and cuticle of helminths, and the cyst wall of the human parasites *Giardia* and *Entamoeba.* Receptors for chitin are poorly understood with little information available concerning the structure that is recognized by the immune system in mammals. Receptors that have affinity for terminal residue GlcNAc include galectins [52,53] and the macrophage mannose receptor [54]. Another receptor, FIBCD1, is

highly expressed in intestinal epithelial cells and appears to recognize acetylated structures, including chitin [55,56]. Two other motifs that recognize chitin, LysM and glyco_18, have been described in mammalian proteins. A crystal structure of YKL-40, a glyco_18 motif containing protein, shows that $(GlcNAc)_5$ can bind at two overlapping sites within the chitin binding domain and a model of $(GlcNAc)_9$ fills the entire binding domain [57]. While YKL-40 is highly expressed in patients with asthma and plays a critical role in Th2 allergic responses, is does not seem to be required for responses to chitin itself [58]. Recombinant LysM domains from the chitinase-A protein of the fern *Pteris ryukyuensis* were found to bind GlcNAc oligosaccharides with increasing affinity as the length of the polymer increased from three to five residues [59]. In *Arabidopsis*, the LysM-containing protein CERK1 mediates antifungal immunity via direct recognition of chitin oligosaccharides [60]. Interestingly, while $(GlcNac)_5$ binds to CERK1 with high affinity, the oligosaccharide inhibits antifungal immunity, whereas $(GlcNAc)_8$ induces dimerization of CERK1 and activates the antifungal response [61]. Although they do not bind to chitin directly [35], dectin-1 and TLR2 have been implicated in macrophage responses to chitin [62,63].

Airway epithelial cells: the active barrier

Airway epithelial cells line the conducting airways of the lung and represent the initial point of contact for inhaled pathogens, allergens, and toxins. The cells maintain an active barrier to exclude pathogens, sense danger signals, and modulate the activities of inflammatory cells. Airway epithelial cells actively participate in all aspects of pulmonary inflammation including initiation, termination, and tissue repair. Inflammation in the lung is particularly deleterious as it is associated with respiratory compromise.

Thus, airway epithelial cells serve a critical function by closely regulating inflammatory responses.

An intact epithelial layer forms a robust initial defense against inhaled pathogens and maintains an anti-inflammatory environment in the lung. Airway epithelial cells maintain a physical barrier through tight junctions and desmosomes near their apical surfaces to prevent the paracellular passage of antigen or pathogens to the submucosal space [64]. In addition to blocking the invasion of fungi, epithelial cells mitigate the impact of fungal exposure via a variety of active mechanisms. First, airway epithelial cells constitutively secrete into the fluid layer that lines the airway a number of molecules with antifugal activity including surfactants [65], complement [66], β-defensins [67,68], cathelicidins [69], lactoferrin [70], and mucins [71]. The rich carbohydrate and protein matrix at the apical surface traps inhaled fungal spores, exposing them to high concentrations of these antifungal molecules and sweeping the spores out of the airway via ciliary action. Thus, the airway surface represents a dynamic surface with antifungal activity.

Airway epithelial cells also have a sentinel function. Spores that avoid the antifungal mucus layer, and that evade capture by immune phagocytes, can be sensed and responded to by airway epithelial cells. Airway epithelial cells express a broad range of PRR including Toll-like receptors [72], C-type lectins [73], protease activated receptors, and NOD-like receptors that allow the cells to react to incoming foreign stimuli. Activation of TLR on airway epithelial cells triggers increased production of antifungal molecules and inflammatory cytokines. While many PRR are not expressed at the surface in the absence of inflammation, triggering of TLR can also upregulate expression of other PRR such as dectin-1 [73], allowing for further amplification of the inflammatory response.

Airway epithelial cells further control inflammatory responses in the lung through modulation of immune cell function. Airway epithelial cells influence immune cells in the lung by direct and indirect mechanisms. In the absence of inflammation, epithelial cells enforce tolerance in the airway through secretion of TGF-beta and presentation of antigen on MHCII to induce Foxp3+Treg cells [74,75]. Airway epithelial cells further promote an anti-inflammatory environment through constitutive expression of CD200 [76], the vitamin D activating enzyme 1α-hydrolase [77], production of nitric oxide [78], and surfactant-dependent inhibition of SIRPα [79], all of which inhibit DC maturation and macrophage activation. Thus, airway epithelial cells possess numerous mechanisms to actively control inflammation in the lung.

Airway epithelial cells mediate sensitization to inhaled antigen

Exposure to fungal spores disrupts the normal function of airway epithelial cells, leading to the breaking of tolerance and the sensitization to fungal antigens. Fungal proteases cleave and activate protease-activated receptors, as well as tight junction proteins [28]. This has the effect of allowing for paracellular leakage of antigen into the subepithelial space, impacting polarity of the epithelial cells, and inducing the production of proinflammatory cytokines. Damage induced by fungal products also results in the release of endogenous danger signals such as free ATP and uric acid [80] that further enhance inflammation.

Activated epithelial cells secrete a number of cytokines that instruct the maturation and activation of DC subsets in the lung. Upon stimulation, airway epithelial cells produce TSLP [81], IL25 [82], and IL33 [83] which promote the ability of DC to polarize T cells toward the allergy associated Th2 phenotype [84]. Activated epithelial

cells also produce chemokines which recruit effector and memory T cells to the lung potentating allergen-specific inflammatory responses [85].

Once more unto the breach: fungal carbohydrates as mediators of epithelial activation and allergic sensitization

While fungal protease effects on airway epithelial cells are well characterized, the effects of fungal carbohydrates are less studied. Beta-glucan exposure increases epithelial cell production of IL-8 *in vitro* [86] whereas GXM mediates attachment of *Cryptococcus* to airway epithelial cells [87] and also triggers production of IL-8 [88]. Airway epithelial cells also react to house dust mite antigens in a beta-glucan dependent fashion suggesting a role for beta glucan in sensitization to fungal and insect antigens [89].

At the outset of this project, it was reported that chitin exposure induced innate allergic inflammation in the lung characterized by alternatively activated macrophages and eosinophilia [90], yet co-incubation of macrophages with chitin particles *in vitro* led to the generation of classically activated macrophages [62,63,91,92]. Because chitin is a common component of multiple common environmental allergens derived from fungi, insects, and helminths we speculated that chitin exposure could bias the immune response to co-administered antigen toward an allergic phenotype. We also hypothesized that the effects of chitin exposure were centrally mediated by airway epithelial cells rather than alveolar macrophages as had been reported in the literature. This hypothesis led to the following specific aims for this dissertation. First, to elucidate the role of chitin-exposed epithelial cells in promoting innate allergic inflammation and

second, to investigate the role of chitin-exposed epithelial cells in promoting fungal specific T cell polarization in a model of asthma induced by antigens from the fungus *Aspergillus fumigatus*. Briefly, this dissertation demonstrates that chitin exposure promotes the release of CCL2 from airway epithelial cells and that CCR2 - the receptor for CCL2 - is required for chitin-induced innate allergic inflammation. In addition, this dissertation establishes a role for complement in chitin-dependent allergic sensitization and suggests that chitin can act as an adjuvant to prime fungal specific CD4+ T cells in the lung through a mechanism that requires activation of airway epithelial cells by chitin.

REFERENCES

1. Blackwell M (2011) The Fungi: 1, 2, 3… 5.1 million species? American Journal of Botany 98: 426-438.

2. Milgroom MG, Wang K, Zhou Y, Lipari SE, Kaneko S (1996) Intercontinental population structure of the chestnut blight fungus, Cryphonectria parasitica. Mycologia 179-190.

3. Pennisi E (2010) Armed and dangerous. Science 327: 804-805.

4. Cutler JE, Deepe GSJ, Klein BS (2007) Advances in combating fungal diseases: vaccines on the threshold. Nat Rev Microbiol 5: 13-28.

5. Romani L (2011) Immunity to fungal infections. Nat Rev Immunol 11: 275-288.

6. Perfect JR (2012) The impact of the host on fungal infections. Am J Med 125: S39-51.

7. Chakrabarti A, Slavin MA (2011) Endemic fungal infections in the Asia-Pacific region. Med Mycol 49: 337-344.

8. Queiroz-Telles F, Nucci M, Colombo AL, Tobon A, Restrepo A (2011) Mycoses of implantation in Latin America: an overview of epidemiology, clinical manifestations, diagnosis and treatment. Med Mycol 49: 225-236.

9. Pfaller MA, Diekema DJ (2010) Epidemiology of invasive mycoses in North America. Crit Rev Microbiol 36: 1-53.

10. (2010) Emergence of Cryptococcus gattii-- Pacific Northwest, 2004-2010. MMWR Morb Mortal Wkly Rep 59: 865-868.

11. Byrnes EJr, Li W, Lewit Y, Ma H, Voelz K et al. (2010) Emergence and pathogenicity of highly virulent Cryptococcus gattii genotypes in the northwest United States. PLoS Pathog 6: e1000850.

12. Tebbets B, Stewart D, Lawry S, Nett J, Nantel A et al. (2012) Identification and characterization of antifungal compounds using a Saccharomyces cerevisiae reporter bioassay. PLoS ONE 7: e36021.

13. Pfaller MA (2012) Antifungal drug resistance: mechanisms, epidemiology, and consequences for treatment. Am J Med 125: S3-13.

14. Brown GD, Denning DW, Levitz SM (2012) Tackling human fungal infections.

Science 336: 647.

15. Knutsen AP, Bush RK, Demain JG, Denning DW, Dixit A et al. (2012) Fungi and allergic lower respiratory tract diseases. J Allergy Clin Immunol 129: 280-91; quiz 292-3.

16. Beezhold DH, Green BJ, Blachere FM, Schmechel D, Weissman DN et al. (2008) Prevalence of allergic sensitization to indoor fungi in West Virginia. Allergy Asthma Proc 29: 29-34.

17. Horner WE, Helbling A, Salvaggio JE, Lehrer SB (1995) Fungal allergens. Clin Microbiol Rev 8: 161-179.

18. Frohlich-Nowoisky J, Pickersgill DA, Despres VR, Poschl U (2009) High diversity of fungi in air particulate matter. Proc Natl Acad Sci U S A 106: 12814-12819.

19. Dales RE, Cakmak S, Burnett RT, Judek S, Coates F et al. (2000) Influence of ambient fungal spores on emergency visits for asthma to a regional children's hospital. Am J Respir Crit Care Med 162: 2087-2090.

20. Shea KM, Truckner RT, Weber RW, Peden DB (2008) Climate change and allergic disease. J Allergy Clin Immunol 122: 443-53; quiz 454-5.

21. Gange AC, Gange EG, Sparks TH, Boddy L (2007) Rapid and recent changes in fungal fruiting patterns. Science 316: 71.

22. Kauffman HF, Tomee JF, van de Riet MA, Timmerman AJ, Borger P (2000) Protease-dependent activation of epithelial cells by fungal allergens leads to morphologic changes and cytokine production. J Allergy Clin Immunol 105: 1185-1193.

23. Heyder J (2004) Deposition of inhaled particles in the human respiratory tract and consequences for regional targeting in respiratory drug delivery. Proc Am Thorac Soc 1: 315-320.

24. Aimanianda V, Bayry J, Bozza S, Kniemeyer O, Perruccio K et al. (2009) Surface hydrophobin prevents immune recognition of airborne fungal spores. Nature 460: 1117-1121.

25. Asgharian B (2004) A model of deposition of hygroscopic particles in the human lung. Aerosol science and technology 38: 938-947.

26. Kyriazis I, Ellul J, Katsakiori P, Panayiotakopoulos G, Flordellis C (2012) The multiple layers of signaling selectivity at protease-activated receptors. Curr Pharm Des 18: 161-174.

27. Ebeling C, Forsythe P, Ng J, Gordon JR, Hollenberg M et al. (2005) Proteinase-activated receptor 2 activation in the airways enhances antigen-mediated airway inflammation and airway hyperresponsiveness through different pathways. J Allergy Clin Immunol 115: 623-630.

28. Kiss A, Montes M, Susarla S, Jaensson EA, Drouin SM et al. (2007) A new mechanism regulating the initiation of allergic airway inflammation. J Allergy Clin Immunol 120: 334-342.

29. Latge JP (2007) The cell wall: a carbohydrate armour for the fungal cell. Mol Microbiol 66: 279-290.

30. Perlin DS (2011) Current perspectives on echinocandin class drugs. Future Microbiol 6: 441-457.

31. Nix DE, Swezey RR, Hector R, Galgiani JN (2009) Pharmacokinetics of nikkomycin Z after single rising oral doses. Antimicrob Agents Chemother 53: 2517-2521.

32. Torosantucci A, Bromuro C, Chiani P, De Bernardis F, Berti F et al. (2005) A novel glyco-conjugate vaccine against fungal pathogens. J Exp Med 202: 597-606.
33. Janeway CAJ, Medzhitov R (1998) Introduction: the role of innate immunity in the adaptive immune response. Semin Immunol 10: 349-350.

34. Latge JP (2010) Tasting the fungal cell wall. Cell Microbiol 12: 863-872.

35. Brown GD, Gordon S (2001) Immune recognition. A new receptor for beta-glucans. Nature 413: 36-37.

36. Means TK, Mylonakis E, Tampakakis E, Colvin RA, Seung E et al. (2009) Evolutionarily conserved recognition and innate immunity to fungal pathogens by the scavenger receptors SCARF1 and CD36. J Exp Med 206: 637-653.

37. Adams EL, Rice PJ, Graves B, Ensley HE, Yu H et al. (2008) Differential high-affinity interaction of dectin-1 with natural or synthetic glucans is dependent upon primary structure and is influenced by polymer chain length and side-chain branching. J Pharmacol Exp Ther 325: 115-123.

38. Underhill DM, Rossnagle E, Lowell CA, Simmons RM (2005) Dectin-1 activates Syk tyrosine kinase in a dynamic subset of macrophages for reactive oxygen production. Blood 106: 2543-2550.

39. Gross O, Gewies A, Finger K, Schafer M, Sparwasser T et al. (2006) Card9 controls a non-TLR signalling pathway for innate anti-fungal immunity. Nature 442:

651-656.

40. Goodridge HS, Reyes CN, Becker CA, Katsumoto TR, Ma J et al. (2011) Activation of the innate immune receptor Dectin-1 upon formation of a ‘phagocytic synapse’. Nature 472: 471-475.

41. Rappleye CA, Eissenberg LG, Goldman WE (2007) Histoplasma capsulatum alpha-(1,3)-glucan blocks innate immune recognition by the beta-glucan receptor. Proc Natl Acad Sci U S A 104: 1366-1370.

42. Chai LY, Vonk AG, Kullberg BJ, Verweij PE, Verschueren I et al. (2011) Aspergillus fumigatus cell wall components differentially modulate host TLR2 and TLR4 responses. Microbes Infect 13: 151-159.

43. Bozza S, Clavaud C, Giovannini G, Fontaine T, Beauvais A et al. (2009) Immune sensing of Aspergillus fumigatus proteins, glycolipids, and polysaccharides and the impact on Th immunity and vaccination. J Immunol 183: 2407-2414.

44. Netea MG, Gow NA, Munro CA, Bates S, Collins C et al. (2006) Immune sensing of Candida albicans requires cooperative recognition of mannans and glucans by lectin and Toll-like receptors. J Clin Invest 116: 1642-1650.

45. Wheeler RT, Fink GR (2006) A drug-sensitive genetic network masks fungi from the immune system. PLoS Pathog 2: e35.

46. Lam JS, Huang H, Levitz SM (2007) Effect of differential N-linked and O-linked mannosylation on recognition of fungal antigens by dendritic cells. PLoS ONE 2: e1009.

47. Saijo S, Ikeda S, Yamabe K, Kakuta S, Ishigame H et al. (2010) Dectin-2 recognition of alpha-mannans and induction of Th17 cell differentiation is essential for host defense against Candida albicans. Immunity 32: 681-691.

48. Fromtling RA, Shadomy HJ, Jacobson ES (1982) Decreased virulence in stable, acapsular mutants of cryptococcus neoformans. Mycopathologia 79: 23-29.

49. Yauch LE, Mansour MK, Shoham S, Rottman JB, Levitz SM (2004) Involvement of CD14, toll-like receptors 2 and 4, and MyD88 in the host response to the fungal pathogen Cryptococcus neoformans in vivo. Infect Immun 72: 5373-5382.

50. Monari C, Kozel TR, Paganelli F, Pericolini E, Perito S et al. (2006) Microbial immune suppression mediated by direct engagement of inhibitory Fc receptor. J Immunol 177: 6842-6851.

51. Chiapello L, Iribarren P, Cervi L, Rubinstein H, Masih DT (2001) Mechanisms for

induction of immunosuppression during experimental cryptococcosis: role of glucuronoxylomannan. Clin Immunol 100: 96-106.

52. Chang YY, Chen SJ, Liang HC, Sung HW, Lin CC et al. (2004) The effect of galectin 1 on 3T3 cell proliferation on chitosan membranes. Biomaterials 25: 3603-3611.

53. Krzeslak A, Lipinska A (2004) Galectin-3 as a multifunctional protein. Cell Mol Biol Lett 9: 305-328.

54. McGreal EP, Miller JL, Gordon S (2005) Ligand recognition by antigen-presenting cell C-type lectin receptors. Curr Opin Immunol 17: 18-24.

55. Schlosser A, Thomsen T, Moeller JB, Nielsen O, Tornoe I et al. (2009) Characterization of FIBCD1 as an acetyl group-binding receptor that binds chitin. J Immunol 183: 3800-3809.

56. Thomsen T, Moeller JB, Schlosser A, Sorensen GL, Moestrup SK et al. (2010) The recognition unit of FIBCD1 organizes into a noncovalently linked tetrameric structure and uses a hydrophobic funnel (S1) for acetyl group recognition. J Biol Chem 285: 1229-1238.

57. Fusetti F, Pijning T, Kalk KH, Bos E, Dijkstra BW (2003) Crystal structure and carbohydrate-binding properties of the human cartilage glycoprotein-39. J Biol Chem 278: 37753-37760.

58. Lee CG, Hartl D, Lee GR, Koller B, Matsuura H et al. (2009) Role of breast regression protein 39 (BRP-39)/chitinase 3-like-1 in Th2 and IL-13-induced tissue responses and apoptosis. J Exp Med 206: 1149-1166.

59. Ohnuma T, Onaga S, Murata K, Taira T, Katoh E (2008) LysM domains from Pteris ryukyuensis chitinase-A: a stability study and characterization of the chitin-binding site. J Biol Chem 283: 5178-5187.

60. Iizasa E, Mitsutomi M, Nagano Y (2010) Direct binding of a plant LysM receptor-like kinase, LysM RLK1/CERK1, to Chitin in vitro. J Biol Chem 285: 2996-3004.

61. Liu T, Liu Z, Song C, Hu Y, Han Z et al. (2012) Chitin-induced dimerization activates a plant immune receptor. Science 336: 1160-1164.

62. Da Silva CA, Hartl D, Liu W, Lee CG, Elias JA (2008) TLR-2 and IL-17A in chitin-induced macrophage activation and acute inflammation. J Immunol 181: 4279-4286.

63. Da Silva CA, Chalouni C, Williams A, Hartl D, Lee CG et al. (2009) Chitin is a size-dependent regulator of macrophage TNF and IL-10 production. J Immunol 182:

3573-3582.

64. Davies JA, Garrod DR (1997) Molecular aspects of the epithelial phenotype. BioEssays 19: 699-704.

65. Vieira DB, Carmona-Ribeiro AM (2006) Cationic lipids and surfactants as antifungal agents: mode of action. J Antimicrob Chemother 58: 760-767.

66. Cheng SC, Sprong T, Joosten LA, van der Meer JW, Kullberg BJ et al. (2012) Complement plays a central role in Candida albicans-induced cytokine production by human PBMCs. Eur J Immunol 42: 993-1004.

67. Jiang Y, Wang Y, Wang B, Yang D, Yu K et al. (2010) Antifungal activity of recombinant mouse beta-defensin 3. Lett Appl Microbiol 50: 468-473.

68. Alekseeva L, Huet D, Femenia F, Mouyna I, Abdelouahab M et al. (2009) Inducible expression of beta defensins by human respiratory epithelial cells exposed to Aspergillus fumigatus organisms. BMC Microbiol 9: 33.

69. Lopez-Garcia B, Lee PH, Gallo RL (2006) Expression and potential function of cathelicidin antimicrobial peptides in dermatophytosis and tinea versicolor. J Antimicrob Chemother 57: 877-882.

70. Andres MT, Viejo-Diaz M, Fierro JF (2008) Human lactoferrin induces apoptosis-like cell death in Candida albicans: critical role of K+-channel-mediated K+ efflux. Antimicrob Agents Chemother 52: 4081-4088.

71. Situ H, Bobek LA (2000) In vitro assessment of antifungal therapeutic potential of salivary histatin-5, two variants of histatin-5, and salivary mucin (MUC7) domain 1. Antimicrob Agents Chemother 44: 1485-1493.

72. Muir A, Soong G, Sokol S, Reddy B, Gomez MI et al. (2004) Toll-like receptors in normal and cystic fibrosis airway epithelial cells. Am J Respir Cell Mol Biol 30: 777-783.

73. Sun WK, Lu X, Li X, Sun QY, Su X et al. (2012) Dectin-1 is inducible and plays a crucial role in Aspergillus-induced innate immune responses in human bronchial epithelial cells. Eur J Clin Microbiol Infect Dis [Epub ahead of print].

74. Gereke M, Jung S, Buer J, Bruder D (2009) Alveolar type II epithelial cells present antigen to CD4(+) T cells and induce Foxp3(+) regulatory T cells. Am J Respir Crit Care Med 179: 344-355.

75. Mayer AK, Bartz H, Fey F, Schmidt LM, Dalpke AH (2008) Airway epithelial cells modify immune responses by inducing an anti-inflammatory microenvironment. Eur

J Immunol 38: 1689-1699.

76. Jiang-Shieh YF, Chien HF, Chang CY, Wei TS, Chiu MM et al. (2010) Distribution and expression of CD200 in the rat respiratory system under normal and endotoxin-induced pathological conditions. J Anat 216: 407-416.

77. Hansdottir S, Monick MM, Hinde SL, Lovan N, Look DC et al. (2008) Respiratory epithelial cells convert inactive vitamin D to its active form: potential effects on host defense. J Immunol 181: 7090-7099.

78. Neri T, Conti I, Cerri C, Tavanti L, Paggiaro P et al. (2010) Divergent effects of nitric oxide on airway epithelial cell activation. Biol Res 43: 467-473.

79. Janssen WJ, McPhillips KA, Dickinson MG, Linderman DJ, Morimoto K et al. (2008) Surfactant proteins A and D suppress alveolar macrophage phagocytosis via interaction with SIRP alpha. Am J Respir Crit Care Med 178: 158-167.

80. Willart MA, Lambrecht BN (2009) The danger within: endogenous danger signals, atopy and asthma. Clin Exp Allergy 39: 12-19.

81. Lambrecht BN, Hammad H (2010) The role of dendritic and epithelial cells as master regulators of allergic airway inflammation. Lancet 376: 835-843.

82. Angkasekwinai P, Park H, Wang YH, Wang YH, Chang SH et al. (2007) Interleukin 25 promotes the initiation of proallergic type 2 responses. J Exp Med 204: 1509-1517.

83. Kurowska-Stolarska M, Stolarski B, Kewin P, Murphy G, Corrigan CJ et al. (2009) IL-33 Amplifies the Polarization of Alternatively Activated Macrophages That Contribute to Airway Inflammation. J Immunol 183: 6469-77.

84. Holgate ST (2012) Innate and adaptive immune responses in asthma. Nat Med 18: 673-683.

85. Islam SA, Luster AD (2012) T cell homing to epithelial barriers in allergic disease. Nat Med 18: 705-715.

86. Carmona EM, Lamont JD, Xue A, Wylam M, Limper AH (2010) Pneumocystis cell wall beta-glucan stimulates calcium-dependent signaling of IL-8 secretion by human airway epithelial cells. Respir Res 11: 95.

87. Barbosa FM, Fonseca FL, Holandino C, Alviano CS, Nimrichter L et al. (2006) Glucuronoxylomannan-mediated interaction of Cryptococcus neoformans with human alveolar cells results in fungal internalization and host cell damage. Microbes Infect 8: 493-502.

88. Barbosa FM, Fonseca FL, Figueiredo RT, Bozza MT, Casadevall A et al. (2007) Binding of glucuronoxylomannan to the CD14 receptor in human A549 alveolar cells induces interleukin-8 production. Clin Vaccine Immunol 14: 94-98.

89. Nathan AT, Peterson EA, Chakir J, Wills-Karp M (2009) Innate immune responses of airway epithelium to house dust mite are mediated through beta-glucan-dependent pathways. J Allergy Clin Immunol 123: 612-618.

90. Reese TA, Liang HE, Tager AM, Luster AD, Van Rooijen N et al. (2007) Chitin induces accumulation in tissue of innate immune cells associated with allergy. Nature 447: 92-96.

91. Nishiyama A, Tsuji S, Yamashita M, Henriksen RA, Myrvik QN et al. (2006) Phagocytosis of N-acetyl-D-glucosamine particles, a Th1 adjuvant, by RAW 264.7 cells results in MAPK activation and TNF-alpha, but not IL-10, production. Cell Immunol 239: 103-112.

92. Shibata Y, Metzger WJ, Myrvik QN (1997) Chitin particle-induced cell-mediated immunity is inhibited by soluble mannan: mannose receptor-mediated phagocytosis initiates IL-12 production. J Immunol 159: 2462-2467.

Chapter 2

Chitin elicits CCL2 from airway epithelial cells and induces CCR2-dependent innate allergic inflammation in the lung

René M. Roy, Marcel Wüthrich, and Bruce S. Klein

This chapter has been accepted for publication as:
Roy RM, Wuthrich M, Klein BS (2012) Chitin elicites CCL2 from airway epithelial cells and induces CCR2-dependent innate allergic inflammation in the lung. J Immunol 189 (5) In Press.

ABSTRACT

Chitin exposure in the lung induces eosinophilia and alternative activation of macrophages, and is correlated with allergic airway disease. However, the mechanism underlying chitin-induced polarization of macrophages is poorly understood. Here, we show that chitin induces alternative activation of macrophages *in vivo,* but does not do so directly *in vitro*. We further show that airway epithelial cells bind chitin *in vitro* and produce CCL2 in response to chitin both *in vitro* and *in vivo*. Supernatants of chitin exposed epithelial cells promoted alternative activation of macrophages *in vitro*, whereas antibody neutralization of CCL2 in the supernate abolished the alternative activation of macrophages. CCL2 acted redundantly *in vivo*, but mice lacking the CCL2 receptor, CCR2, showed impaired alternative activation of macrophages in response to chitin, as measured by arginase I, CCL17 and CCL22 expression. Furthermore, CCR2KO mice exposed to chitin had diminished ROS products in the lung, blunted eosinophil and monocyte recruitment, and impaired eosinophil functions as measured by expression of CCL5, IL13 and CCL11. Thus, airway epithelial cells secrete CCL2 in response to chitin and CCR2 signaling mediates chitin-induced alternative activation of macrophages and allergic inflammation *in vivo*.

INTRODUCTION

Exposure to fungal- and insect-related antigens early in life are a significant risk factor in the development of allergy and asthma (1). Besides intrinsic protease activity present in many allergens, the additional presence of pathogen-associated molecular patterns (PAMP) such as lipopolysaccharide and β-glucan contributes to the allergenicity of inhaled environmental allergens (2, 3). Common to the cell wall of fungi and the exoskeleton of insects and crustaceans is the polysaccharide chitin, a linear chain of β-1,4-N-acetylglucosamine sugars. Chitin is among the most abundant polymers on our planet and is recognized by, and elicits responses from, organisms across the kingdoms of life. As an example, N-acetylglucosamine oligosaccharides trigger antifungal immune responses in plants via specific chitin receptors that share homology with mammalian chitnases and chitinase-like proteins (4, 5). In humans, elevated chitin exposure in the workplace and at home is correlated with asthma and other allergic diseases (6-8). Furthermore, murine models have demonstrated that exposure to chitin particles results in innate allergic inflammation characterized by alternatively activated macrophages and eosinophilia (9-11). Thus, chitin represents a potential allergy promoting pathogen-associated molecular pattern with a significant public health impact.

Among airway immune cells, macrophages are "ambidextrous" cells capable of initiating or suppressing inflammatory responses (12). In response to environmental or microbial exposures, macrophages are polarized into phenotypically distinct activation states: classical (M1) or alternative (M2). M2 macrophages antagonize pro-inflammatory Th_1 responses and promote the development of Th_2-associated inflammation central to the pathogenesis of allergy and asthma. Although chitin exposure induces M2 polarization *in vivo* (9, 10), macrophages exposed to chitin *in vitro* fail to acquire an M2 phenotype (13-16), suggesting that an intermediary is required for chitin-induced M2 polarization *in vivo*.

Airway epithelial cells are the initial point of contact for inhaled allergens and coordinate with pulmonary dendritic cells (DC) to induce Th_2 responses central to the pathogenesis of asthma. In a model of house dust mite (HDM) induced asthma, activation of epithelial cells was required for the subsequent development of allergic responses in the airway (2). Here, we investigated the intermediary cells and products that facilitate chitin-induced M2 polarization and allergic airway inflammation. We demonstrate that airway epithelial cells produce CCL2 (monocyte chemotactic protein-1, MCP-1) in response to chitin and that the CCL2 receptor CCR2 is required for chitin-induced M2 polarization and allergic inflammation *in vivo.*

MATERIAL AND METHODS

Mice

CCR2 knockout (stock# 004999), CCL2 knockout (stock# 004434) mice, aged 5-8 weeks were obtained from The Jackson Laboratory (Bar Harbor, ME). C57BL/6 wild type mice (strain code 01C55), aged 5-8 weeks, were obtained from NCI (Frederick, MD). Mice were housed and cared for according guidelines from the University of Wisconsin Animal Care and Use Committee, who approved this work.

Reagents and cell culture

Chitin purified from crab shells was purchased from Sigma (C9752). AMJ2-C11 murine macrophages (CRL-2456) and LA-4 murine lung epithelial cells (CCL-196) were obtained from ATCC. AMJ2-C11 cells were maintained in RPMI with 10% heat inactivated fetal bovine serum (FBS) and 1% penicillin/streptomycin (complete RPMI). LA-4 cells were maintained in F-12 Ham's media with 15% FBS and 1% penicillin/ streptomycin. Anti-CCL2 neutralizing antibody (MAB479) and mouse cytokine antibody array (ARY006) were purchased from R&D Systems.

Chitin purification

Ground chitin particles were dissolved in 12.5M HCl and incubated for 30 minutes at 40ºC with frequent agitation. The solution was transferred to a cooled beaker and slowly neutralized with ice cold NaOH. The insoluble fraction was collected and washed in H_2O three times followed by a wash in ethanol. The purified chitin particles were then dried in a speedvac before storage at -20ºC. Before use, chitin particles were resuspended in endotoxin-free PBS, sonicated, then filtered through a 10µm nylon filter. Protein was less than 2% by mass as determined by BCA assay. Endotoxin levels as measured by Pyrogent Plus assay (Lonza) were less than 0.03EU/mL.

Binding Assays

For chitin binding assays only, chitin particles less than 10μm were labeled with flourescein isothiocyante (FITC) as previously described (17). For all other exposures, unlabeled chitin particles were used. AMJ2-C11 macrophages or LA-4 lung epithelial cells were incubated with chitin particles over varying doses and time intervals. Cell samples were washed three times, fixed with 0.5% paraformaldehyde, and analyzed by fluorescence microscopy. All binding assays were performed at 4ºC. Binding index is calculated as number of particles/100 cells.

Administration of Chitin

Mice were anesthetized via an intraperitoneal injection of etomidate. The anesthetized mouse was then suspended from their front incisors and intubated using a BioLite Intubation System (18). Chitin particles were suspended at indicated concentrations in 20μL PBS and administered via the intubation tube into the airway.

Bronchoalveolar Lavage

At varied intervals after chitin administration, mice were anesthetized with isoflurane and euthanized by exsanguination. 1mL of PBS/2mM EDTA was administered via intratracheal catheter to lavage the airway. BALF was placed on ice prior to centrifugation at 300 x g for 5 minutes. Cell-free supernatants were frozen at -20°C for later analysis. The BALF cell pellet was resuspended in PBS/1%BSA for analysis by flow cytometry or lysed for RNA extraction. For isolation of alveolar macrophages, the BALF cell pellet was resuspended in PBS/1%BSA, incubated with anti-mouse CD11c-biotin antibody (BD Bioscience) on ice for 30 minutes, washed, and incubated with streptavidin coated magnetic beads (BD Bioscience). For chemokine secretion experiments, isolated CD11c+ cells were resuspended in RPMI with 10% FBS and 1% penicillin/streptomycin and incubated overnight in 24-well plates at 37°C.

Mouse Airway Epithelial Cell Isolation

Airway epithelial cells were isolated as previously described (19) with slight modifications. The pulmonary vasculature was perfused with 5mL PBS via the right ventricle and Liberase (Roche) was instilled via a catheter placed in the trachea, followed by 1mL of 1% low melt agarose (ISCBioExpress). The animal was placed on ice to harden the agarose prior to removing the lungs, which were then placed in 2mL Liberase solution for 1 hour at room temperature. Lungs were then teased apart with forceps in DMEM with 1% penicillin/streptomycin (Hyclone) and shaken for 10 minutes at 200r/min. The resulting suspension was filtered through a 40µm filter, centrifuged at 250 x g for 10 minutes. After centrifugation, the cells were stained with anti-mouse CD45-biotin antibody (eBioscience) on ice for 30 minutes, washed, and incubated with streptavidin coated magnetic beads (BD Bioscience) for CD45+ cell depletion. The CD45-depleted suspension was stained with anti-mouse CD326-PE antibody (eBioscience) on ice for 20 minutes, washed, and incubated with anti-PE coated magnetic beads (BD Bioscience). The CD326+ cells were resuspended in DMEM with 10% FBS and 1% penicillin/streptomycin and incubated overnight in 6-well plates at 37°C. A portion of the cells was analyzed by flow cytometry to assess purity.

Measurement of chemokines

Following overnight incubation at 37°C, cell-free supernatants were collected and stored at -20°C for later analysis by ELISA. ELISA kits for CCL2, CCL17, CCL22, and Ym1 were obtained from R&D Systems.

Flow Cytometry

Lung cell suspensions were prepared by mincing lungs through a 70µm filter using a 3mL syringe plunger. The resulting homogenate was digested with Liberase/DNAse I and the red blood cells were lysed with ammonium chloride/potassium bicarbonate buffer. All samples were blocked with anti-mouse CD16/32 antibody prior to staining

with fluorochrome-conjugated antibodies. Events were gated on FSC/SSC parameters to exclude debris and on live cells based on Violet Fixable Live-Dead stain (Molecular Probes) Fluorochrome-conjugated antibodies used were Mac-3-FITC, Siglec F-PE, CD90.2-PerCP-Cy5.5, CD11b-PECy7, Ly6C-APC, CD11c-Alexa700, Ly6G-APC-Cy7. Antibodies were obtained from BD Biosciences, eBioscience, and Biolegend. Cells were collected for analysis on a BD Biosciences LSRII cytometer and data analyzed with FloJo software (Tree Star).

Real-Time PCR

Total RNA was isolated from lung homogenates or isolated cell populations using a Qiagen RNeasy mini kit and cDNA was prepared using the BioRad iScript cDNA synthesis kit. cDNA was amplified using BioRad SSoFast EvaGreen Supermix in a BioRad MyIQ Real Time PCR detection system. Primers were designed using Primer-BLAST (20). Relative transcript quantity was calculated using the comparative Ct method with β-actin transcript as the control transcript (21).

ROS measurement

The presence of reactive oxygen species (ROS) in cell-free BALF was assessed using 2'-7'-dichlorofluorescin diacetate (DCF), which becomes fluorescent after exposure to peroxidase and hydrogen peroxide (22). 80μL of BALF or PBS was added to 120μL of DCF/HBSS solution in 96-well black opaque plates. After a 20-minute incubation in the dark, fluorescence intensity above an empty control 96-well black plate was measured using a Bio-Rad Versadoc5000MP imaging system.

Statistics

The means of fold change in transcript, chemokine protein content, or numbers of leukocytes were compared to control using an unpaired t-test with a two-tailed p-value < 0.05 considered statistically significant. For experiments where percent reduction vs.

wild type mice were reported, a one-sample t-test was used to compare values to a hypothetical value of zero (i.e. no change) with a p-value < 0.05 considered statistically significant. All statistical analysis was performed using Prism software (Graph Pad). In all figures, error bars represent the standard deviation of the data.

RESULTS

Interaction of chitin with macrophages *in vitro* and *in vivo*

To understand the direct effect of chitin exposure on macrophages, we investigated the binding of chitin particles to macrophages and the activation profile of the cells after they were exposed to chitin particles *in vitro*. AMJ2-C11 macrophages bound FITC-labeled chitin particles in a dose- and time-dependent, saturable manner (Fig 1A, 1B). Because FITC may alter surface binding properties of particles, we confirmed our findings with unlabeled chitin particles that were stained with the chitin selective dye Uvitex 2B following binding. To assess the activation state of macrophages exposed to chitin, we measured expression of arginase I (ArgI), a canonical product of the M2 phenotype (23, 24). Chitin particles failed to induce ArgI expression in AMJ2-C11 macrophages, but did activate the cells and induce production of TNF-α, a marker of classical activation *in vitro* (Fig 1C). Chitin also failed to induce ArgI expression in alveolar macrophages *in vitro* (data not shown). Because the context of chitin exposure likely affects the activation state of macrophages, we also evaluated the activation of macrophages *in vivo*. Accordingly, ArgI expression was strongly induced in the lung following intratracheal exposure to chitin particles (Fig 1D). Thus, chitin promotes disparate macrophage activation states *in vitro* and *in vivo* and the cells exhibit an M2 phenotype only *in vivo*.

Chitin binds to airway epithelial cells and elicits CCL2 *in vitro*

Due to the apparent dichotomy of macrophage activation observed above, we hypothesized that chitin was alternatively activating macrophages indirectly *in vivo*. Epithelial cells form a barrier to particles and high molecular weight molecules in the airway and are activated by chitin-containing allergens such as house dust mite (2, 3). To test whether chitin interacts with airway epithelial cells, we exposed LA-4 murine

epithelial cells to FITC-labeled chitin particles *in vitro*. LA-4 cells bound FITC-labeled chitin particles in a dose- and time-dependent, saturable manner (Fig 2A, 2B). Unlabeled chitin particles bound to LA-4 epithelial cells in a similar fashion. To determine if LA-4 cells were activated by exposure to chitin particles, we used a proteomic array to investigate chitin-induced release of cytokine and chemokine into the cell supernate. Exposure to chitin particles induced a dose-dependent increase in CCL2 secretion, but did not induce any of the other 39 targets in the array (Fig 2C). Notably, chitin exposure to LA-4 epithelial cells failed to induce IL-4 or IL-13 production, cytokines that promote the alternative activation of macrophages. In addition, CCL7, which shares a receptor with CCL2, was also not produced by chitin-exposed epithelial cells *in vitro.* We confirmed the dose-dependent increase in CCL2 production by chitin-exposed epithelial cells by measuring CCL2 in epithelial cell supernatants in amounts ranging up to 300 pg/ml (Fig 2D).

Chitin exposed airway epithelial cells alternatively activate macrophages in a CCL2-dependent manner *in vitro*

To further investigate whether chitin-exposed epithelial cells could promote the alternative activation of macrophages, we incubated AMJ2-C11 macrophages in supernatants from chitin-exposed LA-4 cells. Supernatants from chitin-exposed epithelial cells resulted in a chitin dose-dependent increase in ArgI expression in the macrophages (Fig 3A). Given our observation that chitin induces CCL2 secretion from epithelial cells *in vitro,* and prior work that demonstrated an impairment in alternative activation of macrophages in CCL2-deficient animals (25, 26), we investigated whether CCL2 in epithelial cell supernatant is required for alternative activation of macrophages *in vitro*. We used a CCL2-neutralizing antibody to block the product in chitin-exposed epithelial cell supernatants added to the macrophages. In the presence of neutralizing CCL2 antibody, chitin-exposed epithelial cell supernatant lost the ability to induce ArgI

expression in macrophages (Fig 3B). However, unlike recombinant IL-13, recombinant CCL2 alone was not sufficient to induce ArgI expression in macrophages (Fig 3C). Therefore, CCL2 is necessary but not sufficient to mediate ArgI expression in macrophages exposed to chitin-stimulated epithelial cells *in vitro*.

Chitin induces CCL2 from airway epithelial cells *in vivo*

Next, we investigated whether CCL2 is produced by lung epithelial cells after exposure to chitin particles *in vivo*. Following chitin administration into the airway, we found a dose-dependent increase in CCL2 expression in whole lung homogenates (Fig 4A). While CCL2 protein in cell-free BALF was increased in a dose-dependent fashion by chitin exposure (Fig 4B), we found no increase in CCL2 in the BALF cell pellet (Fig 4A), suggesting a lung parenchymal source of CCL2. To investigate whether lung epithelial cells produce CCL2 in response to chitin exposure, we isolated these cells from chitin- and PBS control-exposed lungs. We achieved a nearly 20-fold enrichment of epithelial cells from whole lung homogenates by depleting hematopoietic cells (CD45+) and selecting for cells expressing the epithelial marker CD326 (EpCAM) (27) (Fig 4C). Following overnight culture of cells *ex vivo*, the CD45+ cell populations from chitin-exposed mice did not increase CCL2 production. In contrast, CD326+ enriched epithelial cells from chitin-exposed mice secreted significantly more CCL2 than PBS control-exposed mice (Fig 4D). Hence, CD326+ epithelial cells represent a source of CCL2 *in vivo* following chitin exposure in the airway.

Chitin induced alternative activation of macrophages is CCR2 dependent *in vivo*

To see if CCL2 plays a role in chitin-induced alternative activation of macrophages *in vivo*, we analyzed the expression kinetics of CCL2 and the alternative activation marker ArgI in the lung. CCL2 is expressed as early as 2 hours following exposure to chitin

while ArgI is not expressed until 16 hours (Fig 5A), temporally supporting a role for CCL2 in the induction of ArgI. To determine whether CCL2 is necessary for ArgI expression in the lung, we administered chitin to the airways of CCL2KO mice. We found no impairment in Arg I expression. However, we observed that CCL2KO mice had a significant compensatory increase in CCL7 expression in response to chitin (Fig 5B).

Because CCL7 signals through the same receptor as CCL2 – that is, CCR2 (28, 29) – and contributes to CCR2-mediated activity in parallel with CCL2 (30), we investigated whether CCR2 is required for chitin-induced ArgI expression *in vivo*. Whole lung homogenates showed significantly delayed and reduced ArgI expression after chitin exposure in CCR2KO mice compared to wild-type mice (Fig 5C). To determine if the CCR2-dependent reduction in ArgI expression occurred in alveolar macrophages, and therefore reflected an impaired M2 phenotype, we isolated and analyzed CD11c+ cells from BAL. Isolated CD11c+ cells were >95% $CD11b^{lo}$/Mac-3+, indicating their identity as macrophages rather than dendritic cells. CD11c+ cells from CCR2KO mice had significantly lower levels of ArgI expression than did WT mice (Fig 5D). To substantiate a defect in M2 polarization in CCR2KO mice, we also measured the expression of other M2 signature chemokines in isolated CD11c+ cells. Both CCL17 and CCL22 also were expressed at significantly lower levels in CD11c+ cells from CCR2KO mice compared to WT mice (Fig 5D). Similarly, CD11c+ cells isolated from the BALF chitin-exposed CCR2KO mice secreted less CCL17, CCL22, and Ym1 following overnight incubation *ex vivo* than CD11c+ cells isolated from the BAL of chitin-exposed wild type mice (Figure 5E-G). Therefore, CCR2 signaling is required for chitin-induced M2 polarization in the lung.

Chitin exposure elicits neutrophilic and eosinophilic inflammation and recruits monocytes in a CCR2-dependent manner

To characterize and compare the allergic inflammatory response in the lungs of wild-type and CCR2KO mice, we quantified leukocyte subsets in whole lung homogenates following chitin exposure. Overall cell numbers, influx of CD11c+/Mac3+/CD11b^{lo} macrophages, Ly6G^{hi} neutrophils, and Thy-1+ T-cells were all unaffected in CCR2KO mice (Fig 6A,B,D, and F). However, recruitment of CD11b+/Ly6C^{hi} monocytes was dependent on CCR2 in response to chitin exposure (Fig 6E). Furthermore, chitin-induced recruitment of SiglecF+/CD11c- eosinophils was significantly reduced in CCR2KO mice (Fig 6C). Thus, CCR2 was linked functionally to the recruitment of eosinophils into the lung following exposure to chitin.

Eosinophils have an activation defect in chitin-exposed CCR2 deficient mice

Because we found alterations in the numbers of eosinophils and other innate immune cells recruited to the lung, we investigated whether eosinophil function and other inflammatory parameters in CCR2KO mice were otherwise altered in their response to chitin exposure. Exposure to allergens increases the production of ROS in the airway (31, 32), however the role of CCR2 in allergen or chitin-induced ROS production remains undefined. BAL obtained from chitin-exposed mice converted significantly more of the redox-sensitive H_2DCF dye to fluorescent DCF in WT mice as compared to CCR2KO mice (Fig 7A). To further investigate eosinophil function during innate allergic inflammation in chitin-exposed mice, we sorted these cells by FACS and analyzed the expression of products associated with eosinophil activation(33). Sorted SiglecF+/ CD11c- eosinophils from whole lung homogenates of chitin-exposed animals showed that CCR2KO mice had 60-to-80% less expression of CCL5, IL13, and CCL11 than similarly exposed WT mice (Fig 7B), and also had reduced surface expression of the activation marker CD69 (Fig 7C). Thus, CCR2 is required for recruitment, activation and function of allergic innate immune cells such as eosinophils after chitin exposure *in vivo*.

DISCUSSION

Our work provides new insight into the cellular mechanisms that drive M2 polarization during innate allergic inflammation in response to chitin. Our study suggests that macrophages are not M2 polarized directly on exposure to chitin in the lung. Instead, we demonstrate that chitin stimulates CCL2 production from airway epithelial cells, and we establish a pivotal role for CCR2 in chitin-induced macrophage polarization and innate allergic inflammation in the airway. Isolated CD326+ cells from chitin-exposed lungs and LA-4 epithelial cells exposed to chitin *in vitro* produced elevated levels of CCL2. Compared to WT mice, CCR2KO mice exposed to chitin demonstrated reduced expression of M2 markers (ArgI, CCL17 and CCL22), eosinophil recruitment and eosinophil activation in the lung. Thus, we propose that the respiratory epithelium modulates M2 polarization of macrophages upon chitin exposure.

Airway epithelial cells are among the earliest cells exposed to inhaled substances and actively collaborate with immune cells to mount innate and adaptive responses. Because chitin is associated with many inhaled allergens, we hypothesize that chitin recognition by airway epithelial cells may promote an epithelial pro-allergy program to otherwise innocuous agents via secretion of CCL2. Multiple lines of evidence underscore the association of CCL2 with asthma and allergic airway disease. Elevated CCL2 levels are present in BALF obtained from individuals with asthma (34) and CCL2 is elicited upon airway allergen challenge in humans (35). In animal models, OVA/alum sensitization and challenge provokes increased CCL2 expression (36). Similarly, chitin-associated cockroach (37) or *Aspergillus fumigatus* antigens (38) also provoke CCL2 production in animal asthma models. Our findings suggest that epithelial cells may be an important source of CCL2 during exposure to chitin-containing allergens, thereby promoting M2 polarization.

Consistent with a role for airway epithelial cell CCL2 in allergic responses, chitin

exposure promotes M2 polarization *in vivo* via an indirect mechanism (10) that is dependent on CCR2. We propose that airway epithelial cell-derived CCL2 is a key chemokine in promoting M2 polarization and innate allergic inflammation in response to chitin. Indeed, CCL2 expression precedes ArgI expression in chitin-exposed lungs. Following chitin exposure, antibody neutralization of CCL2 in chitin-exposed epithelial cell supernatants also inhibits M2 polarization *in vitro*. Airway epithelial cells are an important source of CCL2 in viral infections associated with asthma exacerbations (39, 40). Our findings that CCL2 promotes M2 polarization in a setting of chitin-induced allergic inflammation are consistent with previous reports demonstrating a role for CCL2 in tumor- (41) and thermal injury- (25) associated M2 polarization.

We observed that epithelial cell CCL2 is necessary for M2 polarization in response to chitin *in vitro*, however CCL2 was dispensable for M2 polarization *in vivo*. The upregulation of the CCR2 ligand, CCL7, in CCL2-deficient mice following chitin exposure may obscure the necessary role of CCL2 in chitin-induced M2 polarization we observed *in vitro*. To address this issue, we investigated the host response to chitin in a CCR2-deficient mouse. In the absence of CCR2, chitin exposure failed to elicit alternatively activated macrophages in the lung. Our results reflect the established central role of CCR2 in mediating the effects of both CCL2 and CCL7 *in vivo*. For example, in a model of infection with the fungal pathogen *Histoplasma capsulatum*, CCR2KO mice demonstrated increased susceptibility to the fungus and an increased fungal burden in the lung (42). Neutralization of either CCL2 or CCL7 was not sufficient to increase the fungal burden, however neutralization of both chemokines did. Similarly, CCR2KO mice are more susceptible to *Listeria monocytogenes* infection whereas CCL2KO or CCL7KO mice demonstrate an intermediate susceptibility phenotype (30). Moreover, M2 polarization canonically depends on IL4Rα and its ligands IL4 and IL13. While neither CCL7 nor IL4 or IL13 were detected following epithelial cell exposure to

chitin *in vitro*, all three products are present in the lung following chitin exposure *in vivo*. Our work does not preclude a role for IL-4 in chitin induced innate allergic inflammation. However, future studies should address whether the CCL2-CCR2 axis and IL-4Rα signalling represent linear, convergent, or parallel signaling pathways in chitin-initiated M2 polarization.

CCR2KO mice also demonstrate reduced eosinophil recruitment and activation in response to chitin, further suggesting a role for CCR2 in eosinophilic inflammation. Murine eosinophils contain CCR2 mRNA (43) and may express low levels of CCR2 protein on their cell surface (44). However, this is unlikely to explain the reduction in eosinophil recruitment in CCR2KO mice as eosinophils do not migrate in response to CCL2 (45) and migrate toward CCL7 via a CCR3-dependent mechanism (46). Chitin induced eosinophil recruitment is abrogated in mice lacking the receptor for LTB_4 (9), suggesting a link between eosinophil recruitment and leukotriene signaling following chitin exposure. Because chitin fails to activate eosinophils directly (47), the defect in activation and recruitment in CCR2KO mice must be linked to upstream factors. M2 macrophages elicited by chitin exposure are potent sources of LTB_4 (9). Thus, the reduction in chitin induced eosinophil recruitment in CCR2KO mice may be due to the reduction in M2 polarization.

CCR2 is required for egress (48) and homing (49) of monocytes to sites of inflammation. We show a near-complete reduction of $Ly6C^{hi}$ monocytes recruited to the lung following chitin exposure in CCR2KO mice. $Ly6C^{hi}$ monocytes may differentiate into CD11b+ inflammatory DCs, which accumulate in the allergic airway and are critical mediators of Th_2 adaptive immune response in the airway (50). Recently, CCR2+$Ly6C^{hi}$ monocytes were reported to recruit eosinophils to colonic mucosa via CCL11 in an experimental colitis model (51). The partnering of $Ly6C^{hi}$ monocytes with M2 macrophages to recruit and/or activate eosinophils could represent an intriguing

interaction to therapeutically target in order to reduce eosinophilic inflammation during asthma and allergy.

In conclusion, we show that airway epithelial cells secrete CCL2 and that CCR2 signaling is required for events leading to M2 polarization and recruitment and activation of eosinophils upon chitin exposure. The findings clarify the mechanisms that drive alternative activation of macrophages in response to chitin, and identify possible targets of therapeutic intervention in the setting of chitin induced innate allergic inflammation.

ACKNOWLEDGEMENTS

We thank Marlene Klaila and Titilayo Omobesi for excellent animal care, Dr. Tristan Brandhorst for assistance in preparing and analyzing chitin used in these studies and Dr. Rebecca Brockman-Schneider and Dr. James Gern for advice and assistance with epithelial cell experiments.

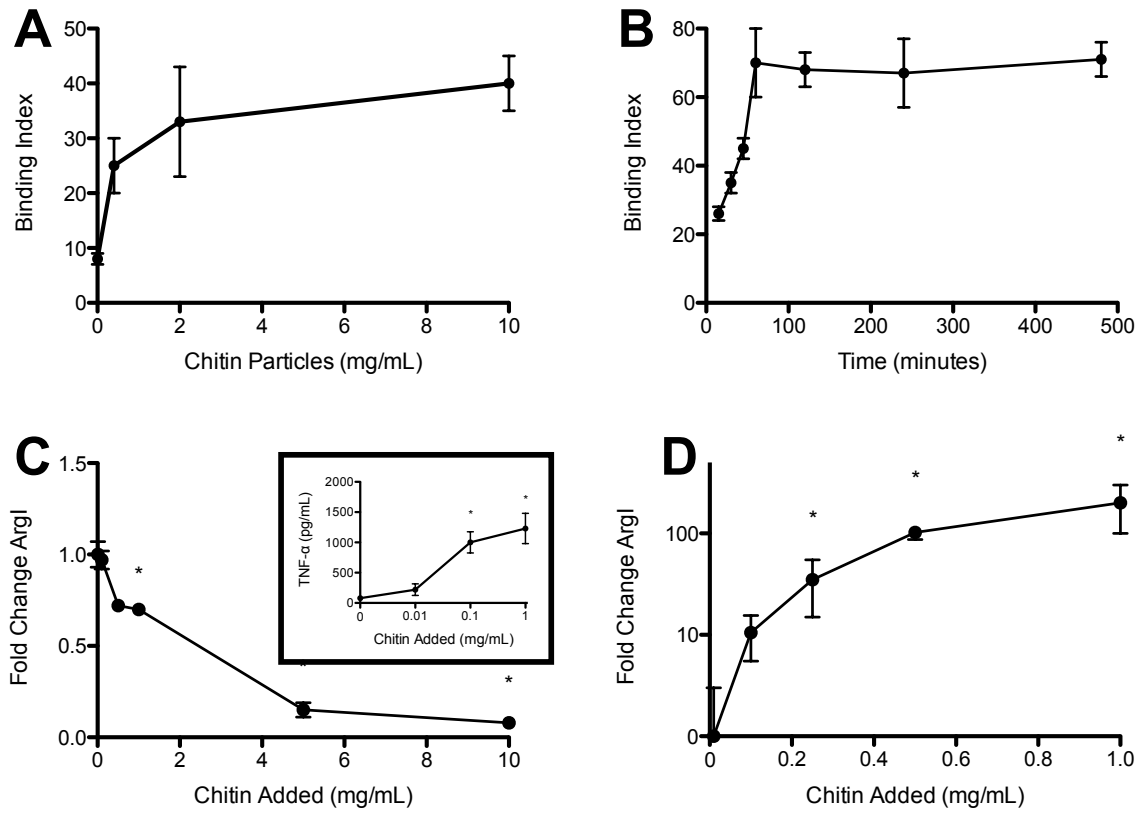

Figure 1

Figure 2-1. Macrophages bind chitin and become M2 polarized in vivo but not in vitro. (A) Dose-dependent, and **(B)** time-dependent binding of chitin particles by AMJ2-C11 macrophages. Binding was performed at 4°C in vitro (n=3). Chitin-induced ArgI expression **(C*)*** and release of TNF-α [inset] *in* vitro (n=3; 5 mice/group), and **(D)** *in vivo* (n=3). **P*<0.05 vs. no chitin control.

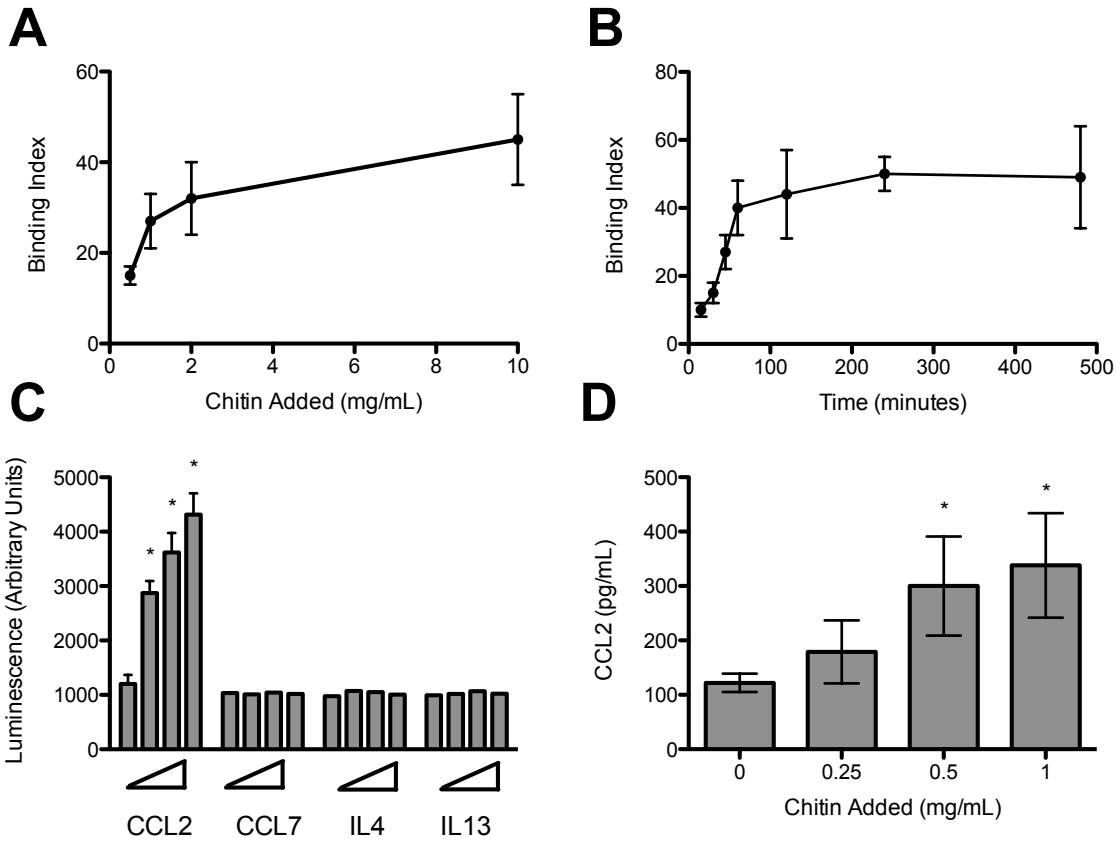

Figure 2

Figure 2-2. Airway epithelial cells bind chitin and produce CCL2 following chitin exposure. (A) Dose-dependent and **(B)** time-dependent binding of chitin particles to LA-4 epithelial cells. Binding was performed at 4°C *in vitro* (n=3). **(C)** Chitin induced CCL2, CCL7, IL-4, and IL-13 production (n=3). Chitin added in amounts of 0, 0.25, 0.5, and 1.0 mg/mL is represented by the crescendo. **(D)** CCL2 production by LA-4 cells 16 hours following chitin exposure (n=3). **P*<0.05 vs. no chitin control.

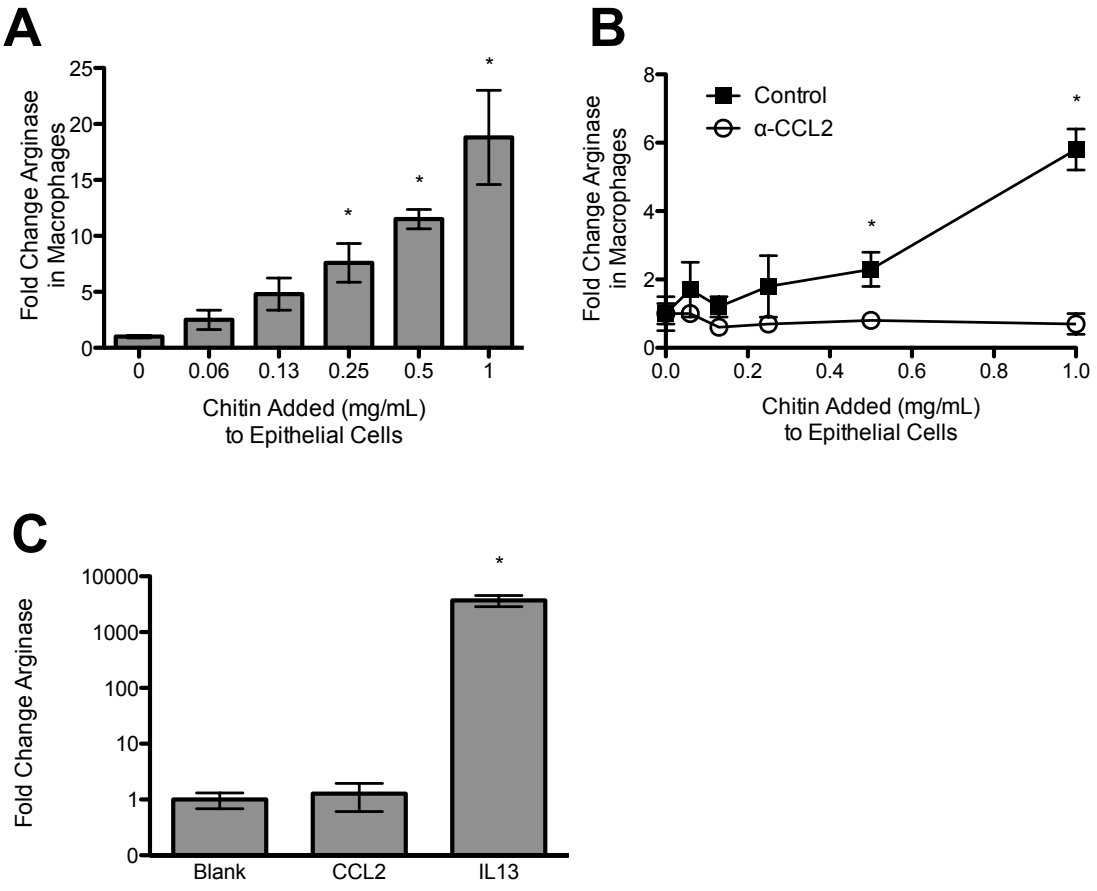

Figure 3

Figure 2-3. Epithelial cell CCL2-dependent M2 polarization in vitro. (A) ArgI expression in macrophages cultured in chitin-exposed epithelial cell supernatant for 16 hours (n=5, **P*<0.05 vs. no chitin added). **(B)** Experiment in panel B done in the presence of 100µg/mL CCL2 neutralizing or isotype control antibody (n=3, **P*<0.05). **(C)** Effect of recombinant CCL2 or IL13 (50ng/mL) on AMJ2-C11 macrophage ArgI expression *in vitro* (n=3, **P*<0.05 vs. PBS).

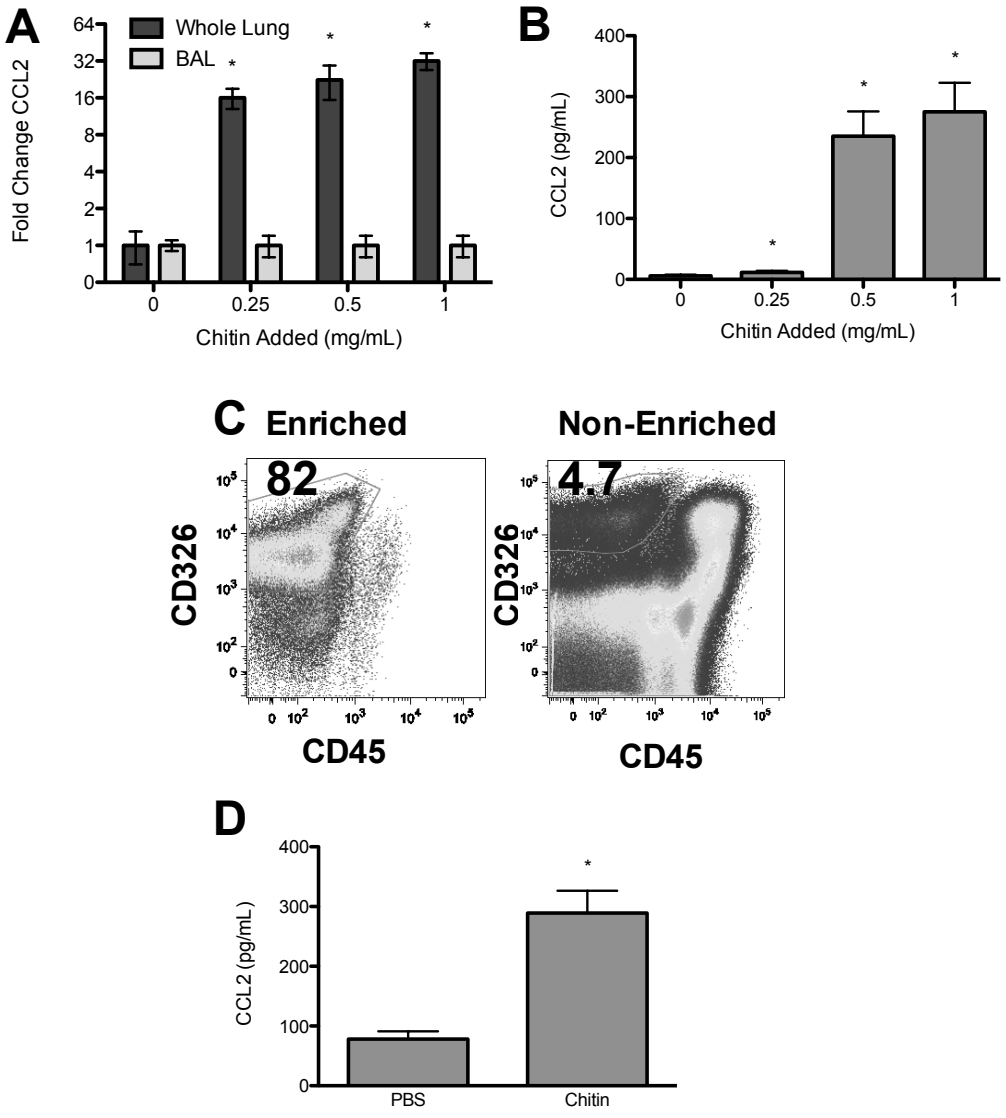

Figure 4

Figure 2-4. Chitin induces epithelial cell CCL2 secretion in vivo. (A) Chitin induced CCL2 transcript expression in whole lung homogenate and BAL and **(B)** CCL2 protein level in BAL (n=4, **P*<0.05). **(C)** To verify an epithelial source of CCL2, CD326+ cells were isolated from chitin- or PBS-exposed lungs. The purity of cell separation was assessed by flow cytometry. **(D)** Chitin-exposed CD326+ cells cultured overnight *ex vivo* following isolation produce CCL2 (n=3, **P*<0.05 vs. PBS).

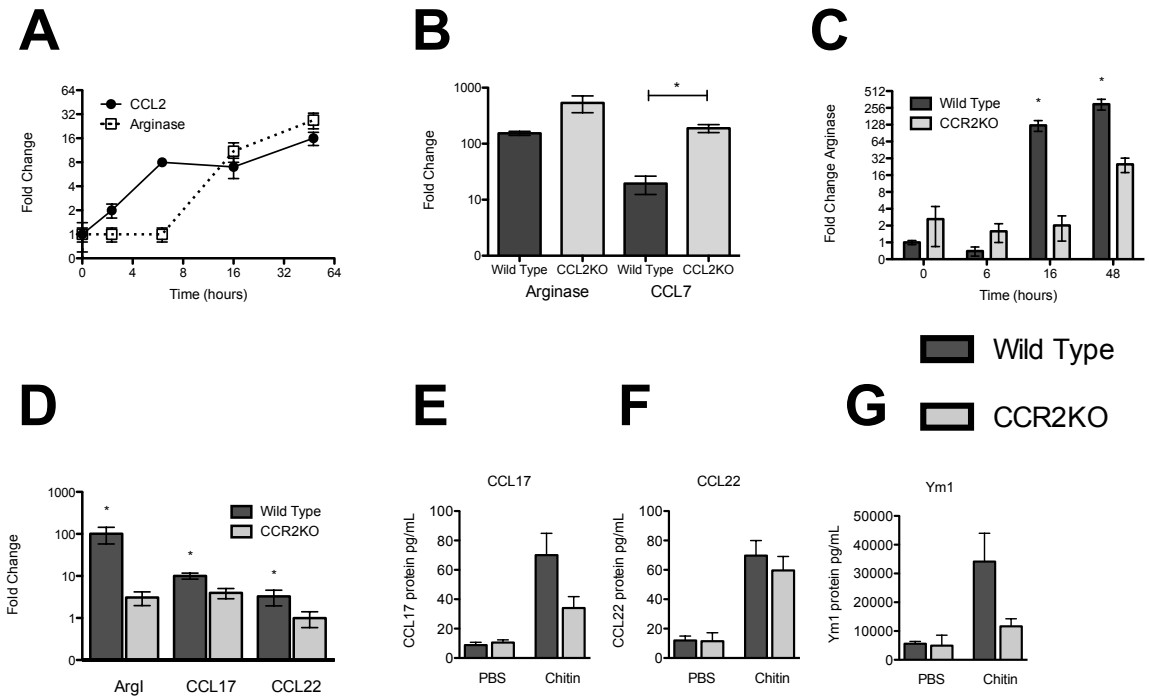

Figure 5

Figure 2-5. Chitin induces CCR2-dependent M2 polarization in vivo. (A) Kinetics of ArgI and CCL2 expression following chitin exposure *in vivo* (n=3; 5 mice/group). **(B)** ArgI and CCL7 expression in wild type and CCL2KO mice (5 mice/group, **P*<0.05). **(C)** Chitin induction of ArgI expression in whole lung in wild-type and CCR2KO mice (n=3; 5mice/group, **P*<0.05, WT vs. CCR2KO). **(D)** Chitin-induction of ArgI, CCL17 and CCL22 expression in CD11c+ cells from BALF of wildtype and CCR2KO mice (n=2; 5mice/group, **P*<0.05, WT vs. CCR2KO).

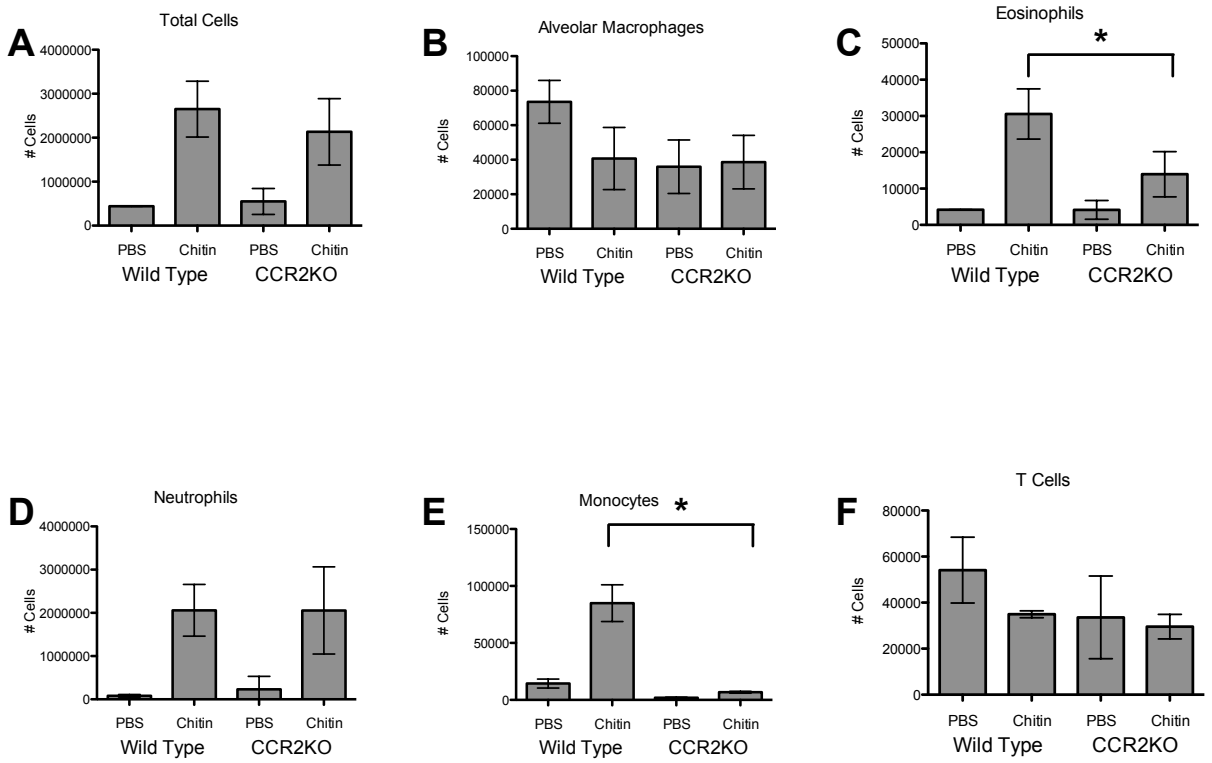

Figure 6

Figure 2-6. Chitin-induced eosinophil and monocyte recruitment is CCR2 dependent. Cell numbers in leukocyte subsets in whole lung homogenate 48 hours after chitin exposure in wildtype and CCR2KO mice (n=3; 5 mice/group, **P*<0.05 WT vs. control). **(A)** Total live cells. **(B)** CD11c+/CD11b^{lo}/Mac3+ Alveolar Macrophages. **(C)** Siglec F+/CD11c-/CD11b+ Eosinophils. **(D)** Ly6G+/SSC^{hi}/CD11b+ Neutrophils. **(E)** CD11b+/Ly6C^{hi}/Ly6G- monocytes. **(F)** Thy1+ T cells.

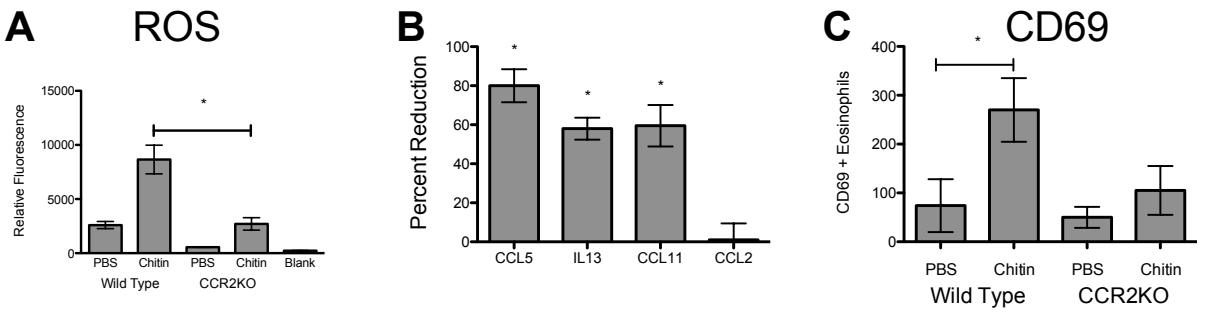

Figure 7

Figure 2-7. Chitin induced ROS production and eosinophil activation is CCR2 dependent. (A) ROS levels in BALF from wildtype and CCR2KO animals 48 hours after chitin exposure (n=3, **P*<0.05 WT vs CCR2KO). Siglec F+/CD11c- lung eosinophils were sorted by FACS from CCR2KO mice vs. wildtype mice 48 hours after chitin exposure. **(B)** Percent reduction of eosinophil CCL5, IL13, and CCL11 expression in CCR2KO vs. WT mice(n=3, **P*<0.05). **(C)** Number of CD69+ eosinophils isolated from mouse lungs 48 hours following exposure. (n=3, **P*<0.05 vs. PBS).

REFERENCES

1. Ahluwalia, S. K., and E. C. Matsui. 2011. The indoor environment and its effects on childhood asthma. *Curr Opin Allergy Clin Immunol* 11: 137-143.

2. Hammad, H., M. Chieppa, F. Perros, M. A. Willart, R. N. Germain, and B. N. Lambrecht. 2009. House dust mite allergen induces asthma via Toll-like receptor 4 triggering of airway structural cells. *Nat Med* 15: 410-416.

3. Nathan, A. T., E. A. Peterson, J. Chakir, and M. Wills-Karp. 2009. Innate immune responses of airway epithelium to house dust mite are mediated through beta-glucan-dependent pathways. *J Allergy Clin Immunol* 123: 612-618.

4. Fusetti, F., T. Pijning, K. H. Kalk, E. Bos, and B. W. Dijkstra. 2003. Crystal structure and carbohydrate-binding properties of the human cartilage glycoprotein-39. *J Biol Chem* 278: 37753-37760.

5. Ohnuma, T., S. Onaga, K. Murata, T. Taira, and E. Katoh. 2008. LysM domains from Pteris ryukyuensis chitinase-A: a stability study and characterization of the chitin-binding site. *J Biol Chem* 283: 5178-5187.

6. Howse, D., D. Gautrin, B. Neis, A. Cartier, L. Horth-Susin, M. Jong, and M. C. Swanson. 2006. Gender and snow crab occupational asthma in Newfoundland and Labrador, Canada. *Environ Res* 101: 163-174.

7. Wu, A. C., J. Lasky-Su, C. A. Rogers, B. J. Klanderman, and A. A. Litonjua. 2010. Fungal exposure modulates the effect of polymorphisms of chitinases on emergency department visits and hospitalizations. *Am J Respir Crit Care Med* 182: 884-889.

8. Van Dyken, S. J., D. Garcia, P. Porter, X. Huang, P. J. Quinlan, P. D. Blanc, D. B. Corry, and R. M. Locksley. 2011. Fungal chitin from asthma-associated home environments induces eosinophilic lung infiltration. *J Immunol* 187: 2261-2267.

9. Reese, T. A., H. E. Liang, A. M. Tager, A. D. Luster, N. Van Rooijen, D. Voehringer, and R. M. Locksley. 2007. Chitin induces accumulation in tissue of innate immune cells associated with allergy. *Nature* 447: 92-96.

10. Satoh, T., O. Takeuchi, A. Vandenbon, K. Yasuda, Y. Tanaka, Y. Kumagai, T. Miyake, K. Matsushita, T. Okazaki, T. Saitoh, K. Honma, T. Matsuyama, K. Yui, T. Tsujimura, D. M. Standley, K. Nakanishi, K. Nakai, and S. Akira. 2010. The Jmjd3-Irf4 axis regulates M2 macrophage polarization and host responses against helminth infection. *Nat Immunol* 11: 936-944.

11. Kogiso, M., A. Nishiyama, T. Shinohara, M. Nakamura, E. Mizoguchi, Y. Misawa, E. Guinet, M. Nouri-Shirazi, C. K. Dorey, R. A. Henriksen, and Y. Shibata. 2011. Chitin particles induce size-dependent but carbohydrate-independent innate eosinophilia. *J Leukoc Biol* 90: 167-176.

12. Peters-Golden, M. 2004. The alveolar macrophage: the forgotten cell in asthma. *Am J Respir Cell Mol Biol* 31: 3-7.

13. Bueter, C. L., C. K. Lee, V. A. Rathinam, G. J. Healy, C. H. Taron, C. A. Specht, and S. M. Levitz. 2011. Chitosan but not chitin activates the inflammasome by a mechanism dependent upon phagocytosis. *J Biol Chem* 286: 35447-35455.

14. Da Silva, C. A., D. Hartl, W. Liu, C. G. Lee, and J. A. Elias. 2008. TLR-2 and IL-17A in chitin-induced macrophage activation and acute inflammation. *J Immunol* 181: 4279-4286.

15. Da Silva, C. A., C. Chalouni, A. Williams, D. Hartl, C. G. Lee, and J. A. Elias. 2009. Chitin is a size-dependent regulator of macrophage TNF and IL-10 production. *J Immunol* 182: 3573-3582.

16. Nishiyama, A., S. Tsuji, M. Yamashita, R. A. Henriksen, Q. N. Myrvik, and Y. Shibata. 2006. Phagocytosis of N-acetyl-D-glucosamine particles, a Th1 adjuvant, by RAW 264.7 cells results in MAPK activation and TNF-alpha, but not IL-10, production. *Cell Immunol* 239: 103-112.

17. Nishiyama, A., T. Shinohara, T. Pantuso, S. Tsuji, M. Yamashita, S. Shinohara, Q. N. Myrvik, R. A. Henriksen, and Y. Shibata. 2008. Depletion of cellular cholesterol enhances macrophage MAPK activation by chitin microparticles but not by heat-killed Mycobacterium bovis BCG. *Am J Physiol Cell Physiol* 295: C341-9.

18. Hamacher, J., M. Arras, F. Bootz, M. Weiss, R. Schramm, and U. Moehrlen. 2008. Microscopic wire guide-based orotracheal mouse intubation: description, evaluation and comparison with transillumination. *Lab Anim* 42: 222-230.

19. Corti, M., A. R. Brody, and J. H. Harrison. 1996. Isolation and primary culture of murine alveolar type II cells. *Am J Respir Cell Mol Biol* 14: 309-315.

20. Rozen, S., and H. Skaletsky. 2000. Primer3 on the WWW for general users and for biologist programmers. *Methods Mol Biol* 132: 365-386.

21. Schmittgen, T. D., and K. J. Livak. 2008. Analyzing real-time PCR data by the comparative C(T) method. *Nat Protoc* 3: 1101-1108.

22. Keston, A. S., and R. Brandt. 1965. The fluorometric analysis of ultramicro quantities of hydrogen peroxide. *Anal Biochem* 11: 1-5.

23. Gordon, S., and F. O. Martinez. 2010. Alternative activation of macrophages: mechanism and functions. *Immunity* 32: 593-604.

24. Odegaard, J. I., R. R. Ricardo-Gonzalez, M. H. Goforth, C. R. Morel, V. Subramanian, L. Mukundan, A. Red Eagle, D. Vats, F. Brombacher, A. W. Ferrante, and A. Chawla. 2007. Macrophage-specific PPARgamma controls alternative activation and improves insulin resistance. *Nature* 447: 1116-1120.

25. Shigematsu, K., A. Asai, M. Kobayashi, D. N. Herndon, and F. Suzuki. 2009. Enterococcus faecalis translocation in mice with severe burn injury: a pathogenic role of CCL2 and alternatively activated macrophages (M2aMphi and

M2cMphi). *J Leukoc Biol* 86: 999-1005.

26. Tsuda, Y., H. Takahashi, M. Kobayashi, T. Hanafusa, D. N. Herndon, and F. Suzuki. 2004. CCL2, a product of mice early after systemic inflammatory response syndrome (SIRS), induces alternatively activated macrophages capable of impairing antibacterial resistance of SIRS mice. *J Leukoc Biol* 76: 368-373.

27. McQualter, J. L., K. Yuen, B. Williams, and I. Bertoncello. 2010. Evidence of an epithelial stem/progenitor cell hierarchy in the adult mouse lung. *Proc Natl Acad Sci U S A* 107: 1414-1419.

28. Osterholzer, J. J., J. L. Curtis, T. Polak, T. Ames, G. H. Chen, R. McDonald, G. B. Huffnagle, and G. B. Toews. 2008. CCR2 mediates conventional dendritic cell recruitment and the formation of bronchovascular mononuclear cell infiltrates in the lungs of mice infected with Cryptococcus neoformans. *J Immunol* 181: 610-620.

29. Szymczak, W. A., and G. S. J. Deepe. 2009. The CCL7-CCL2-CCR2 axis regulates IL-4 production in lungs and fungal immunity. *J Immunol* 183: 1964-1974.

30. Jia, T., N. V. Serbina, K. Brandl, M. X. Zhong, I. M. Leiner, I. F. Charo, and E. G. Pamer. 2008. Additive roles for MCP-1 and MCP-3 in CCR2-mediated recruitment of inflammatory monocytes during Listeria monocytogenes infection. *J Immunol* 180: 6846-6853.

31. Boldogh, I., A. Bacsi, B. K. Choudhury, N. Dharajiya, R. Alam, T. K. Hazra, S. Mitra, R. M. Goldblum, and S. Sur. 2005. ROS generated by pollen NADPH oxidase provide a signal that augments antigen-induced allergic airway inflammation. *J Clin Invest* 115: 2169-2179.

32. Ye, Y. L., H. T. Wu, C. F. Lin, C. Y. Hsieh, J. Y. Wang, F. H. Liu, C. T. Ma, C. H. Bei, Y. L. Cheng, C. C. Chen, B. L. Chiang, and C. W. Tsao. 2011. Dermatophagoides pteronyssinus 2 regulates nerve growth factor release to induce airway inflammation via a reactive oxygen species-dependent pathway. *Am J Physiol Lung Cell Mol Physiol* 300: L216-24.

33. Rose, C. E. J., J. A. Lannigan, P. Kim, J. J. Lee, S. M. Fu, and S. S. Sung. 2010. Murine lung eosinophil activation and chemokine production in allergic airway inflammation. *Cell Mol Immunol* 7: 361-374.

34. Alam, R., J. York, M. Boyars, S. Stafford, J. A. Grant, J. Lee, P. Forsythe, T. Sim, and N. Ida. 1996. Increased MCP-1, RANTES, and MIP-1alpha in bronchoalveolar lavage fluid of allergic asthmatic patients. *Am J Respir Crit Care Med* 153: 1398-1404.

35. Holgate, S. T., K. S. Bodey, A. Janezic, A. J. Frew, A. P. Kaplan, and L. M. Teran. 1997. Release of RANTES, MIP-1 alpha, and MCP-1 into asthmatic airways following endobronchial allergen challenge. *Am J Respir Crit Care Med* 156: 1377-1383.

36. Gonzalo, J. A., C. M. Lloyd, D. Wen, J. P. Albar, T. N. Wells, A. Proudfoot, C. Martinez-A, M. Dorf, T. Bjerke, A. J. Coyle, and J. C. Gutierrez-Ramos. 1998.

The coordinated action of CC chemokines in the lung orchestrates allergic inflammation and airway hyperresponsiveness. *J Exp Med* 188: 157-167.

37. Campbell, E. M., I. F. Charo, S. L. Kunkel, R. M. Strieter, L. Boring, J. Gosling, and N. W. Lukacs. 1999. Monocyte chemoattractant protein-1 mediates cockroach allergen-induced bronchial hyperreactivity in normal but not CCR2-/- mice: the role of mast cells. *J Immunol* 163: 2160-2167.

38. Blease, K., B. Mehrad, N. W. Lukacs, S. L. Kunkel, T. J. Standiford, and C. M. Hogaboam. 2001. Antifungal and airway remodeling roles for murine monocyte chemoattractant protein-1/CCL2 during pulmonary exposure to Asperigillus fumigatus conidia. *J Immunol* 166: 1832-1842.

39. Renois, F., J. Jacques, D. Talmud, G. Deslee, N. Leveque, and L. Andreoletti. 2010. Respiratory echovirus 30 and coxsackievirus B5 can induce production of RANTES, MCP-1 and IL-8 by human bronchial epithelial cells. *Virus Res* 152: 41-49.

40. Olszewska-Pazdrak, B., A. Casola, T. Saito, R. Alam, S. E. Crowe, F. Mei, P. L. Ogra, and R. P. Garofalo. 1998. Cell-specific expression of RANTES, MCP-1, and MIP-1alpha by lower airway epithelial cells and eosinophils infected with respiratory syncytial virus. *J Virol* 72: 4756-4764.

41. Roca, H., Z. S. Varsos, S. Sud, M. J. Craig, C. Ying, and K. J. Pienta. 2009. CCL2 and interleukin-6 promote survival of human CD11b+ peripheral blood mononuclear cells and induce M2-type macrophage polarization. *J Biol Chem* 284: 34342-34354.

42. Deepe, G. S. J., M. Wuthrich, and B. S. Klein. 2005. Progress in vaccination for histoplasmosis and blastomycosis: coping with cellular immunity. *Med Mycol* 43: 381-389.

43. Borchers, M. T., T. Ansay, R. DeSalle, B. L. Daugherty, H. Shen, M. Metzger, N. A. Lee, and J. J. Lee. 2002. In vitro assessment of chemokine receptor-ligand interactions mediating mouse eosinophil migration. *J Leukoc Biol* 71: 1033-1041.

44. Rothenberg, M. E., and S. P. Hogan. 2006. The eosinophil. *Annu Rev Immunol* 24: 147-174.

45. Oliveira, S. H., S. Lira, C. Martinez-A, M. Wiekowski, L. Sullivan, and N. W. Lukacs. 2002. Increased responsiveness of murine eosinophils to MIP-1beta (CCL4) and TCA-3 (CCL1) is mediated by their specific receptors, CCR5 and CCR8. *J Leukoc Biol* 71: 1019-1025.

46. Chung, I. Y., Y. H. Kim, M. K. Choi, Y. J. Noh, C. S. Park, D. Y. Kwon, D. Y. Lee, Y. S. Lee, H. S. Chang, and K. S. Kim. 2004. Eotaxin and monocyte chemotactic protein-3 use different modes of action. *Biochem Biophys Res Commun* 314: 646-653.

47. Yoon, J., J. U. Ponikau, C. B. Lawrence, and H. Kita. 2008. Innate antifungal immunity of human eosinophils mediated by a beta2 integrin, CD11b. *J*

Immunol 181: 2907-2915.

48. Shi, C., T. Jia, S. Mendez-Ferrer, T. M. Hohl, N. V. Serbina, L. Lipuma, I. Leiner, M. O. Li, P. S. Frenette, and E. G. Pamer. 2011. Bone marrow mesenchymal stem and progenitor cells induce monocyte emigration in response to circulating toll-like receptor ligands. *Immunity* 34: 590-601.

49. Tsou, C. L., W. Peters, Y. Si, S. Slaymaker, A. M. Aslanian, S. P. Weisberg, M. Mack, and I. F. Charo. 2007. Critical roles for CCR2 and MCP-3 in monocyte mobilization from bone marrow and recruitment to inflammatory sites. *J Clin Invest* 117: 902-909.

50. Robays, L. J., T. Maes, S. Lebecque, S. A. Lira, W. A. Kuziel, G. G. Brusselle, G. F. Joos, and K. V. Vermaelen. 2007. Chemokine receptor CCR2 but not CCR5 or CCR6 mediates the increase in pulmonary dendritic cells during allergic airway inflammation. *J Immunol* 178: 5305-5311.

51. Waddell, A., R. Ahrens, K. Steinbrecher, B. Donovan, M. E. Rothenberg, A. Munitz, and S. P. Hogan. 2011. Colonic eosinophilic inflammation in experimental colitis is mediated by Ly6C(high) CCR2(+) inflammatory monocyte/ macrophage-derived CCL11. *J Immunol* 186: 5993-6003.

Chapter 3

Airway epithelial cell NF-κB signaling and CCR2 mediate chitin-dependent *Aspergillus*-specific Th2 and Th17 differentiation in the lung

René M. Roy, Somashekarappa G. Nanjappa, Kevin Galles, Vanessa LeBert, Fiona Yull, Timothy Blackwell, Marcel Wüthrich, and Bruce S. Klein

ABSTRACT

Chitin particle exposure promotes pulmonary innate allergic inflammation yet its ability promote sensitization to inhaled antigen is unknown. We developed a model of chitin-dependent sensitization to soluble antigen from the allergy associated fungus *Aspergillus fumigatus*. In the presence of chitin, mice sensitized to *Aspergillus fumigatus* antigens exhibited pulmonary eosinophilia, expressed Th2 cytokines in the lung, and had elevated levels of serum IgE compared to mice exposed to chitin or antigens alone. We used transgenic *Aspergillus fumigatus* specific CD4+ T cells in an adoptive transfer system to demonstrate that chitin mediates *Aspergillus* specific Th2 and Th17 polarization of effector T cells in the lung. Chitin dependent sensitization to *Aspergillus fumigatus* antigen was dependent on CCR2 and airway epithelial cell NF-κB signaling. These data demonstrate that chitin can serve as an adjuvant in Th2 and Th17 polarization and implicate NF-κB controlled gene products from airway epithelial cells and CCR2 as key modulators of chitin dependent sensitization to *Aspergillus* antigens in the lung.

INTRODUCTION

Since van Leeuwen described a series of patients with asthma and sensitivity to molds in the aftermath of the First World War [1], fungi have remained an important cause of allergic disease and asthma exacerbations worldwide [2-4]. Following inhalation of conidia, sensitization to fungi, especially *Aspergillus fumigatus*, is mediated in part by fungal proteases that damage epithelial cell tight junctions, promote pro-inflammatory cytokine release, and facilitate exposure of fungal antigens to lung antigen presenting cells [5]. In addition, the cell wall of *Aspergillus* contains carbohydrates, such as β-glucan, that are recognized by pattern recognition receptors [6] and that trigger immune responses from mesenchymal and hematopoeitic cells in the lung [7,8].

Besides β-glucan, *Aspergillus* cell walls contain chitin [9], a linear chain of β-1,4-N-acetylglucosamine sugars, which can trigger innate allergic inflammation that is characterized by eosinophilia and alternatively activated macrophages [10]. Furthermore, following intraperitoneal injection of chitin particles with the model antigen ovalbumin, chitin also serves as an adjuvant that polarizes CD4+ T cells into Th1, Th2, and Th17 cells [11]. However, whether and how chitin might serve as an adjuvant to promote allergic inflammation and sensitization in the lung is unknown. Since many inhaled allergens of insect or fungal origin contain chitin [12,13], understanding the mechanism of chitin induced allergic inflammation in the lung is relevant to understanding allergic sensitization in asthma.

Airway epithelial cells are the initial point of contact for inhaled antigen and are critical regulators of allergic sensitization in the lung [14]. Airway epithelial cells maintain tight junctions near their apical surfaces that effectively form a barrier between inhaled antigen and immune cells, such as dendritic cells, in the submucosal space [15,16]. In patients with asthma, airway epithelial cells display disordered tight junctions and the barrier function is impaired suggesting that epithelial barrier dysfunction may influence

allergic sensitization in the lung [17,18]. Beyond their barrier function, airway epithelial cells secrete cyokines and chemokines that regulate the function of dendritic cells in the airway. Upon exposure to to an activating stimulus, airway epithelial cells secrete the dendritic cell activating cytokines such as, thymic stromal lymphopoeitin (TSLP), IL25, IL33, and GM-CSF which induce maturation and migration of airway DC to the lymph node [16] where the activated DC can prime T cells. We recently demonstrated that upon exposure to chitin, airway epithelial cells become activated and secrete CCL2 [19] and furthermore, that CCR2-the receptor for CCL2-was required for chitin induced innate allergic inflammation. However, our work focused on innate responses to chitin, and left open the question of whether epithelial cell or its products such as CCL2/CCR2 have a role in chitin dependent sensitization to environmental allergens.

In the present study, we sought to determine whether chitin exposure could promote allergic sensitization to *Aspergillus* antigens in the lung. Furthermore, we tested whether airway epithelial cells and CCR2, which are critical to chitin-induced innate allergic inflammation, also mediate chitin-dependent allergic sensitization. To address these questions, we developed a model of chitin-dependent sensitization to *Aspergillus* antigens. Following exposure to chitin, mice exposed to A.f antigen became sensitized and exhibited allergic inflammation characterized by pulmonary eosinophilia, expression of Th2 cytokines, and elevated serum IgE. Mice carrying an airway epithelial cell specific, inducible dominant negative IκBα gene were protected against chitin-dependent sensitization to *Aspergillus* as were CCR2KO mice. By using adoptive transfer of *Aspergillus* specific transgenic CD4+ T cells, we also found that epithelial cell-chitin interactions polarize *Aspergillus* specific T cell into Th2 as well as Th17 cells. In sum, our results demonstrate that chitin serves as an adjuvant that mediates *Aspergillus* specific T cell polarization via activation of airway epithelial cells and CCR2.

METHODS

Mice

CCR2 knockout (stock# 004999) mice aged 5-8 weeks were obtained from The Jackson Laboratory (Bar Harbor, ME). C57BL/6 wild type mice (strain code 01C55), aged 5-8 weeks, were obtained from NCI (Frederick, MD). DNTA (IκBα-DN Trans Activated) mice are an inducible transgenic mouse based on the tet-on system [20]. The generation and characterization of DNTA mice has been reported [21]. DNTA mice express a Myc-His-tagged mutant avian IκBα (NF-κB inhibitor) with S36 and S40 serine–adenine substitutions rendering the protein unable to be phosphorylated or degraded [22]. To achieve selective expression in airway epithelium, mice containing tet-O7-IκBα-DN-Myc-His constructs (DN mice) were crossed to mice expressing reverse tetracycline transactivator under control of the rat CC10 promoter (rtTA mice)(Courtesy Dr. Jeff Whitsett) [20]. Transgene expression was induced by supplementing water in a dark drinking bottle with 1mg/mL doxycyline (Sigma) and 1% sucrose. Doxycycline supplemented water was initiated two days before exposure to chitin and/or *Aspergillus* antigen, was replaced twice per week, and was maintained throughout the experiment.

Af3.16 mice are TCR transgenic mice harboring *Aspergillus* specific transgenic CD4+ T cells (Courtesy Dr. Amariliz Rivera and Dr. Tobias Hohl). The generation and characterization of Af3.16 mice has been reported [23]. Upon arrival at the University of Wisconsin-Madison, DNTA and Af3.16 mice were rederived by transfer of embryos into C57/BL6 surrogate dams. Mice were housed and cared for according guidelines from the University of Wisconsin Animal Care and Use Committee, who approved this work.

Reagents

Chitin purified from crab shells was purchased from Sigma (C9752) and was purified as previously described [19]. *Aspergillus fumigatus* soluble antigens were obtained via the University of Wisconsin Hospital Pharmacy from Greer (M3 Skin Test Vial). Prior to use, *Aspergillus* antigens was heat inactivated for 30 minutes at 60°C followed by drying by SpeedVac and reconstitution at 10mg/mL in sterile PBS.

Administration of Chitin / *Aspergillus* antigens

Mice were anesthetized via inhalation of isoflurane. The anesthetized mouse was then suspended from their front incisors and intubated using a BioLite Intubation System [24]. Chitin particles were suspended at 10mg/mL in PBS. 20μL of PBS, chitin particles, *Aspergillus* antigens, or chitin particles plus *Aspergillus* antigens were administered via the intubation tube into the airway. For sensitization, *Aspergillus* antigens in the presence or absence of chitin were administered every four days for five exposures and mice were euthanized two days following the final exposure (see Figure 1).

Adoptive transfer of Af3.16 T cells and detection of *Aspergillus* specific cytokine producing T cells

One day prior to exposure to chitin and/or *Aspergillus* antigens, 10^6 naive Thy1.1+ Af3.16 T cells isolated from spleen and lymph nodes were transferred into congenic Thy 1.2+ hosts. Mice that received Af3.16 T cells were exposed to PBS, chitin alone, *Aspergillus* antigens alone, or chitin plus *Aspergillus* antigens on day 1, 3, and 5 post-transfer. On day 7 post transfer, lungs and mediastinal lymph nodes were collected. Lung and mediastinal lymph node cell suspensions were stimulated for 5 hours with anti-CD3 and anti-CD28 antibody in the presence of GolgiStop (BD Bioscience). Cells were washed and filtered through a 70μm filter prior to surface staining for CD4, Thy1.1,

CD62L and CD44. Stained cells were fixed and permeabilized in BD Cytofix/Cytoperm at 4°C overnight. Permeabilized cells were stained with anti-IL4, anti-IL13, anti-IFNγ, and anti-IL17A for 30 minutes on ice. To identify cytokine producing Af3.16 T cells, events were gated on CD4, Thy1.1, and $CD44^{hi}$ and expression determined for each cytokine.

Flow Cytometry

Lung cell suspensions were prepared by mincing lungs through a 70µm filter using a 3mL syringe plunger. The resulting homogenate was digested with Liberase/DNAse I and the red blood cells were lysed with ammonium chloride/potassium bicarbonate buffer. All samples were blocked with anti-mouse CD16/32 antibody prior to staining with fluorochrome-conjugated antibodies. Events were gated on FSC/SSC parameters to exclude debris and on live cells based on Violet Fixable Live-Dead stain (Molecular Probes). Eosinophils were defined as Siglec F^{hi} $CD11b^{+}$ SSC^{hi} $CD11c^{-}$ $Ly6G^{-}$ $Thy1^{-}$. Antibodies were obtained from BD Biosciences, eBioscience, and Biolegend. Cells were collected for analysis on a BD Biosciences LSRII cytometer and data analyzed with FloJo software (Tree Star).

Real-Time PCR

Total RNA was isolated from lung homogenates using a Qiagen RNeasy mini kit and cDNA was prepared using the BioRad iScript cDNA synthesis kit. cDNA was amplified using BioRad SSoFast EvaGreen Supermix in a BioRad MyIQ Real Time PCR detection system. Primers were designed using Primer-BLAST [25]. Relative transcript quantity was calculated using the comparative Ct method with β-actin transcript as the control transcript [26].

Measurement of IgE

Following the sensitization protocol, blood was obtained from anesthetized mice by retro-orbital bleed and allowed to clot for 30 minutes at room temperature. Next the samples were centrifuged at 1500 x g for 15 minutes and the serum phase collected. Serum was diluted in RPMI 10-fold and stored at -20°C prior to analysis by ELISA.

Statistics

Samples were compared to control using an unpaired t-test with a two-tailed p-value < 0.05 considered statistically significant. All statistical analysis was performed using Prism software (Graph Pad). In all figures, error bars represent the standard deviation of the mean of the data.

RESULTS AND DISCUSSION

A model to assess chitin-dependent *Aspergillus* antigen sensitization in the lung.

To explore the role of chitin in promoting allergic sensitization to *Aspergillus* antigens, we developed a model of *Aspergillus* exposure to mimic chronic exposure to fungal antigens in the presence or absence of chitin particles. Because we sought to examine the role of lung epithelial cells in chitin dependent sensitization to *Aspergillus*, we chose to administer antigen and chitin intra-tracheally via non-surgical intubation [24]. This method has several advantages: i) it minimizes damage typically wrought by surgical intra-tracheal administration, ii) it allows for repeated exposures, and iii) it limits antigen delivery to the lung bypassing the upper airway and avoiding the gastrointestinal tract. Other published models of *Aspergillus* sensitization inject *Aspergillus* antigen into the peritoneum followed by repeated intranasal administration of antigen [27,28] thus bypassing the potential role of airway epithelial cells and airway DC in the initial sensitization to *Aspergillus* antigens. Figure 1 depicts the exposure protocol used to sensitize mice to *Aspergillus*.

Chitin exposure promotes allergic sensitization to *Aspergillus*

In order to assess chitin-dependent allergic sensitization in our model we compared mice that were sensitized to *Aspergillus* antigen in the presence or absence of chitin, chitin alone or that received PBS (naïve). We monitored eosinophil recruitment to the lung, Th2 cytokine production, and serum IgE levels in each group. Mice sensitized to *Aspergillus* in the presence of chitin had significantly more pulmonary eosinophilia (Fig 2A) than mice sensitized to *Aspergillus* alone or chitin alone. While chitin particles themselves can induce eosinophilia, the effect is transient, and eosinophil numbers drop to pre-exposure levels 7 days following chitin exposure [10,19,29]. Our present results

likewise demonstrate a resolution of eosinophilia 14 days following chitin exposure in the lung. However, when mice are additionally exposed to *Aspergillus* antigen, the initial chitin exposure is sufficient to promote eosinophilic inflammation. In addition to eosinophilia, the expression of the allergy associated Th2 cytokines IL4, IL5, and IL13 was sharply increased in mice sensitized to *Aspergillus* antigen in the presence of chitin compare to those exposed to either *Aspergillus* antigen or chitin alone (Fig 2B-D). Furthermore, IgE levels in the serum were elevated in mice sensitized to *Aspergillus* antigen in the presence of chitin were elevated compared to the other groups (Fig 2E). Together, these results indicate that chitin particles likely possess adjuvanticity and can promote allergic sensitization to antigen in the lung.

Airway epithelial cell NF-kB activity is required for chitin-dependent *Aspergillus* allergic sensitization

Airway epithelial cells represent an initial point of contact for inhaled antigens and play a critical role in shaping immune responses in the lung [16,21,30]. In addition to serving as a physical barrier preventing invasion by pathogens, the airway epithelium actively senses the outside world and directs appropriate responses by hematopoetic cells of the immune system. Activation of or injury to the airway epithelium is central to allergic sensitization and the pathology of asthma [14,31,32]. Indeed, blockade of NF-κB activation in airway epithelial cells protects mice from allergic inflammation [33] whereas activation of airway epithelial cell NF-κB is sufficient to sensitize mice to inhaled antigen [34]. We have shown that chitin alone triggers NF-κB dependent chemokine production by airway epithelial cells [19]. We hypothesized that NF-κB blockade in airway epithelial cells would abrogate chitin-dependent sensitization to *Aspergillus* antigen. To test this hypothesis, mice that harbor a doxycycline-inducible dominant negative IκBα transgene in airway epithelial cells (DNTA mice) [21] were sensitized to

Aspergillus antigen in the presence of chitin. When compared with non-transgenic littermate controls treated with doxycycline or untreated DNTA mice, DNTA mice treated with doxycycline had reduced pulmonary eosinophilia (Fig. 3A), decreased expression of Th2 cytokines in the lung (Fig 3B-D), and lower serum IgE levels (Fig. 3E). Thus, airway epithelial cells promote chitin dependent allergic sensitization to *Aspergillus* antigens via a NF-κB dependent mechanism.

Chitin promotes *Aspergillus*-specific Th2 and Th17 polarizaiton

Chitin promotes sensitization to *Aspergillus* antigens and induces the production of Th2 associated cytokines in the lung. To test whether chitin could serve as an adjuvant to polarize *Aspergillus* specific T cell responses in our model, we adoptively transferred 10^6 Thy1.1+ *Aspergillus* specific CD4+ T cells (Af3.16 cells) [23] into congenic Thy1.2+ wild type mice one day prior to exposure to chitin and/or *Aspergillus* antigens. We then exposed the mice to chitin and/or A.f antigens at 1, 3, and 5 days following transfer of Af3.16 cells. On day 7, we harvested lungs for analysis by flow cytometry. Lungs from mice sensitized to *Aspergillus* antigens in the presence of chitin had higher numbers of Af3.16 cells than did mice sensitized with chitin or *Aspergillus* antigen alone (Fig 4A). Similarly, the frequency of Af3.16 cells among CD4+ T cells was elevated in the lungs of mice sensitized to *Aspergillus* in the presence of chitin compared to the other groups (Fig 4B). Analysis of the cytokine profile of Af3.16 cells revealed that mice sensitized to *Aspergillus* in the presence of chitin had a much higher frequency of IL4 and IL17A producing cells (Fig 4C and 4D) compared to mice exposed to chitin or *Aspergillus* antigen alone. We were unable to detect an increase in the frequency of IL13 or IFNγ producing Af3.16 cells in our model (data not shown). These results suggest that chitin can serve as an adjuvant to polarize *Aspergillus* specific Th2 and Th17 cells. While Th2 cells are viewed as central to the pulmonary inflammation associated with asthma, Th17

cells are increasingly recognized as key players in severe neutrophilic asthma and corticosteroid resistant asthma [35,36]. Our findings showing that chitin can prime Th2 as well as Th17 *Aspergillus* specific CD4+ T cells may explain the high proportion of severe asthma in patients with hypersensitivity to fungi [2,37].

CCR2 is necessary for chitin-dependent *Aspergillus* allergic sensitization

Because CCR2 is required for chitin-induced innate allergic inflammation [19], we hypothesized that CCR2 was also necessary for chitin-induced *Aspergillus* antigen sensitization. A role for CCR2 in allergic Th2-type responses is controversial. CCR2KO mice sensitized to *Aspergillus* were not protected from pulmonary eosinophilia, elevated Th2 chemokine levels, and airway remodeling compared to wild type mice upon challenge with *Aspergillus* conidia [38,39]. Similarly, CCR2KO mice demonstrate a profound Th1 polarization defect and robust Th2 activation in infection models with *Histoplasma capsulatum* [40], *Cryptococcus neoformans* [41], and *Leishmania major* [42]. Conversely, CCR2KO mice were protected from airway hyperresponsiveness in a cockroach antigen model of asthma [43] and the use of a CCR2-blocking monoclonal antibody attenuated allergic inflammation in asthmatic non-human primates [44]. Furthermore, CCR2 was required for Th2 responses in a diesel exhaust particle model of allergic sensitization in mice [45]. CCR2KO mice sensitized to *Aspergillus* antigen in the presence of chitin demonstrated reduced pulmonary eosinophilia (Fig 5A), lowered expression of Th2 cytokines in the lung (Fig 5B-D), and a trend toward decreased IgE levels in the serum (Fig 5E) compared to wild type mice. These results suggest that CCR2 is necessary for chitin-induced allergic sensitization to *Aspergillus* antigen in the lung.

Conclusions

Overall, our data suggest that chitin can promote *Aspergillus* specific polarization of CD4+ T cells toward a Th2 and Th17 phenotype. The polarization of *Aspergillus* specific CD4+ T cells mirrors other markers of allergic inflammation induced by chitin, namely pulmonary eosinophilia and elevated serum IgE levels. Our results also argue that in addition to mediating innate allergic inflammation, CCR2 signaling is required for chitin-induced adaptive immune responses. Finally, we demonstrate a critical role for airway epithelial cell NF-κB dependent gene products in mediating the adjuvant effect of chitin. Taken together, our results point to a chitin-induced inflammatory program mediated by airway epithelial cells and CCR2 that lead to allergic sensitization and that may suggest novel therapeutic options targeting asthma in patients sensitized to fungi.

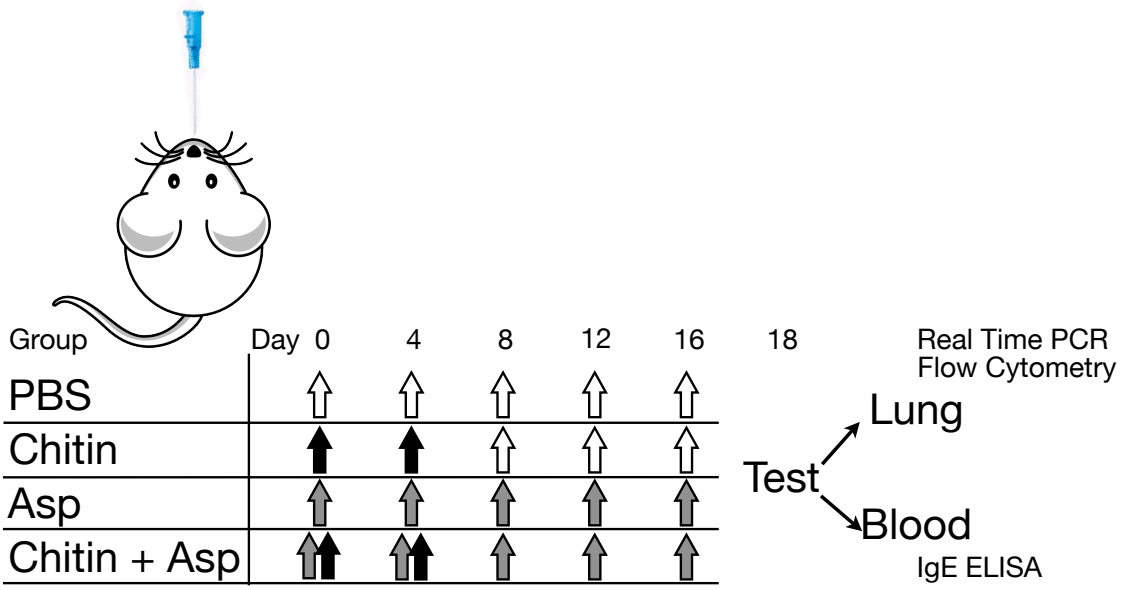

Figure 3-1. A model of chitin dependent sensitization to *Aspergillus*. Mice were exposed via the intratracheal route on day 0, 4, 8, 12, and 16. The PBS group (naive) received PBS (white arrows) at each time point. The Chitin group received chitin on day 0 and 4 (black arrows) and PBS thereafter. The Asp group received soluble *Aspergillus* antigens on each day (gray arrows). The Chitin + Asp group received chitin and soluble *Aspergillus* antigens on day 0 and 4 and *Aspergillus* antigens thereafter. Mice were sacrificed on day 18, the lungs and blood harvested and tested as indicated.

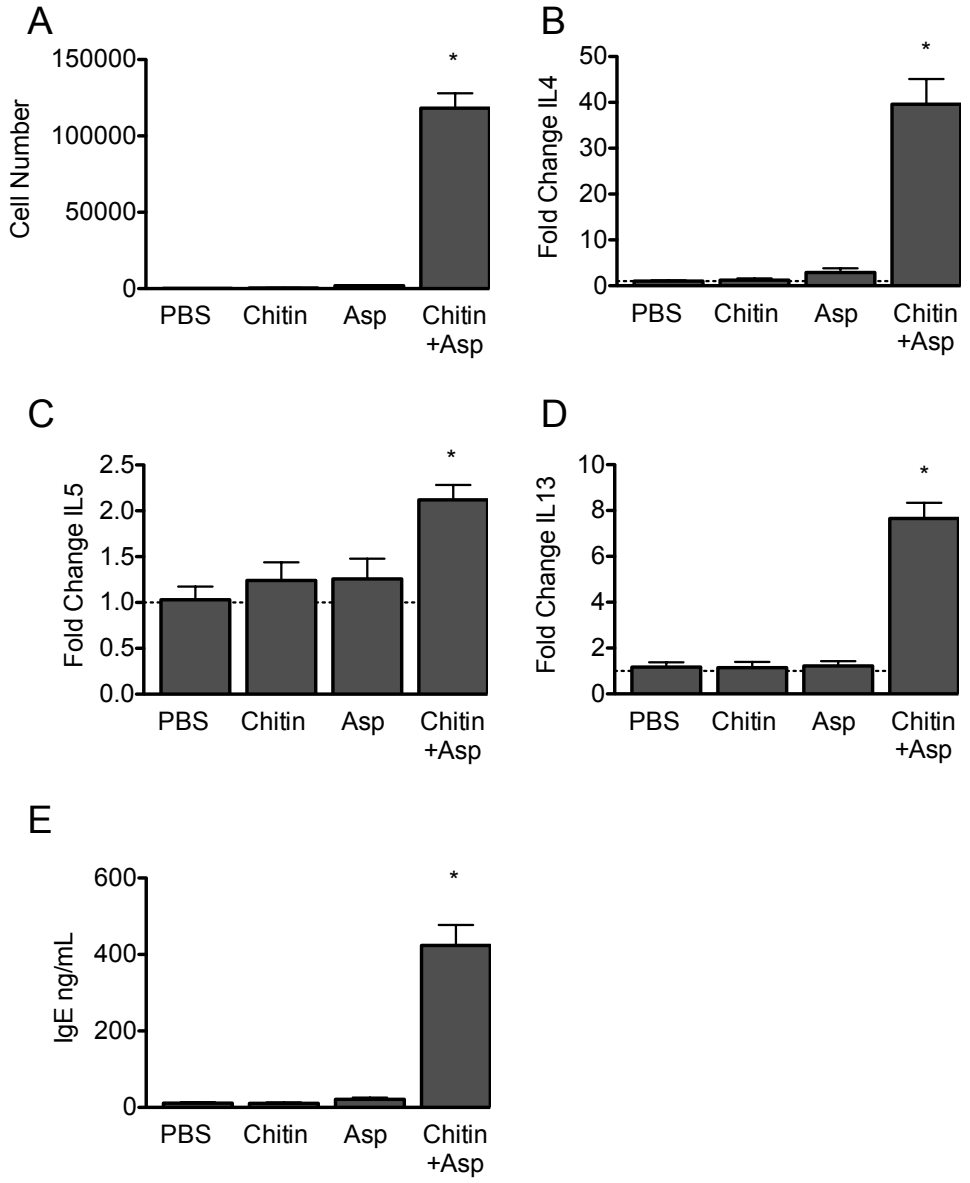

Figure 3-2. Chitin promotes sensitization to *Aspergillus* in the lung. Mice were sensitized to *Aspergillus* in the presence or absence of chitin (5 mice/group). **[A]** Eosinophils were enumerated from lung homogenates by flow cytometry. **[B]** IL4, **[C]** IL5, **[D]** IL13 expression levels were determined by real-time PCR from mRNA isolated from lung homogenates. **[E]** IgE was measured in serum by ELISA. Values are presented as mean +/- SEM, *P<0.05 vs PBS control.

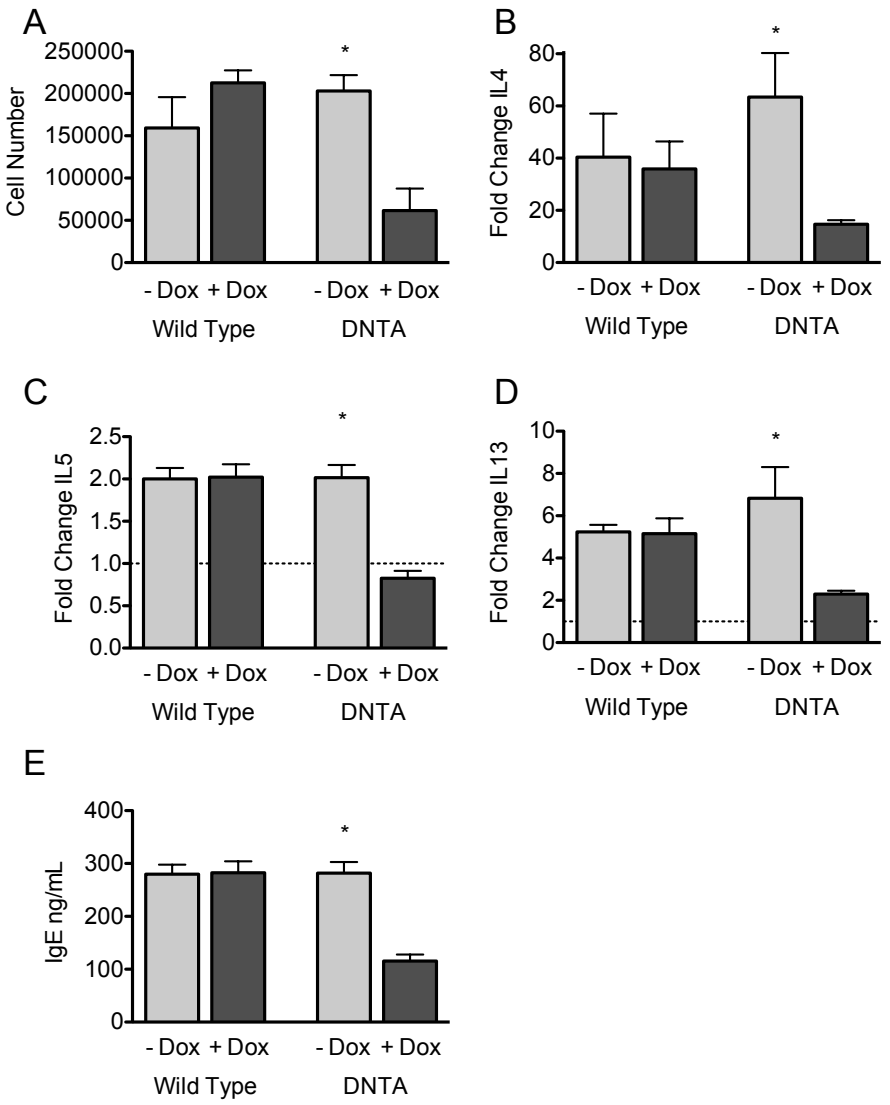

Figure 3-3. Airway epithelial cell NF-κB activity is required for chitin-induced sensitization to *Aspergillus* in the lung. WIld type or DNTA mice were sensitized to *Aspergillus* in the presence of chitin 2 days following addition of doxycycline (+Dox) or vehicle (-Dox) to drinking water (4-6 mice per group). **[A]** Eosinophils were enumerated from lung homogenates by flow cytometry. **[B]** IL4, **[C]** IL5, **[D]** IL13 expression levels were determined by real-time PCR from mRNA isolated from lung homogenates. **[E]** IgE was measured in serum by ELISA. Values are presented as mean +/- SEM, *P<0.05 +Dox vs -Dox.

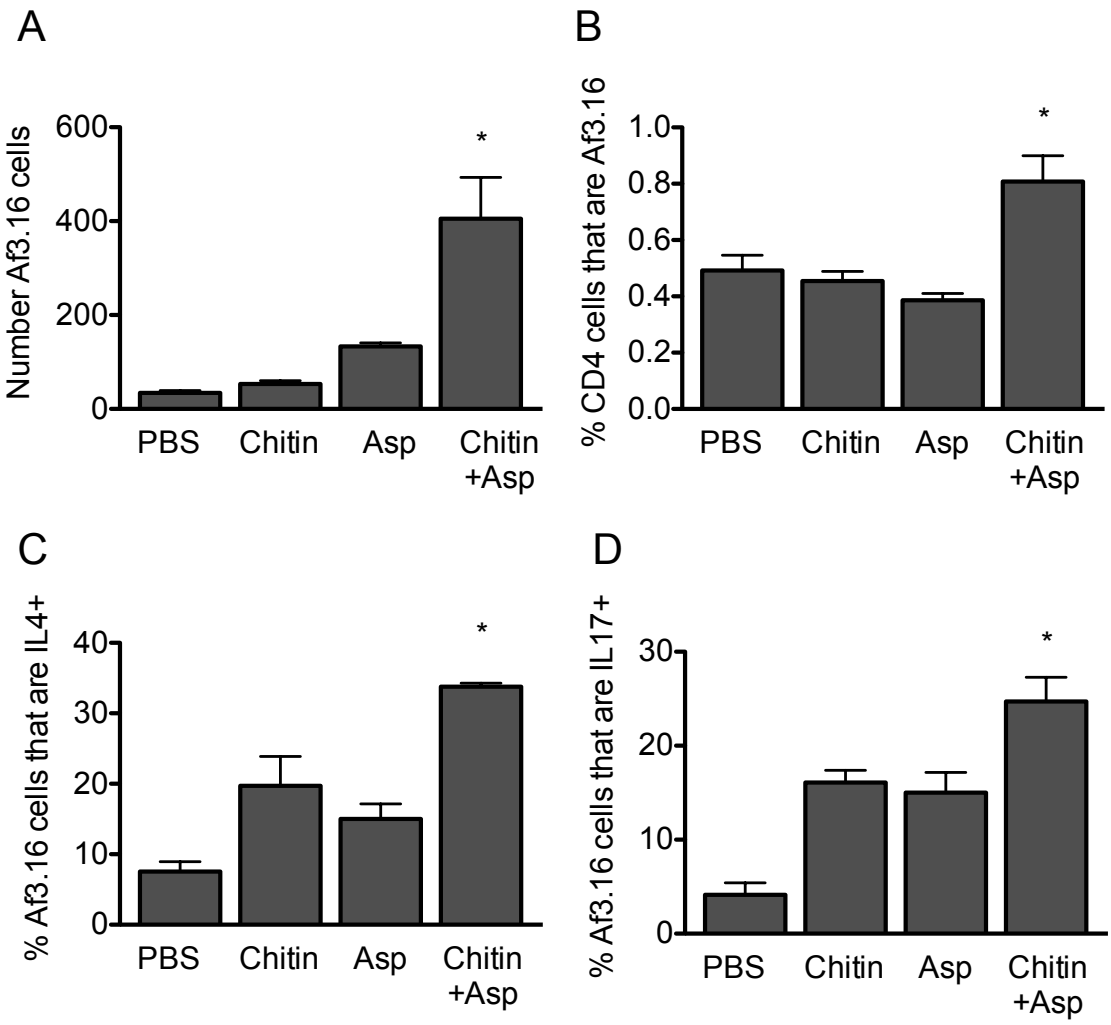

Figure 3-4. Chitin-dependent sensitization to *Aspergillus* promotes recruitment and Th2/Th17 polarization of *Aspergillus*-specific CD4+ T cells (Af 3.16 cells) in the lung. Mice were sensitized to *Aspergillus* in the presence or absence of chitin one day following the receipt of 10^6 Af 3.16 cells. **[A]** Thy 1.1+ CD4+ cells (Af 3.16 cells) were enumerated from lung homogenates by flow cytometry. **[B]** Frequency of Af 3.16 cells among CD4+ T cells in the lung. **[C]** Frequency of Af 3.16 cells producing IL4 in the lung. **[D]** Frequency of Af3.16 cells producing IL17A in the lung. Values are presented as mean +/- SEM, *P<0.05 vs PBS control.

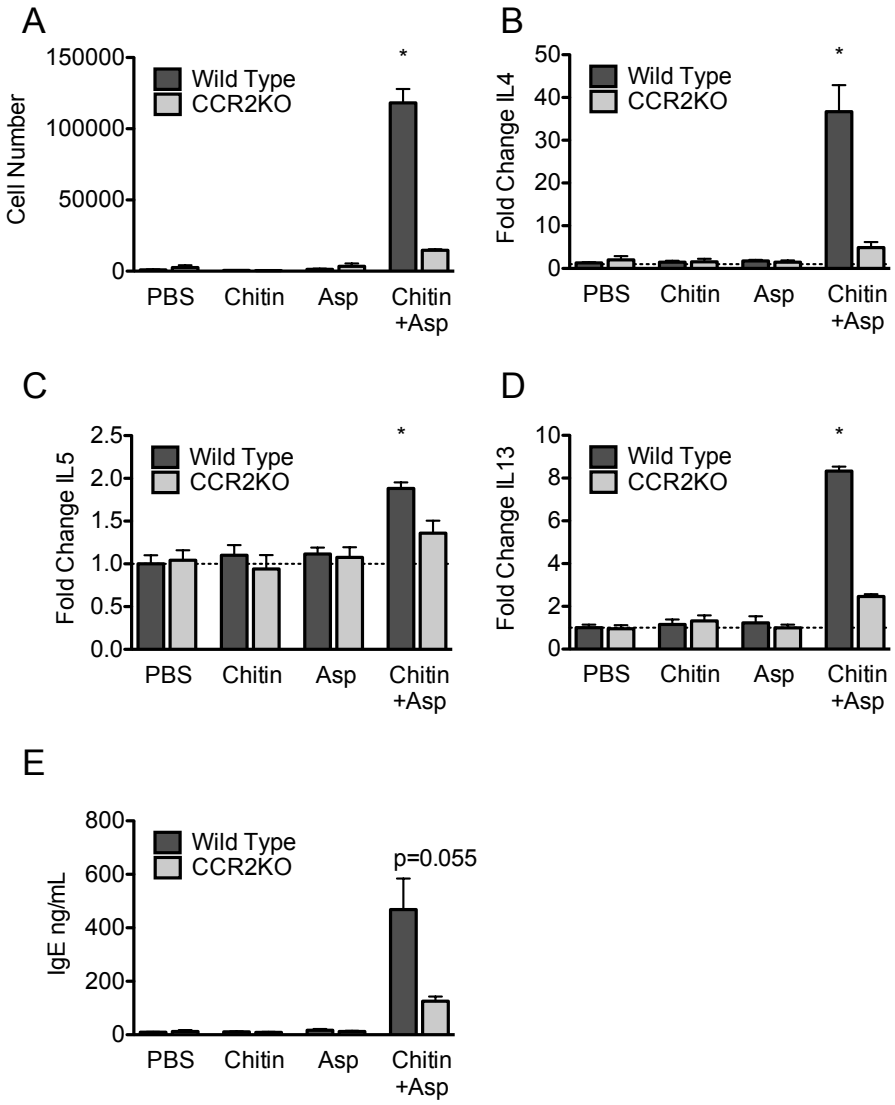

Figure 5. Chitin-dependent sensitization to *Aspergillus* requires CCR2 in the lung. Wild type or CCR2KO mice were sensitized to *Aspergillus* in the presence or absence of chitin (8 mice/group). **[A]** Eosinophils were enumerated from lung homogenates by flow cytometry. **[B]** IL4, **[C]** IL5, **[D]** IL13 expression levels were determined by real-time PCR from mRNA isolated from lung homogenates. **[E]** IgE was measured in serum by ELISA. Exact p-value of wild type vs. CCR2KO for mice sensitized to *Aspergillus* in the presence of chitin is indicated. Values are presented as mean +/- SEM, *P<0.05 wild type vs CCR2KO**.**

REFERENCES

1. van Leeuwen WS (1924) Bronchial Asthma in Relation to Climate. Proc R Soc Med 17: 19-26.

2. Agarwal R, Gupta D (2011) Severe asthma and fungi: current evidence. Med Mycol 49 Suppl 1: S150-7.

3. Kobayashi T, Iijima K, Radhakrishnan S, Mehta V, Vassallo R et al. (2009) Asthma-related environmental fungus, Alternaria, activates dendritic cells and produces potent Th2 adjuvant activity. J Immunol 182: 2502-2510.

4. Denning DW, O'Driscoll BR, Hogaboam CM, Bowyer P, Niven RM (2006) The link between fungi and severe asthma: a summary of the evidence. Eur Respir J 27: 615-626.

5. Kauffman HF, Tomee JF, van de Riet MA, Timmerman AJ, Borger P (2000) Protease-dependent activation of epithelial cells by fungal allergens leads to morphologic changes and cytokine production. J Allergy Clin Immunol 105: 1185-1193.

6. Brown GD, Gordon S (2001) Immune recognition. A new receptor for beta-glucans. Nature 413: 36-37.

7. Kheradmand F, Kiss A, Xu J, Lee SH, Kolattukudy PE et al. (2002) A protease-activated pathway underlying Th cell type 2 activation and allergic lung disease. J Immunol 169: 5904-5911.

8. Kiss A, Montes M, Susarla S, Jaensson EA, Drouin SM et al. (2007) A new mechanism regulating the initiation of allergic airway inflammation. J Allergy Clin Immunol 120: 334-342.

9. Guest GM, Momany M (2000) Analysis of cell wall sugars in the pathogen Aspergillus fumigatus and the saprophyte Aspergillus Nidulans. Mycologia 92: 1047-1052.

10. Reese TA, Liang HE, Tager AM, Luster AD, Van Rooijen N et al. (2007) Chitin induces accumulation in tissue of innate immune cells associated with allergy. Nature 447: 92-96.

11. Da Silva CA, Pochard P, Lee CG, Elias JA (2010) Chitin Particles are Multifaceted Immune Adjuvants. Am J Respir Crit Care Med 182: 1482-1491.

12. Van Dyken SJ, Garcia D, Porter P, Huang X, Quinlan PJ et al. (2011) Fungal chitin from asthma-associated home environments induces eosinophilic lung infiltration. J

Immunol 187: 2261-2267.

13. Dickey BF (2007) Exoskeletons and exhalation. N Engl J Med 357: 2082-2084.

14. Holgate ST, Roberts G, Arshad HS, Howarth PH, Davies DE (2009) The role of the airway epithelium and its interaction with environmental factors in asthma pathogenesis. Proc Am Thorac Soc 6: 655-659.

15. Fanning AS, Van Itallie CM, Anderson JM (2012) Zonula occludens-1 and -2 regulate apical cell structure and the zonula adherens cytoskeleton in polarized epithelia. Mol Biol Cell 23: 577-590.

16. Lambrecht BN, Hammad H (2010) The role of dendritic and epithelial cells as master regulators of allergic airway inflammation. Lancet 376: 835-843.

17. De Boer WI, Sharma HS, Baelemans SMI, Hoogsteden HC, Lambrecht BN et al. (2008) Altered expression of epithelial junctional proteins in atopic asthma: possible role in inflammation. Canadian journal of physiology and pharmacology 86: 105-112.

18. Xiao C, Puddicombe SM, Field S, Haywood J, Broughton-Head V et al. (2011) Defective epithelial barrier function in asthma. J Allergy Clin Immunol 128: 549-56.e1-12.

19. Roy RM, Wuthrich M, Klein BS (2012) Chitin elicites CCL2 from airway epithelial cells and induces CCR2-dependent innate allergic inflammation in the lung. J Immunol 189: In Press.

20. Perl AK, Tichelaar JW, Whitsett JA (2002) Conditional gene expression in the respiratory epithelium of the mouse. Transgenic Res 11: 21-29.

21. Cheng DS, Han W, Chen SM, Sherrill TP, Chont M et al. (2007) Airway epithelium controls lung inflammation and injury through the NF-kappa B pathway. J Immunol 178: 6504-6513.

22. Sadikot RT, Han W, Everhart MB, Zoia O, Peebles RS et al. (2003) Selective I kappa B kinase expression in airway epithelium generates neutrophilic lung inflammation. J Immunol 170: 1091-1098.

23. Rivera A, Ro G, Van Epps HL, Simpson T, Leiner I et al. (2006) Innate immune activation and CD4+ T cell priming during respiratory fungal infection. Immunity 25: 665-675.

24. Rayamajhi M, Redente EF, Condon TV, Gonzalez-Juarrero M, Riches DW et al. (2011) Non-surgical intratracheal instillation of mice with analysis of lungs and lung

draining lymph nodes by flow cytometry. J Vis Exp e2702.

25. Rozen S, Skaletsky H (2000) Primer3 on the WWW for general users and for biologist programmers. Methods Mol Biol 132: 365-386.

26. Schmittgen TD, Livak KJ (2008) Analyzing real-time PCR data by the comparative C(T) method. Nat Protoc 3: 1101-1108.

27. Blease K, Mehrad B, Lukacs NW, Kunkel SL, Standiford TJ et al. (2001) Antifungal and airway remodeling roles for murine monocyte chemoattractant protein-1/CCL2 during pulmonary exposure to Asperigillus fumigatus conidia. J Immunol 166: 1832-1842.

28. Samarasinghe AE, Hoselton SA, Schuh JM (2011) A comparison between intratracheal and inhalation delivery of Aspergillus fumigatus conidia in the development of fungal allergic asthma in C57BL/6 mice. Fungal Biol 115: 21-29.

29. Kogiso M, Nishiyama A, Shinohara T, Nakamura M, Mizoguchi E et al. (2011) Chitin particles induce size-dependent but carbohydrate-independent innate eosinophilia. J Leukoc Biol 90: 167-176.

30. Mayer AK, Bartz H, Fey F, Schmidt LM, Dalpke AH (2008) Airway epithelial cells modify immune responses by inducing an anti-inflammatory microenvironment. Eur J Immunol 38: 1689-1699.

31. Trompette A, Divanovic S, Visintin A, Blanchard C, Hegde RS et al. (2009) Allergenicity resulting from functional mimicry of a Toll-like receptor complex protein. Nature 457: 585-588.

32. Hammad H, Chieppa M, Perros F, Willart MA, Germain RN et al. (2009) House dust mite allergen induces asthma via Toll-like receptor 4 triggering of airway structural cells. Nat Med 15: 410-416.

33. Poynter ME, Cloots R, van Woerkom T, Butnor KJ, Vacek P et al. (2004) NF-kappa B activation in airways modulates allergic inflammation but not hyperresponsiveness. J Immunol 173: 7003-7009.

34. Ather JL, Hodgkins SR, Janssen-Heininger YM, Poynter ME (2011) Airway epithelial NF-kappaB activation promotes allergic sensitization to an innocuous inhaled antigen. Am J Respir Cell Mol Biol 44: 631-638.

35. Nakagome K, Matsushita S, Nagata M (2012) Neutrophilic inflammation in severe asthma. Int Arch Allergy Immunol 158 Suppl 1: 96-102.

36. Wilson RH, Whitehead GS, Nakano H, Free ME, Kolls JK et al. (2009) Allergic

sensitization through the airway primes Th17-dependent neutrophilia and airway hyperresponsiveness. Am J Respir Crit Care Med 180: 720-730.

37. Agarwal R, Nath A, Aggarwal AN, Gupta D, Chakrabarti A (2010) Aspergillus hypersensitivity and allergic bronchopulmonary aspergillosis in patients with acute severe asthma in a respiratory intensive care unit in North India. Mycoses 53: 138-143.

38. Blease K, Mehrad B, Standiford TJ, Lukacs NW, Gosling J et al. (2000) Enhanced pulmonary allergic responses to Aspergillus in CCR2-/- mice. J Immunol 165: 2603-2611.

39. Koth LL, Rodriguez MW, Bernstein XL, Chan S, Huang X et al. (2004) Aspergillus antigen induces robust Th2 cytokine production, inflammation, airway hyperreactivity and fibrosis in the absence of MCP-1 or CCR2. Respir Res 5: 12.

40. Szymczak WA, Deepe GSJ (2009) The CCL7-CCL2-CCR2 axis regulates IL-4 production in lungs and fungal immunity. J Immunol 183: 1964-1974.

41. Traynor TR, Kuziel WA, Toews GB, Huffnagle GB (2000) CCR2 expression determines T1 versus T2 polarization during pulmonary Cryptococcus neoformans infection. J Immunol 164: 2021-2027.

42. Sato N, Ahuja SK, Quinones M, Kostecki V, Reddick RL et al. (2000) CC chemokine receptor (CCR)2 is required for langerhans cell migration and localization of T helper cell type 1 (Th1)-inducing dendritic cells. Absence of CCR2 shifts the Leishmania major-resistant phenotype to a susceptible state dominated by Th2 cytokines, b cell outgrowth, and sustained neutrophilic inflammation. J Exp Med 192: 205-218.

43. Campbell EM, Charo IF, Kunkel SL, Strieter RM, Boring L et al. (1999) Monocyte chemoattractant protein-1 mediates cockroach allergen-induced bronchial hyperreactivity in normal but not CCR2-/- mice: the role of mast cells. J Immunol 163: 2160-2167.

44. Mellado M, Martin de Ana A, Gomez L, Martinez C, Rodriguez-Frade JM (2008) Chemokine receptor 2 blockade prevents asthma in a cynomolgus monkey model. J Pharmacol Exp Ther 324: 769-775.

45. Provoost S, Maes T, Joos GF, Tournoy KG (2012) Monocyte-derived dendritic cell recruitment and allergic T(H)2 responses after exposure to diesel particles are CCR2 dependent. J Allergy Clin Immunol 129: 483-491.

Chapter 4

Chitin dependent allergic sensitization to *Aspergillus fumigatus* but not chitin induced innate allergic inflammation requires C3 and C3aR

René M. Roy, Hugo C. Paes, Marcel Wüthrich, and Bruce S. Klein

ABSTRACT

Levels of the anaphylatoxin C3a are increased in patients with asthma compared with non-asthmatics and increase further still during asthma exacerbations. However, the role of C3a during sensitization to allergen is relatively unstudied. Sensitization to fungal allergens, such as *Aspergillus fumigatus*, is a strong risk factor for the development of asthma. Exposure to chitin, a structural polysaccharide of the fungal cell wall, induces innate allergic inflammation and may promote sensitization to fungal allergens. Coincubation of serum with chitin or intratracheal administration of chitin resulted in the generation of C3a. We next developed a model of chitin-dependent sensitization to soluble *Aspergillus* antigens to test the ability of chitin to promote allergic sensitization. Using C3KO and C3aRKO mice, we examined the role of complement activation in chitin-dependent allergic sensitization. Analysis of lung homogenates from mice sensitized to *Aspergillus* in the presence of chitin revealed that C3 and C3aR mice were protected from chitin dependent sensitization to *Aspergillus*. To investigate the mechanism of protection in complement deficient mice, we analyzed costimulatory marker expression on dendritic cell subsets in the lung. Dendritic cells from complement deficient mice had a tolerogenic profile after chitin exposure compared with dendritic cells from wild type mice. Taken together, our data suggest that chitin dependent sensitization to *Aspergillus* antigen depends on C3a mediated suppression of regulatory dendritic cells in the lung and that chitin itself directly generates C3a in the lung.

INTRODUCTION

Environmental exposure to molds, such as *Aspergillus fumigatus*, are correlated with an increased risk of asthma. Moreover, in patients with severe acute onset asthma, more than half are hypersensitive to *Aspergillus* [1]. In addition, detection of *Aspergillus* in sputum culture and IgE sensitization to *Aspergillus* are predictive for poor lung function in patients with asthma [2]. Following the inhalation of conidia or hyphae, sensitization to *Aspergillus* is mediated by fungal proteases that cleave and activate protease activated receptors (PAR) and by fungal wall components that activate pattern recognition receptors (PRR) on structural and hematopoeitic cells in the lung [3,4]. These diverse signals generated upon exposure to *Aspergillus* drive the Th2 adaptive response in individuals with asthma.

Integrating the signals generated in the lung following exposure to *Aspergillus* are the dendritic cells (DC). Immature DC line the airways and parenchyma of the lung and consist of plasmacytoid DC (pDC), CD11b+ DC, and CD103+ DC [5,6]. In the absence of robust stimulation via PRR or cytokines, inhaled antigen taken up by DC induces tolerance by promoting the development of regulatory T cells (Treg) [7]. On the other hand, exposure to an antigen in the context of another inflammatory stimulus such as LPS, enhances the ability of DC to migrate from the lung to the lymph node [8] and upregulates costimulatory molecules [9] leading to the priming of effector T cells. The presence of inflammation also recruits $Ly6C^{hi}$ monocytes to the lung which differentiate into inflammatory or monocyte-derived DC [10] which can also prime effector T cells. DC subsets vary in their ability to instruct T cell polarization and the ultimate outcome of the DC-T cell interaction is dependent on the presented antigen, the tissue microenvironment, including cytokine and chemokine levels, and the interaction of costimulatory molecules on the DC and T cells. During sensitization to allergen in the

lung, DC can be activated directly via PRR [11] or indirectly via PRR activation on lung stromal cells [12]. This activation results in the maturation of dendritic cells (DC) characterized by increased expression of CD80, CD86, CD273 (B7-DC or PD-L2), and CD274 (B7-H1 or PD-L1) [13]. Thus, DC are able to modulate and direct inflammation in the lung following antigen exposure by influencing the balance between tolerance and inflammation.

In coordination with DC, the complement system also critically maintains the balance between tolerance and inflammation in the lung. The complement system is an evolutionarily ancient protein cascade of the animal immune system that augments innate immune function by opsonizing targeted surfaces, modifying pathogenic or damaged cell surfaces to promote lysis, and recruiting innate effector cells to the site of inflammation [14]. Complement factor 3 (C3) is the lynchpin of the complement cascade and the initial cleavage of C3 produces the anaphylatoxin C3a and a larger fragment, C3b. C3a mediates its effects via its receptor, C3aR, which is expressed on lymphoid and myeloid cells [15] and on pulmonary epithelial and smooth muscle cells [16]. On DC, engagement of C3aR leads to cAMP-dependent increased antigen uptake and augments the ability of DC to promote T cell polarization [17]. Thus C3a is well suited to act on lung parenchymal cells as well as lung-resident and recruited immune cells to direct the immune response to encountered antigen.

Chitin is a ubiquitous polysaccharide common to the cell walls of fungi including *Aspergillus* [18]. Upon exposure, chitin triggers responses from organisms across the kingdoms of life identifying it as an evolutionarily conserved and stimulatory molecular pattern [19-22]. In the lung, chitin exposure promotes innate allergic inflammation that is characterized by alternatively activated macrophages, eosinophilia, and neutrophilia [21,22]. Following intraperitoneal injection of chitin particles with the model antigen ovalbumin, chitin can also serve as an adjuvant that drives polarization of CD4+ T cells

into Th1, Th2, and Th17 cells [23]. However, whether chitin can serve as an adjuvant to promote allergic inflammation and sensitization in the lung is unknown. Since many inhaled allergens of insect or fungal origin contain chitin [24,25], understanding the mechanism of chitin induced allergic inflammation in the lung is relevant to understanding allergic sensitization in asthma.

In the present study, we sought to determine whether chitin-induced allergic inflammation is dependent on C3 and C3aR signaling in the lung and to evaluate the impact of chitin administration on the maturation of DC in the lung during sensitization to *Aspergillus* antigens. We demonstrate that chitin activates complement and that C3 and C3aR mediate adaptive allergic inflammation in a model of chitin-induced allergy to *Aspergillus* via modulation of DC function in the lung.

MATERIALS AND METHODS

Mice

C3aR knockout (stock# 005712), C3 knockout (stock# 003641) mice, aged 5-8 weeks were obtained from The Jackson Laboratory (Bar Harbor, ME). C57BL/6 wild type mice (strain code 01C55), and BALB/c wild type mice (strain code 01B05) aged 5-8 weeks, were obtained from NCI (Frederick, MD). For all experiments, five mice were used per group. Mice were housed and cared for according guidelines from the University of Wisconsin Animal Care and Use Committee, who approved this work.

Reagents

Chitin purified from crab shells was purchased from Sigma (C9752) and was purified as previously described [22]. *Aspergillus fumigatus* antigens were obtained via the University of Wisconsin Hospital Pharmacy from Greer (M3 Skin Test Vial). Prior to use, *Aspergillus* antigens were dried by SpeedVac and reconstituted at 10mg/mL in sterile PBS.

Measurement of C3a

Whole blood was obtained from healthy human volunteers or from C57BL/6 mice and mixed with heparin to prevent clotting. Following centrifugation, plasma was incubated for 1 hour with chitin particles, *Aspergillus* antigens, with blocking antibodies to C1q or Factor B as indicated.

Following exposure to chitin, C3a levels in plasma or in lung homogenate were determined by ELISA. Prior to lung homogenization, the pulmonary vasculature was perfused with 5mL PBS via the right ventricle to minimize blood in the homogenate. The human C3a ELISA was obtained from Hycult Biotech and the mouse C3a ELISA was obtained from BD Bioscience.

Administration of Chitin / *Aspergillus* antigens

Mice were anesthetized via inhalation of isoflurane. The anesthetized mouse was then

suspended from their front incisors and intubated using a BioLite Intubation System [26]. Chitin particles were suspended at 10mg/mL in PBS. 20μL of PBS, chitin particles, *Aspergillus* antigens, or chitin particles plus *Aspergillus* antigens were administered via the intubation tube into the airway. For sensitization, *Aspergillus* antigens in the presence or absence of chitin were administered every four days for five exposures and mice were euthanized two days following the final exposure.

Flow Cytometry

Lung cell suspensions were prepared by mincing lungs through a 70μm filter using a 3mL syringe plunger. The resulting homogenate was digested with Liberase/DNAse I and the red blood cells were lysed with ammonium chloride/potassium bicarbonate buffer. All samples were blocked with anti-mouse CD16/32 antibody prior to staining with fluorochrome-conjugated antibodies. Events were gated on FSC/SSC parameters to exclude debris and on live cells based on Violet Fixable Live-Dead stain (Molecular Probes). Eosinophils were defined as Siglec F^{hi} $CD11b^{+}$ SSC^{hi} $CD11c^{-}$ $Ly6G^{-}$ $Thy1^{-}$. Neutrophils were defined as $CD11b^{+}$ SSC^{hi} $CD11c^{-}$ $Ly6G^{+}$ $Thy1^{-}$. Plasmacytoid DC were defined as CD11b+ $CD11c^{dim}$ CD62L+ SiglecH+. CD11b+ DC were defined as CD11b+ CD11c+ Ly6C-. CD103+ DC were defined as CD103+ CD11b- CD11c+ Langerin+. Inflammatory DC were defined as CD11b+ CD11c+ Ly6C+. Antibodies were obtained from BD Biosciences, eBioscience, and Biolegend. Cells were collected for analysis on a BD Biosciences LSRII cytometer and data analyzed with FloJo software (Tree Star).

Real-Time PCR

Total RNA was isolated from lung homogenates using a Qiagen RNeasy mini kit and cDNA was prepared using the BioRad iScript cDNA synthesis kit. cDNA was amplified using BioRad SSoFast EvaGreen Supermix in a BioRad MyIQ Real Time PCR detection system. Primers were designed using Primer-BLAST [27]. Relative transcript quantity was calculated using the comparative Ct method with β-actin transcript as the

control transcript [28].

Statistics

Samples were compared to control using an unpaired t-test with a two-tailed p-value < 0.05 considered statistically significant. All statistical analysis was performed using Prism software (Graph Pad). In all figures, error bars represent the standard deviation of the data.

RESULTS

Chitin activates complement in vitro and in vivo

To investigate whether chitin particles are able to activate complement directly, we measured the production of the anaphylatoxin C3a in chitin-exposed human serum. Chitin particles induced the production of C3a in human serum (Fig 1A) and mouse serum (Fig 1B). Because chitin is a surface component of various pathogens such as fungi, parasite cysts, and helminth eggs, activation of complement could proceed via the antibody-mediated classical pathway or the antibody independent alternative pathway. In addition to antibodies potentially generated by exposure to environmental sources of chitin, natural IgM antibodies to chitin have been described in animals across the evolutionary spectrum [29]. To delineate the mechanism of chitin-induced complement activation we added chitin to serum in the presence of neutralizing antibody against C1q to block the classical activation pathway or against Factor B to block the alternative complement activation pathway. Neutralizing antibodies to Factor B but not to C1q blocked the activation of complement by chitin particles in serum suggesting that the major route of complement activation by chitin is via the alternative pathway (Fig 1C).

To determine if chitin could activate complement in the lung, we assayed lung homogenates from naive and chitin exposed mice for the presence of C3a by ELISA. Lung homogenate from chitin exposed mice had significantly more C3a than naive mice lung homogenates (Fig 1D). Thus chitin promotes C3a generation in vitro and in vivo in the lung.

A model of chitin dependent sensitization to *Aspergillus* antigens

We have established a model of chitin-dependent sensitization to allergen utilizing soluble *Aspergillus* proteins (unpublished observations and below), which can be important in the development of allergic asthma [30]. Protease allergens from *Aspergillus* possess the ability to cleave C3 directly [31,32] and could conceivably drive

complement activation. We therefore tested whether the soluble *Aspergillus* protein antigens themselves could activate complement directly. Incubation of serum with *Aspergillus* antigens before or after heat-treatment (to neutralize potential protease activity) failed to result in the production of C3a (Fig 2A). Thus, soluble *Aspergillus* antigens alone lack the ability to generate C3a *in vitro*.

Chitin-induced allergic sensitization is C3-C3a dependent

Aspergillus antigens alone fail to induce markers of allergic inflammation in the lung, whereas mice exposed to chitin particles during sensitization to *Aspergillu*s demonstrate increased pulmonary eosinophilia (Fig 2B). Furthermore, mice sensitized in the presence of chitin, had increased serum IgE levels and increased expression of the allergy associated cytokines IL-4, IL-5 and, IL-13 in lung homogenates compared with naive, chitin-exposed or *Aspergillus* antigen alone exposed mice (Fig 2B). Thus, chitin acts as an adjuvant during *Aspergillus* induced allergic sensitization.

Becasue chitin can activate complement we tested whether complement was required for chitin-dependent allergic inflammation. C3KO mice were protected against allergic sensitization in this model exhibiting lower pulmonary eosinophilia, reduced expression of IL-4, IL-5, and IL-13, and lower levels of serum IgE (Fig 2B). To test whether the anaphylotoxin C3a was required for chitin-induced allergic inflammation to *Aspergillus* antigens, we sensitized wild-type and C3aRKO mice to *Aspergillus* in the presense or absence of chitin. Mirroring the results from C3KO mice, C3aRKO mice had reduced pulmonary eosinophilia, lower IL-4, IL-5 and IL-13 expression in the lung, and lower serum IgE levels than wild type mice (Fig 2C). Thus, the ability of chitin particles to promote sensitization to *Aspergillus and* adaptive allergic inflammation is dependent on C3 and signalling via C3aR.

Chitin-induced innate allergic inflammation is not dependent on C3 or C3aR

Because chitin can induce innate allergic inflammation characterized by alternatively activated macrophages and recruitment of eosinophils, we tested whether C3 or signaling via C3aR was required for chitin induced innate allergic inflammation. Forty-eight hours following chitin exposure, we compared the expression of the macrophage alternative activation marker Arginase I in lung homognates from wild type, C3KO, and C3aRKO mice. Neither C3KO mice nor C3aRKO mice demonstrated a defect in chitin induced alternative activation of macrophages as measured by Arginase I expression (Fig 3A). We also quantified the recruitment of SiglecF+/CD11c- eosinophils to the lung following chitin exposure. Eosinophil recruitment in C3KO or C3aRKO mice was not different than wild type mice following chitin exposure (Fig 3B). Severe asthma and allergic bronchopulmonary aspergillosis (ABPA) are associated with airway neutrophilia [33-35] as is exposure to chitin [21,22]. Following exposure to chitin, wild type, C3, and C3aR mice did not demonstrate a difference in recruited neutrophils in the lung (Fig 3C). Therefore, C3 or signaling via C3aR are not required for chitin induced innate pulmonary eosinophilia, neutrophilia or alternative activation of macrophages.

C3/C3aR signaling blocks lung DC from acquiring a tolerogenic phenotype following chitin exposure

DC play a critical role in shaping the adaptive immune response to antigen. Since C3KO and C3aRKO mice failed to mount a robust allergic response to *Aspergillus* antigens in the presence of chitin, we tested whether chitin exposure modulated DC maturation in a C3 and C3aR dependent fashion. The failure to mount an allergic response to *Aspergillus* in the presence of chitin could be the result of either a reduction in the ability of DC to stimulate T cells or an increase in the ability of DC to suppress T cell activation. In the lung, pDC promote tolerance to inhaled antigen by suppressing effector T cells and promoting regulatory T cells [36] a process that depends on the expression of CD273 and CD274 [37]. Upon exposure to chitin, pDC in the lungs of wild

type mice failed to upregulate CD273 or CD274 (Fig 4A, 4B). However, pDC from chitin-exposed C3KO mice and C3aRKO mice significantly increased expression of CD273 and CD274 (Fig 4A, 4B). Tolerance to antigen is correlated with an elevated ratio of CD274 to CD86 expression on plasmacytoid DC [38]. Following exposure to chitin, pDC from C3KO and C3aRKO mice had a significantly increased CD274/CD86 expression ratio whereas pDC from wild type mice did not (Fig 4C). These data suggest that pDC from chitin-exposed C3KO and C3aRKO mice acquire a tolerogenic phenotype whereas pDC from wild type mice fail to acquire a tolerogenic phenotype.

Chitin promotes robust CD80/CD86 activation on CD11b+ and inflammatory DC subsets in the lung

We next tested whether C3 or C3aR signaling also promoted the activation of myeloid DC subsets in the lung by measuring the surface expression of the co-stimulatory molecules CD80 and CD86 on CD11b+, CD103+, and inflammatory DC 48 hours following chitin exposure. Chitin exposure failed to increase CD80 or CD86 expression on CD103+ DC from wild type, C3KO, or C3aRKO mice (data not shown). Resident CD11b+ DC upregulated CD80 and CD86 expression following chitin exposure as did monocyte-derived inflammatory DC (Fig 5A, 5B). The upregulation of CD80 and CD86 on CD11b+ DC and inflammatory DC was equivalent in wild type, C3KO, and C3aRKO mice (Fig 5A, 5B). These data suggest that chitin exposure induces the maturation of certain myeloid DC subsets in the lung in a C3- and C3aR-independent manner.

DISCUSSION

The fungal cell wall contains a variety of carbohydrate polymers that are recognized by the mammalian immune system and that shape the ultimate immune response. Exposure to chitin particles triggers innate allergic inflammation however the role of chitin in promoting allergic sensitization in the lung is unknown. We developed our model to test whether chitin particles could promote allergic sensitization to *Aspergillus* antigens and to assess the role of C3 in chitin dependent allergic sensitization. Our study further establishes that exposure to chitin particles promotes allergic inflammation in the lung. Furthermore, we demonstrate that chitin exposure impacts the maturation of DC in the lung and promotes the development of allergic sensitization to *Aspergillus* antigens. Finally, we establish a role for C3, the central component of the complement cascade, and the anaphylatoxin receptor C3aR in mediating chitin-dependent allergic sensitization in the lung.

The ability of chitin to generate C3a in the lung and to promote C3aR dependent allergic inflammation has relevance for human disease, particularly asthma. Polymorphisms in C3 and C3aR are linked to an increased risk of asthma [39] and in individuals with asthma exacerbations, plasma concentrations of C3a rise and higher C3a levels are associated with increased hospitalizations [40]. Other environmental exposures linked to asthma such as ozone, diesel exhaust, and cigarette smoke, also generate C3a, and drive airway pathology [41-43]. Our study demonstrates that environmental exposure to chitin particles also triggers the production of C3a via the alternative pathway potentially linking chitin exposure to the development of allergic airway pathology. While chitin particles can generate C3a directly in plasma, the elevated C3a levels we observed in the lung following chitin exposure could proceed by one of two pathways both of which are physiologically relevant. First, chitin particles could activate C3 already present in the lung via the alternative pathway (as with

plasma) or trigger additional C3 production from lung resident cells. Second, because chitin particles trigger robust innate inflammation, plasma proteins from the blood could leak across into the inflamed airways. C3 present in the plasma could then be activated by chitin particles via the alternative pathway or via the activation of thrombin in the setting of inflammation [44]. In each case, exposure to chitin particles results in an increase in C3a in the lung which can drive allergic sensitization and inflammation [45].

Consistent with a role for C3a in the pathophysiology of allergic inflammation, we found that C3KO and C3aRKO mice were protected against chitin-dependent sensitization to *Aspergillus* antigens. Our results agree with previous studies using C3KO or C3aRKO mice which found protection against pulmonary eosinophilia, elevated Th2 cytokines, and elevated IgE in response to ambient particulate matter, house dust mite, or the model antigen ovalbumin [41,46,47]. While blockade of C3a or C3aR protects the airways from allergic inflammation following challenge with an allergen, less is known about the role of C3a in the sensitization to allergen. Upon engagement of C3aR by C3a, DC demonstrate an increase in the ability to phagocytose antigen and to activate T cells [17]. Furthermore, C3aR signaling leads to reduced expression of C5aR on the surface of DC [37] shifting DC from a C5aR-dependent tolerogenic phenotype toward an activated phenotype capable of promoting Th2 cytokine production from T cells. Our results demonstrate that in the absence of C3 or C3aR, chitin exposure promotes the expression of the regulatory co-stimulatory molecules CD273 and CD274 on pDC. This suggests that production of C3a following chitin exposure helps to suppress the expression of the regulatory molecules CD273 and CD274, thereby promoting the sensitization to *Aspergillus* antigen.

While clearly impacting adaptive immune responses, the absence of C3 or C3aR had no impact on innate allergic inflammation or the expression of the co-stimulatory markers on myeloid DC following chitin administration. C3a mediates the adhesion of

eosinophils to the walls of postcapillary venules but is unable to affect transmigration in vivo whereas C5a can mediate adhesion and transmigration [48]. In addition, chitin induced eosinophilia has been shown to be dependent on CCR2 [22] and LTB4 [21] which likely represent complement independent eosinophil recruitment pathways. Furthermore, chitin particles trigger cytokine production in vitro in experiments using complement inactivated serum which argues against a role for complement in innate immune responses to chitin [22,49]. While myeloid DC in the lung expressed the co-stimulatory markers CD80 and CD86 in the absence of C3 and C3aR, C3KO and C3aRKO mice had abundant CD273 and CD274 expression on pDC. CD273 and CD274 expressing pDC suppress the ability of myeloid DC to activate T cells [37,45]. This may explain why C3KO and C3aRKO mice were protected against chitin-induced allergic sensitization to *Aspergillus* antigens.

Preparations of chitin vary widely between studies of allergic inflammation, and may impact the results and conclusions of studies. Our work was done with commercial preparations of chitin that were acid extracted to remove impurities [22]. They were tested to ensure limited residual protein and endotoxin contamination. Though there may be impurities beyond pure N-acetyl glucosamine that could influence our results, and the role of complement in the events studied, we believe that our results may mimic the mix of material in chitin from environmental sources. For example, chitin inhaled along with environmental allergens is not likely to represent purified N-acetyl glucosamine. Thus, while we cannot exclude a role for other constituents in complement activation, we feel our results reasonably model the role of complement in *Aspergillus* sensitization that occurs when allergens are inhaled with chitin as adjuvant.

In conclusion, our study demonstrates that chitin exposure can promote allergic sensitization to *Aspergillus* antigens. Furthermore, we add chitin particles to the list of environmental insults that can generate C3a in the lung and link C3a generation to the

ability of chitin to promote allergic inflammation. Finally, we suggest that chitin exposure modulates co-stimulatory molecule expression on lung DC subsets in order to potentiate allergic responses. These results illuminate the potential role of complement in mediating chitin-dependent allergic sensitization.

ACKNOWLEDGEMENTS

We thank Marlene Klaila and Titilayo Omobesi for excellent animal care and Dr. Jenny Gumperz and Dr. Subramanya Hegde for assistance in obtaining human blood samples.

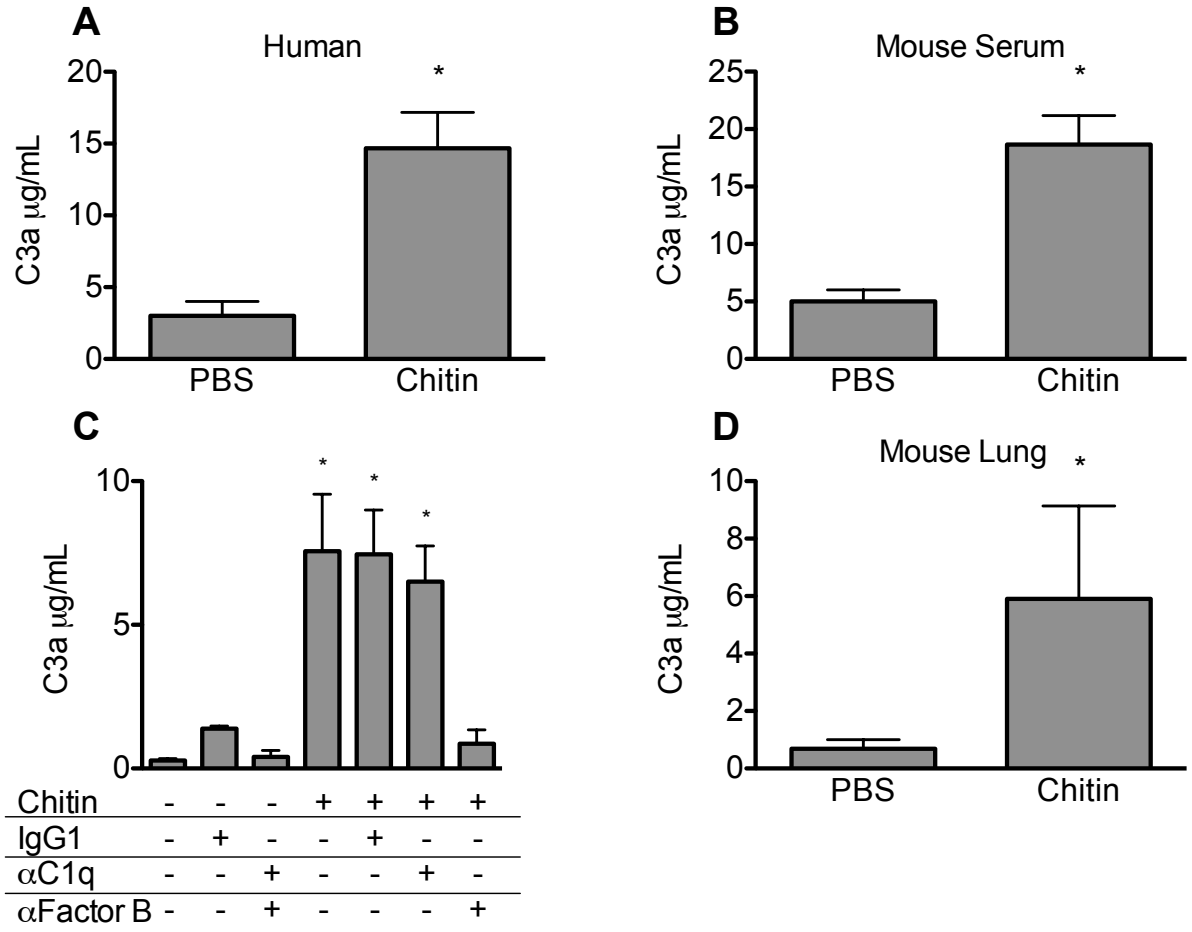

Figure 4-1. Chitin particles generate C3a in vivo and via the alternative pathway in vitro. Chitin particles or Aspergillus antigens were co-incubated with plasma and neutralizing antibodies; C3a levels were determined by ELISA. **[A]** Chitin induced C3a generation in human plasma (n=3); **[B]** in mouse plasma (n=3). **[C]** Chitin induces C3a generation in human plasma via the alternative pathway, IgG1=isotype control Ab, αC1q=C1q neutralizing Ab, αFactorB=Factor B neutralizing Ab (n=3). **[D]** Chitin particles or PBS was administered i.t. Following overnight incubation, perfused lung homogenate was obtained and C3a levels were determined by ELISA (n=5). Values are presented as mean +/- SEM, *P<0.05 vs PBS.

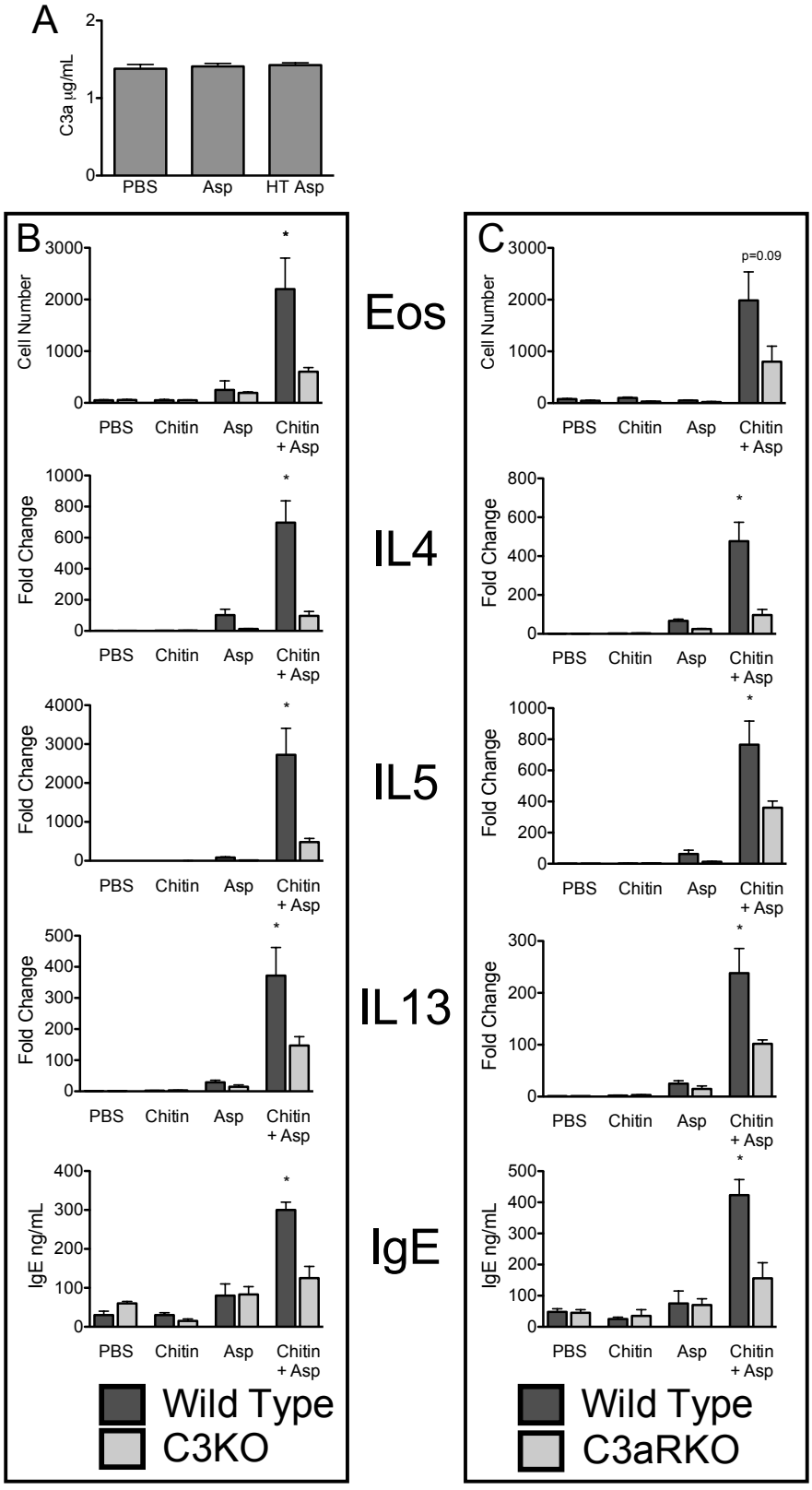
A
C3a µg/mL
PBS
Asp
HT Asp
B
C
Eos
IL4
IL5
IL13
IgE
Cell Number
Fold Change
IgE ng/mL
PBS
Chitin
Asp
Chitin + Asp
p=0.09
Wild Type
C3KO
C3aRKO

Figure 4-2. Chitin promotes C3- and C3aR-dependent allergic inflammation to *Aspergillus* antigens. [A] Aspergillus antigens fail to generate C3a in human plasma, HT Asp=heat-treated aspergillus antigens, (n=3). Values are presented as mean +/- SEM, *P<0.05 vs PBS. Wild type, C3KO, and C3aRKO were sensitized to *Aspergillus* as described in the Methods. **[B]** C3KO mice vs. wild type (n=5). **[C]** C3aRKO mice vs. wild type (n=5). Eosinophils were enumerated from lung homogenates by flow cytometry. IL4, IL5, and IL13 expression levels were determined by real-time PCR from mRNA isolated from lung homogenates. IgE was measured in serum by ELISA. Values are presented as mean +/- SEM, *P<0.05 wild type vs respective KO.

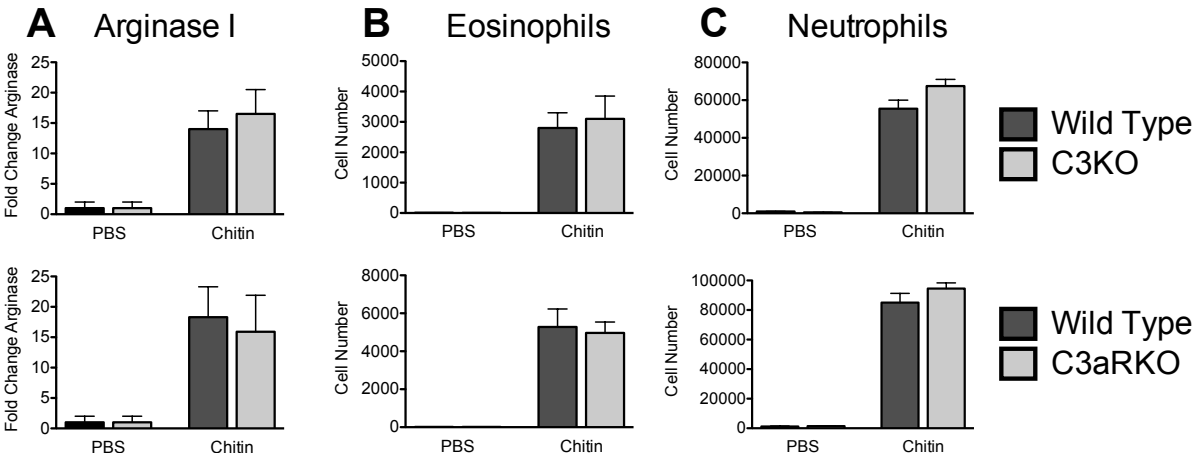

Figure 4-3. Chitin induced innate allergic inflammation is not C3- or C3aR-dependent. 48 hours following chitin exposure, lung homogenates were obtained. **[A]** Arginase I expression was determined by realtime PCR (n=5). Values are presented as mean fold change in arginase expression relative to PBS +/- SEM **[B]** Eosinophils and **[C]** neutrophils were enumerated from lung homogenates by flow cytometry (n=5). Values are presented as mean +/- SEM.

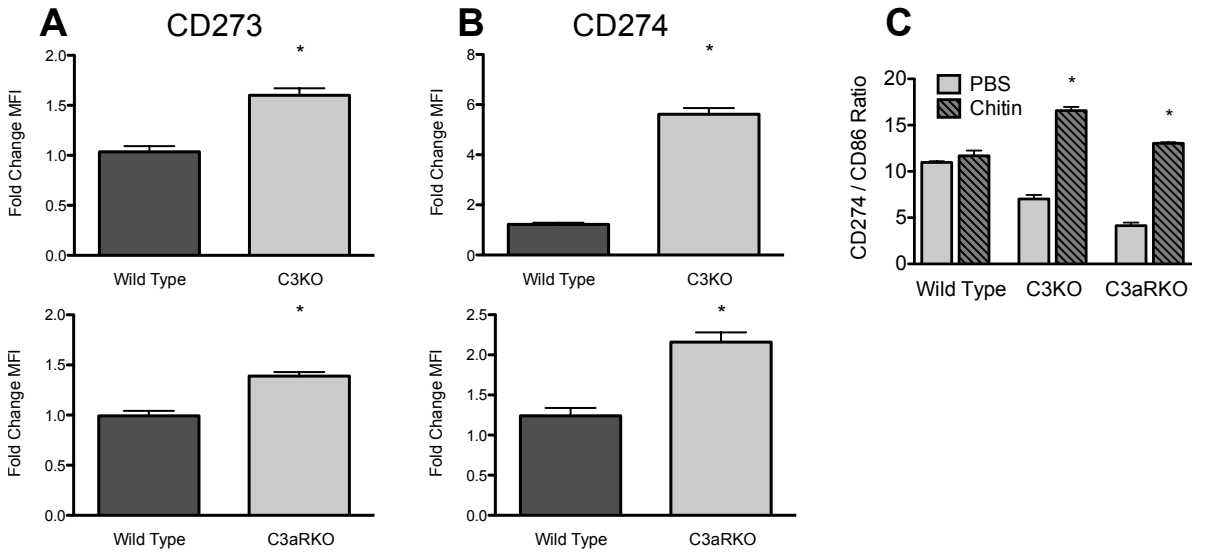

Figure 4-4. Chitin induced a tolerogenic phenotype on lung pDC in the absence of C3 and C3aR. 48 hours following chitin exposure, lung homogenates were obtained and the expression of CD273, CD274, and CD86 on pDC was determined by flow cytometry. pDC were defined as CD11b+, CD11clow, CD62L+, Siglec H+. **[A]** Expression of CD273 on lung pDC (n=5). Values are mean fold change +/- SEM of the mean fluorescent intensity (MFI) of chitin exposed mice vs. PBS exposed mice. *P<0.05 KO vs. wild type. **[B]** Expression of CD274 on lung pDC (n=5). Values are mean fold change +/- SEM of the MFI of chitin exposed mice vs. PBS exposed mice. *P<0.05 KO vs. wild type. **[C]** The tolerogenic phenotype of pDC in the absence of C3 and C3aR. Values are the ratio +/- SEM between the MFI of CD274 and the MFI of CD86 on lung pDC. *P<0.05 chitin vs PBS.

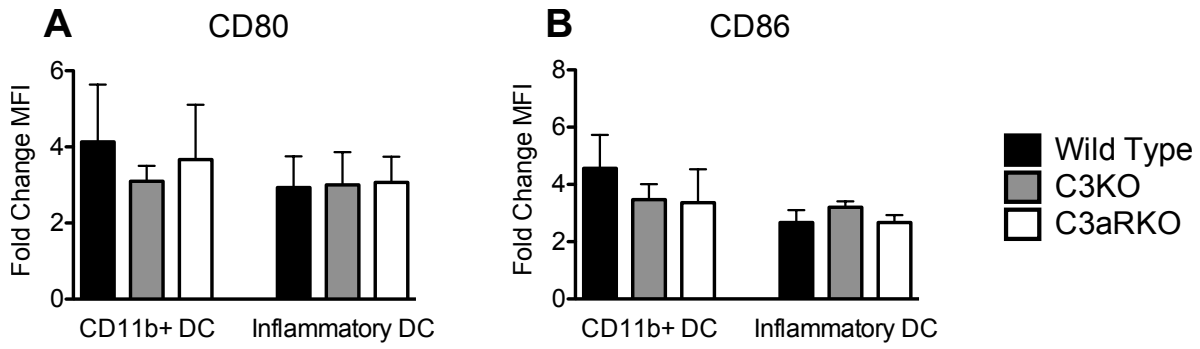

Figure 4-5. Chitin induced CD80 and CD86 expression on pulmonary myeloid DC is not C3- or C3aR-dependent.

48 hours following chitin exposure, lung homogenates were obtained and the expression of CD80 and CD86 on myeloid DC subsets was determined by flow cytometry. CD11b+ DC were defined as CD11b+ CD11c+ Ly6C- CD103-. Inflammatory DC were defined as CD11b+ CD11c+ Ly6C+. **[A]** Expression of CD80 on lung CD11b+ and inflammatory DC (n=5). Values are mean fold change +/- SEM of the mean fluorescent intensity (MFI) of chitin exposed mice vs. PBS exposed mice. **[B]** Expression of CD86 on lung CD11b+ and inflammatory DC (n=5). Values are mean fold change +/- SEM of the mean fluorescent intensity (MFI) of chitin exposed mice vs. PBS exposed mice.

REFERENCES

1. Agarwal R, Nath A, Aggarwal AN, Gupta D, Chakrabarti A (2010) Aspergillus hypersensitivity and allergic bronchopulmonary aspergillosis in patients with acute severe asthma in a respiratory intensive care unit in North India. Mycoses 53: 138-143.

2. Fairs A, Agbetile J, Hargadon B, Bourne M, Monteiro WR et al. (2010) IgE sensitization to Aspergillus fumigatus is associated with reduced lung function in asthma. Am J Respir Crit Care Med 182: 1362-1368.

3. Kheradmand F, Kiss A, Xu J, Lee SH, Kolattukudy PE et al. (2002) A protease-activated pathway underlying Th cell type 2 activation and allergic lung disease. J Immunol 169: 5904-5911.

4. Kiss A, Montes M, Susarla S, Jaensson EA, Drouin SM et al. (2007) A new mechanism regulating the initiation of allergic airway inflammation. J Allergy Clin Immunol 120: 334-342.

5. Schon-Hegrad MA, Oliver J, McMenamin PG, Holt PG (1991) Studies on the density, distribution, and surface phenotype of intraepithelial class II major histocompatibility complex antigen (Ia)-bearing dendritic cells (DC) in the conducting airways. J Exp Med 173: 1345-1356.

6. Sung SS, Fu SM, Rose CEJ, Gaskin F, Ju ST et al. (2006) A major lung CD103 (alphaE)-beta7 integrin-positive epithelial dendritic cell population expressing Langerin and tight junction proteins. J Immunol 176: 2161-2172.

7. Akbari O, Freeman GJ, Meyer EH, Greenfield EA, Chang TT et al. (2002) Antigen-specific regulatory T cells develop via the ICOS-ICOS-ligand pathway and inhibit allergen-induced airway hyperreactivity. Nat Med 8: 1024-1032.

8. Dieu MC, Vanbervliet B, Vicari A, Bridon JM, Oldham E et al. (1998) Selective recruitment of immature and mature dendritic cells by distinct chemokines expressed in different anatomic sites. J Exp Med 188: 373-386.

9. Hochweller K, Anderton SM (2005) Kinetics of costimulatory molecule expression by T cells and dendritic cells during the induction of tolerance versus immunity in vivo. Eur J Immunol 35: 1086-1096.

10. Osterholzer JJ, Chen GH, Olszewski MA, Curtis JL, Huffnagle GB et al. (2009) Accumulation of CD11b+ lung dendritic cells in response to fungal infection results from the CCR2-mediated recruitment and differentiation of Ly-6Chigh monocytes. J Immunol 183: 8044-8053.

11. Trompette A, Divanovic S, Visintin A, Blanchard C, Hegde RS et al. (2009) Allergenicity resulting from functional mimicry of a Toll-like receptor complex protein. Nature 457: 585-588.

12. Hammad H, Chieppa M, Perros F, Willart MA, Germain RN et al. (2009) House dust mite allergen induces asthma via Toll-like receptor 4 triggering of airway structural cells. Nat Med 15: 410-416.

13. van Rijt LS, Jung S, Kleinjan A, Vos N, Willart M et al. (2005) In vivo depletion of lung CD11c+ dendritic cells during allergen challenge abrogates the characteristic features of asthma. J Exp Med 201: 981-991.

14. Carroll MC (1998) The role of complement and complement receptors in induction and regulation of immunity. Annu Rev Immunol 16: 545-568.

15. Zwirner J, Gotze O, Begemann G, Kapp A, Kirchhoff K et al. (1999) Evaluation of C3a receptor expression on human leucocytes by the use of novel monoclonal antibodies. Immunology 97: 166-172.

16. Drouin SM, Kildsgaard J, Haviland J, Zabner J, Jia HP et al. (2001) Expression of the complement anaphylatoxin C3a and C5a receptors on bronchial epithelial and smooth muscle cells in models of sepsis and asthma. J Immunol 166: 2025-2032.

17. Li K, Anderson KJ, Peng Q, Noble A, Lu B et al. (2008) Cyclic AMP plays a critical role in C3a-receptor-mediated regulation of dendritic cells in antigen uptake and T-cell stimulation. Blood 112: 5084-5094.

18. Maubon D, Park S, Tanguy M, Huerre M, Schmitt C et al. (2006) AGS3, an alpha(1-3)glucan synthase gene family member of Aspergillus fumigatus, modulates mycelium growth in the lung of experimentally infected mice. Fungal Genet Biol 43: 366-375.

19. Kaku H, Nishizawa Y, Ishii-Minami N, Akimoto-Tomiyama C, Dohmae N et al. (2006) Plant cells recognize chitin fragments for defense signaling through a plasma membrane receptor. Proc Natl Acad Sci U S A 103: 11086-11091.

20. Cuesta A, Esteban MA, Meseguer J (2003) In vitro effect of chitin particles on the innate cellular immune system of gilthead seabream (Sparus aurata L.). Fish Shellfish Immunol 15: 1-11.

21. Reese TA, Liang HE, Tager AM, Luster AD, Van Rooijen N et al. (2007) Chitin induces accumulation in tissue of innate immune cells associated with allergy. Nature 447: 92-96.

22. Roy RM, Wuthrich M, Klein BS (2012) Chitin elicites CCL2 from airway epithelial cells and induces CCR2-dependent innate allergic inflammation in the lung. J

Immunol 189: In Press.

23. Da Silva CA, Pochard P, Lee CG, Elias JA (2010) Chitin Particles are Multifaceted Immune Adjuvants. Am J Respir Crit Care Med 182: 1482-1491.

24. Van Dyken SJ, Garcia D, Porter P, Huang X, Quinlan PJ et al. (2011) Fungal chitin from asthma-associated home environments induces eosinophilic lung infiltration. J Immunol 187: 2261-2267.

25. Dickey BF (2007) Exoskeletons and exhalation. N Engl J Med 357: 2082-2084.

26. Rayamajhi M, Redente EF, Condon TV, Gonzalez-Juarrero M, Riches DW et al. (2011) Non-surgical intratracheal instillation of mice with analysis of lungs and lung draining lymph nodes by flow cytometry. J Vis Exp e2702.

27. Rozen S, Skaletsky H (2000) Primer3 on the WWW for general users and for biologist programmers. Methods Mol Biol 132: 365-386.

28. Schmittgen TD, Livak KJ (2008) Analyzing real-time PCR data by the comparative C(T) method. Nat Protoc 3: 1101-1108.

29. Rapaka RR, Ricks DM, Alcorn JF, Chen K, Khader SA et al. (2010) Conserved natural IgM antibodies mediate innate and adaptive immunity against the opportunistic fungus Pneumocystis murina. J Exp Med 207: 2907-2919.
30. Koth LL, Rodriguez MW, Bernstein XL, Chan S, Huang X et al. (2004) Aspergillus antigen induces robust Th2 cytokine production, inflammation, airway hyperreactivity and fibrosis in the absence of MCP-1 or CCR2. Respir Res 5: 12.

31. Behnsen J, Lessing F, Schindler S, Wartenberg D, Jacobsen ID et al. (2010) Secreted Aspergillus fumigatus protease Alp1 degrades human complement proteins C3, C4, and C5. Infect Immun 78: 3585-3594.

32. Nagata S, Glovsky MM (1987) Activation of human serum complement with allergens. I. Generation of C3a, C4a, and C5a and induction of human neutrophil aggregation. J Allergy Clin Immunol 80: 24-32.

33. Fei M, Bhatia S, Oriss TB, Yarlagadda M, Khare A et al. (2011) TNF-alpha from inflammatory dendritic cells (DCs) regulates lung IL-17A/IL-5 levels and neutrophilia versus eosinophilia during persistent fungal infection. Proc Natl Acad Sci U S A 108: 5360-5365.

34. Hastie AT, Moore WC, Meyers DA, Vestal PL, Li H et al. (2010) Analyses of asthma severity phenotypes and inflammatory proteins in subjects stratified by sputum granulocytes. J Allergy Clin Immunol 125: 1028-1036.e13.

35. Wark PA, Saltos N, Simpson J, Slater S, Hensley MJ et al. (2000) Induced sputum

eosinophils and neutrophils and bronchiectasis severity in allergic bronchopulmonary aspergillosis. Eur Respir J 16: 1095-1101.

36. de Heer HJ, Hammad H, Soullie T, Hijdra D, Vos N et al. (2004) Essential role of lung plasmacytoid dendritic cells in preventing asthmatic reactions to harmless inhaled antigen. J Exp Med 200: 89-98.

37. Zhang X, Lewkowich IP, Kohl G, Clark JR, Wills-Karp M et al. (2009) A protective role for C5a in the development of allergic asthma associated with altered levels of B7-H1 and B7-DC on plasmacytoid dendritic cells. J Immunol 182: 5123-5130.

38. Abe M, Wang Z, de Creus A, Thomson AW (2005) Plasmacytoid dendritic cell precursors induce allogeneic T-cell hyporesponsiveness and prolong heart graft survival. Am J Transplant 5: 1808-1819.

39. Hasegawa K, Tamari M, Shao C, Shimizu M, Takahashi N et al. (2004) Variations in the C3, C3a receptor, and C5 genes affect susceptibility to bronchial asthma. Hum Genet 115: 295-301.

40. Nakano Y, Morita S, Kawamoto A, Suda T, Chida K et al. (2003) Elevated complement C3a in plasma from patients with severe acute asthma. J Allergy Clin Immunol 112: 525-530.

41. Walters DM, Breysse PN, Schofield B, Wills-Karp M (2002) Complement factor 3 mediates particulate matter-induced airway hyperresponsiveness. Am J Respir Cell Mol Biol 27: 413-418.

42. Kanemitsu H, Nagasawa S, Sagai M, Mori Y (1998) Complement activation by diesel exhaust particles (DEP). Biol Pharm Bull 21: 129-132.

43. Park JW, Taube C, Joetham A, Takeda K, Kodama T et al. (2004) Complement activation is critical to airway hyperresponsiveness after acute ozone exposure. Am J Respir Crit Care Med 169: 726-732.

44. Amara U, Flierl MA, Rittirsch D, Klos A, Chen H et al. (2010) Molecular intercommunication between the complement and coagulation systems. J Immunol 185: 5628-5636.

45. Zhang X, Kohl J (2010) A complex role for complement in allergic asthma. Expert Rev Clin Immunol 6: 269-277.

46. Drouin SM, Corry DB, Kildsgaard J, Wetsel RA (2001) Cutting edge: the absence of C3 demonstrates a role for complement in Th2 effector functions in a murine model of pulmonary allergy. J Immunol 167: 4141-4145.

47. Drouin SM, Corry DB, Hollman TJ, Kildsgaard J, Wetsel RA (2002) Absence of the

complement anaphylatoxin C3a receptor suppresses Th2 effector functions in a murine model of pulmonary allergy. J Immunol 169: 5926-5933.

48. DiScipio RG, Daffern PJ, Jagels MA, Broide DH, Sriramarao P (1999) A comparison of C3a and C5a-mediated stable adhesion of rolling eosinophils in postcapillary venules and transendothelial migration in vitro and in vivo. J Immunol 162: 1127-1136.

49. Da Silva CA, Hartl D, Liu W, Lee CG, Elias JA (2008) TLR-2 and IL-17A in chitin-induced macrophage activation and acute inflammation. J Immunol 181: 4279-4286.

Chapter 5

Conclusions and future directions

This dissertation only begins to scratch the surface of the role of chitin exposure in allergic inflammation. Using a combination of *in vitro* and *in vivo* approaches I have outlined a role for airway epithelial cells in the recognition and response to chitin. Upon chitin recognition, airway epithelial cells are activated and secrete CCL2. Signaling via the CCR2 - the receptor for CCL2 - is required for both chitin-induced innate allergic inflammation and chitin-dependent allergic sensitization to the allergy-associated fungus *Aspergillus fumigatus*. Finally, NF-κB dependent gene expression in airway epithelial cells and complement play a critical role in mediating chitin-dependent *Aspergillus* sensitization. Together, these results sketch the outline of a model where airway epithelial cell centrally mediate allergic responses to chitin and chitin containing allergens.

The next steps are even more exciting. Through the use of DNTA mice and Af3.16 transgenic T cells I expect that one would be able to tease apart the requisite role of epithelial cells in antigen specific T cell polarization. Because I can modulate Nf-κB activity in airway epithelial cells, and I know airway epithelial cells secrete the NF-κB dependent chemokine CCL2 in response to chitin, it is likely that chitin recognition by airway epithelial cells results in additional cytokine and chemokine production. Investigation of the identity of these cytokines would yield new understanding into the mechanism of chitin induced allergic inflammation. Of particular interest is whether chitin can induce the production of allergy associated cytokines such as IL25, IL33, and TSLP in airway epithelial cells.

The production of allergy associated cytokines as a result of chitin exposure leads one to consider the target of those cytokines, dendritic cells. I have found that chitin exposure activates DC in the airway and that this activation depends on complement factor 3 and the anaphylatoxin receptor C3aR. Airway DC interact closely with airway epithelial cells so it is likely that airway DC will be impacted in DNTA mice following chitin exposure. What remains to be seen however, is whether chitin can induce activity in DC directly or whether airway epithelial cells, which play a key role in macrophage activation, will also control the activation of DC. In addition, chitin exposure induces the recruitment of monocytes in a CCR2 dependent fashion which differentiate into inflammatory DC. Due to the striking decrease in innate and allergic sensitization following chitin exposure in CCR2KO mice, the impact of chitin exposure on this particular DC subset deserves special attention.

Finally, I expect one could investigate the mechanism by which chitin promotes *Aspergillus* specific T cell polarization using the adoptive transfer model pioneered in this dissertation. Recently, the ability of fungal carbohydrates to impact T cell polarization through effects on DC and through direct effects on T cells has benefited from an increased knowledge of the mechanisms by which carbohydrates are recognized and improvements in characterizing the structure of the fungal polysaccharides. Chitin should be no different. Although, the precise mechanism of chitin recognition is unknown, I have demonstrated that chitin does activate signaling pathways leading to NF-κB activation. Admittedly this does not narrow the field possibilities considerably however it does help point searchers in the right direction. Once discovered, the chitin receptor could be the target of clinical interventions to decrease asthma and allergy.

In the end, the studies examining the interaction between carbohydrates and the immune are in their adolescent phase, full of promise and difficulties. Detailed

knowledge regarding carbohydrate immunogenic structures and recognition mechanisms are a lacking. Also, we are just beginning to understand a broader range of fungi and it will be interesting to note how well discoveries in *Aspergillus* and *Candida* extend to the fungal field as a whole. While much of the focus regarding the immune recognition of fungal carbohydrates has focused on myeloid and lymphoid cells, airway epithelial cells represent the initial point of contact of inhaled fungal spores and their activity, far from passively blocking the way, could critically direct responses to fungi in the lung.

APPENDIX I

Dendritic Cells in Anti-Fungal Immunity and Vaccine Design

René M. Roy and Bruce S. Klein

This appendix appeared in print as:

Roy RM, Klein BS (2012) Dendritic cells in antifungal immunity and vaccine design. Cell Host Microbe 11: 436-446.

ABSTRACT

Life-threatening fungal infections have increased in recent years while treatment options remain limited. The development of vaccines against fungal pathogens represents a key advance sorely needed to combat the increasing fungal threat. Dendritic cells (DC) are uniquely able to shape anti-fungal immune responses by initiating and modulating naive T cell responses. Targeting DC may allow for the generation of potent vaccines against fungal pathogens. In the context of anti-fungal vaccine design, we describe the characteristics of the varied DC subsets, how DC recognize fungi, their function in immunity against fungal pathogens, and how DC can be targeted in order to create new anti-fungal vaccines. Ongoing studies continue to highlight the critical role of DC in anti-fungal immunity and will help guide DC-based vaccine strategies.

INTRODUCTION

Fungal pathogens are a serious emerging infectious disease threat which are the subject of efforts to develop novel vaccines. The rising danger of mycoses is compounded by both the limited and toxic pharmacological armamentarium used to treat these infections and the immunocompromised status of the large majority of patients with fungal infections. While fungi are commonly encountered by humans in their environment, particularly as inhaled spores or conidia, few fungal species are human pathogens. Fungi also exist as useful commensal organisms until the host becomes immunodeficient or a systemic portal like a venous catheter is colonized whereupon commensal fungi can cause life threatening infections. Thus, the development of fungal vaccines faces the dual challenge of providing protection to immunocompromised patients and protection against primary pathogens which cause lethal infections in healthy individuals.

The rising incidence of fungal infections is linked to the increase in immunocompromised patients, specifically, patients with AIDS, patients with cancer, and recipients of solid organ or hematopoietic stem cell transplants. Candida species are the second leading cause of infectious disease related death in premature infants and the fourth leading cause of hospital bloodstream infections (Benjamin et al., 2010; Pfaller and Diekema, 2007). A rise in the incidence of zygomycosis is also noted in patients with diabetes mellitus (Bitar et al., 2009) augmenting clinical challenges in this growing patient population. Major endemic mycoses can lead to lethal systemic infections in apparently healthy individuals and can reactivate in the setting of immune suppression. Also, fungal-associated allergy and asthma contribute significantly to the human health burden due to fungi.

Encounters with fungi require a coordinated host innate and adaptive immune response to successfully eradicate the fungus and to promote long-lived immunological

memory of the encounter. Iatrogenic risk factors for fungal infections such as granulocytopenia, compromised mucosal barriers, and T cell supressing drugs demonstrate the important roles for both innate and adaptive responses to fungi. In fungal infections, both $CD4^+$ and $CD8^+$ T cells are necessary for the elimination of the pathogen (Wuthrich et al., 2002) Most fungi also elicit antibodies, some of which are protective, that can neutralize fungal pathogens or promote fungal uptake by phagocytes. Phagocytes and other innate immune cells play a critical role in combating fungal pathogens (reviewed by Brown, 2011). Activated phagocytes and neutrophils kill fungi either following phagocytosis or via the production of fungicidal chemicals including reactive oxygen and nitrogen species. Epithelial cells also produce fungicidal compounds such as β-defensin and provide a mechanical barrier at mucosal sites exposed to fungi. Expectedly, genetic or acquired deficiency in either the innate or adaptive immune response significantly increases the risk of fungal infection.

At the intersection of innate and adaptive immunity are dendritic cells (DC), unique cells capable of taking up and processing antigen for presentation by major histocompatibility complex (MHC) class I or MHCII molecules to naive T cells. DC recognize fungi via a broad array of surface and intracellular pattern recognition receptors (PRR). Recognition of fungi results in the secretion of cytokines by DC and the expression of co-stimulatory molecules on the DC surface both of which are required to drive naive $CD4^+$ T cell differentiation into a T-helper (T_h) phenotype. Clearance of fungi with limited damage to the host requires a finely tuned balance between T_h1, T_h17, and T_{reg} subsets; the precise response needed is based on the anatomical location and the specific fungal pathogen. DC oversee and calibrate this balance of T_h responses thus orchestrating T cell responses and integrating the innate and adaptive immune response to fungi.

The unique ability of DC to initiate and engage anti-fungal immunity position DC

as a logical cellular target for the development of fungal vaccines. In this review, we describe the panoply of DC subsets and their function in anti-fungal immunity, identify how DC recognize fungi, and discuss strategies to target DC in the development of novel anti-fungal vaccines.

Characterization and function of DC and monocyte subsets

Four decades ago, Steinman and Cohn reported the identification of a cell with "continually elongating, retracting, and reorienting" long cytoplasmic processes in the spleen and lymph nodes of mice (Steinman and Cohn, 1973). These cells, now known as DC, are hematopoietic cells that function as professional antigen presenting cells and are capable on initiating a T cell response. When DC recognize antigen at the immunological frontier, sites such as the skin or the airways of the lung, or in the draining nodes of the lymphatic system, DC amplify the innate immune response by secreting cytokines that recruit and activate other leukocytes. Following engulfment, processing, and presentation of the antigen, DC initiate and shape the adaptive response by promoting naïve T cell differentiation into effector or regulatory T cells. Since their discovery, a plethora of DC subsets characterized by anatomical location, function, and surface marker expression have been described (Fig. 1). Indeed, it is the specialized functions of the diverse DC subsets that augment the challenge of targeting DC in the development of anti-fungal vaccines. Therefore, ongoing efforts to characterize the function of DC subsets will enhance the rational design of DC-targeted anti-fungal vaccines.

In the steady state, monocytes and DC share a common progenitor cell in the bone marrow, the macrophage-dendritic cell progenitor (MDP) (Fogg et al., 2006; Liu et al., 2009). From the MDP, a common-DC progenitor and monocytes are produced. The common-DC progenitor (CDC), which is restricted to the bone marrow gives rise to

three broad groupings of DC: plasmacytoid DC (pDC), conventional DC, and migratory DC. While monocytes and pDC mature in the bone marrow and are released into the blood for circulation to lymphoid tissues, resident and migratory DC precursors known as preDC exit the bone marrow and circulate via the blood before either entering the high endothelial venules of lymphoid tissues or seeding peripheral tissues.

Plasmacytoid DC

pDC are typified by their high production of interferon-α (IFN-α) in response to the sensing of nucleic acids by endosomal Toll-like receptors and are further characterized in part by the high surface expression of sialic acid binding immunoglobulin-like lectin H (Siglec H). Using a Siglec H-DTR depleter mouse, a recent study further elucidated the roles of pDC in vivo (Takagi et al., 2011). Besides nucleic acid sensing, pDC induced IL-10 producing $CD4^+$ $Foxp3^+$ Treg cells, limited T_h1 and T_h17 cell polarization at mucosal sites, and activated $CD8^+$ T cells. Furthermore, pDC controlled viral infection via the induction of $CD8^+$ T cells, but impaired bacterial clearance and contributed to septic shock. While pDC carry out a well-characterized role in anti-viral immunity, the role of pDC in fungal infections is less clear. pDC recognize Aspergillus fumigatus DNA via TLR9 and are linked with resistance to A. fumigatus infection in mice (Ramirez-Ortiz et al., 2011). Moreover, pDC inhibited fungal growth in vitro and accumulated in the lungs in a murine model of Aspergillus pulmonary infection, hinting that pDC may recognize and combat fungi directly in vivo. A second subset of pDC exists that develops in the context of elevated IFN-α and is similar to pDC found in Peyer's patches of the gut (Li et al., 2011). Uncharacteristically, this pDC subset fails to produce IFN-α after stimulation with TLR ligands; however, this pDC subset secreted elevated levels of IL-6 and IL-23 and primed robust antigen specific T_h17 cells in vivo. This suggests a potential role for IFN-α elicited pDC in the polarization of anti-fungal T_h17 cells. Combined with the recent findings that pDC are critical mediators of Treg / T_h17 balance

at mucosal surfaces, recognition of fungi by pDC or IFN-α elicited pDC at mucosal surfaces may tilt the balance toward tolerance or inflammation.

Conventional DC

Conventional DC, also known as resident DC, exist in the lymphoid tissue and are comprised of two major subpopulations, $CD8^+$ and $CD4^+CD8^-$ resident DC. In addition, the spleen contains a third minor population of so-called double-negative DC, which lack CD4 and CD8 surface expression and appear to be largely similar in function to $CD4^+$CD8- DC (Luber et al., 2010). $CD8^+$ resident DC are identified by the surface phenotype $CD8^+CD4^-CD11b^-CD11c^+MHCII^+DEC205^+$ and are located primarily in the T cell zone of the spleen and lymph nodes (Idoyaga et al., 2009). A major function of $CD8^+$ DC is the cross-presentation of antigens via MHCI to $CD8^+$ cytotoxic T lymphocytes (CTL) (den Haan et al., 2000). $CD8^+$ DC obtain antigen via the engulfment of live or apoptotic cells or antigen containing apoptotic vesicles. $CD4^+CD8^-$ resident DC are identified by the surface phenotype $CD8^-CD4^+CD11b^+CD11c^+MHCII^+33D1^+$ and are present in the red pulp and bridging channels of the spleen and the marginal zones and high endothelial venules of the lymph nodes (Liu and Nussenzweig, 2010). In contrast to $CD8^+$ DC, $CD4^+CD8^-$ DC are not efficient at presenting antigens via MHCI and instead present antigen via MHCII (Dudziak et al., 2007).

Relative to other pathogen classes such as viruses, information regarding the role of resident DC in priming T cell responses to fungi is limited. Direct evidence that resident DC prime anti-fungal T cell responses was demonstrated in a vaccine model to generate immunity to Blastomyces dermatitidis. Lymph node resident DC acquired and displayed antigen and primed antigen specific $CD4^+$ T cells, however acquisition of the antigen depended on ferrying of the yeast from the skin to the lymph node by migratory and monocyte derived DC (Ersland et al., 2010). Less is known about cross-presentation of fungal antigens in vivo. Bone marrow derived DC acquire and cross-

present Histoplasma capsulatum antigens to CTL via ingestion of live or killed Histoplasma capsulatum yeasts or via engulfment of Histoplasma containing apoptotic macrophages (Lin et al., 2005). Subcutaneous injection of apoptotic phagocytes containing CFSE labeled heat-killed Histoplasma results in the accumulation of CFSE in $CD11c^+$ cells in skin draining lymph nodes and $CD11c^+$-dependent CTL-mediated protection against Histoplasma challenge (Hsieh et al., 2011). While these studies provide evidence that fungal antigens can be acquired and presented by resident DC, the precise resident DC subpopulation or subpopulations involved in vivo remain undefined. Unexpectedly, $CD4^+CD8^-$ resident DC may be important for the cross-presentation of fungal antigens. In experiments using an OVA-expressing strain of the model yeast Saccharomyces cerevisiae, both $CD8^+$ and $CD4^+CD8^-$ DC isolated from mouse spleen and primed with OVA-S. cerevisiae induced robust OVA-specific $CD4^+$ T cell proliferation ex vivo however only $CD4^+CD8^-$ DC stimulated an OVA-specific $CD8^+$ T cell response (Backer et al., 2008). To that end, further studies will be needed to unravel the specific contributions of resident DC subpopulations to $CD4^+$ T cell and CTL activation and polarization in vivo.

Migratory DC

Migratory DC, also referred to as tissue DC, are immature DC that are located principally in peripheral tissues such as the skin, the lung, and the gut. Following uptake of antigen, migratory DC exit the tissue and undergo maturation characterized by (1) enhanced antigen processing and presentation, (2) downregulation of tissue homing receptors, (3) upregulation of CCR7 and (4) increased surface expression of co-stimulatory molecules. $CCR7^+$ DC migrate to the T cell zone of lymphoid tissue where they can initiate activation of naive T cells or transfer antigen to resident DC (Banchereau and Steinman, 1998; Allan et al., 2006). With the exception of Langerhans cell in the epidermis, the majority of migratory DC appear to derive from the same

circulating precursor as conventional DC, the preDC. Migratory DC have some capacity for division and self-renewal in situ, while monocyte subsets also contribute to replenishment of migratory DC in certain circumstances. Migratory DC line the surfaces of the body that are exposed to the environment and, as such, are likely to encounter fungi along with other pathogens and antigens. While the migratory DC networks that line the skin, lung, and intestine share similarities, each site has functional differences that are important in anti-fungal immunity and deserve individual discussion.

Skin

The skin is lined by a dense network of DC which can be broadly divided into the epidermis associated Langerhans cell (LC) and a collection of dermis associated dermal DC (Henri et al., 2010a). LC are unique among migratory DC as they arise from a MDP-like cell seeded into the epidermis in utero followed by a wave of expansion within days of birth (Chorro et al., 2009). In addition to their epidermal location, LC are characterized by surface expression of the eponymous langerin (CD207), CD11c, and MHCII. The dermis contains LC that migrate to the draining lymph node, $CD207^{+}CD103^{+}$ dermal DC, and a diverse group of $CD207^{-}CD103^{-}$ DC (Henri et al., 2010b). Upon subcutaneous administration of a B. dermatitidis vaccine, DEC205 expressing skin-derived DC migrated to the skin draining lymph node in a CCR7-dependent fashion, presented the model antigen expressed by the fungus, and activated $CD4^{+}$ T cells (Ersland et al., 2010).

Specialized antigen presentation and T cell polarization functions for skin-associated DC subsets – specifically LC, $CD207^{+}$ dermal DC, and $CD207^{-}$ dermal DC – were elegantly assessed in a cutaneous epidermal exposure model to Candida albicans (Igyarto et al., 2011). LC were necessary and sufficient for the generation of antigen-specific T_h17 cells via the production of elevated levels of IL-6, IL-1β, and IL-23, cytokines which promote and stabilize T_h17 development. In contrast, LC were not

necessary for the generation of CTL. $CD207^+$ dermal DC were required for CTL and also T_h1 polarization. Compared with LC, $CD207^+$ dermal DC produced higher levels of IL-12 and IL-27, and lower levels of IL-1β and IL-6, and no IL-23, making them poor promoters of T_h17. Moreover, the $CD207^+$ dermal DC inhibited the ability of LC and $CD207^-$ dermal DC to promote T_h17 responses. Since IL-12 and IL-27, as well as IFN-γ from T_h1 cells, inhibit T_h17 differentiation and proliferation, $CD207^+$ dermal DC likely block Candida-specific T_h17 cells by promoting T_h1 differentiation. Thus, exposure of LC and $CD207^+$ dermal DC to Candida can promote opposing effects, through the elaboration of polarizing cytokines that enable the development of T_h1 or T_h17 responses. Importantly, this study identified a subset of DC that, when targeted, skews differentiation toward T_h17 cells, which are instrumental in anti-fungal immunity (Ersland et al., 2010; Igyarto et al., 2011).

Lung

DC in the lung and conducting airways deal with constant exposure to inhaled fungal spores and hyphal fragments. Dense network of DC line the airways, sampling inhaled antigen for subsequent shuttling to mediastinal lymph nodes. Indeed, the airway is currently a target for intranasally delivered vaccine against influenza and may represent a candidate vaccine site against inhaled fungi. Besides pDC, lung DC subsets include two broad divisions: $CD103^+$DC and $CD11b^+$ DC. $CD103^+$ lung DC also express CD207 making them similar to $CD207^+CD103^+$ dermal DC in the skin. $CD103^+$DC express tight junction proteins, which allow the DC to intimately associate with airway epithelial cells and to extend dendrites into the airway lumen to sample antigen without disturbing the epithelial barrier (Sung et al., 2006; Jahnsen et al., 2006). Steady state migration of $CD103^+$ DC and $CD11b^+$ DC in the absence of inflammation is responsible for the induction of tolerance to inhaled antigen. $CD103^+$ DC can acquire both soluble and apoptotic cell associated antigens from the airway following which $CD103^+$ DC migrate

to the mediastinal lymph node under both steady state and inflammatory conditions. In the mediastinal lymph node $CD103^+$ DC cross-present antigen to and activate CTL (Desch et al., 2011). $CD11b^+$ DC differ from monocyte derived DC and specialize in cytokine and chemokine production (Beaty et al., 2007) as well as presenting antigen via MHCII to $CD4^+$ T cells in the mediastinal lymph node following migration (del Rio et al., 2007). Rapid recruitment of $Ly6C^+$ monocyte derived DC to the lung upon inflammation clouds analysis of the function of lung $CD11b^+$ DC which lack Ly6C surface expression. Upon pulmonary exposure to A. fumigatus conidia, $CD103^+$ DC failed to take up and transport conidia to the mediastinal lymph node, whereas $CD11b^+$ DC did transport them (Hohl et al., 2009). In this model, lung $CD11b^+$ DC were reduced relative to wild type mice in $CCR2^{-/-}$ mice following A. fumigatus exposure. Conversely, naive $CCR2^{-/-}$ mice had similar lung $CD11b^+$ DC numbers to wild type mice suggesting that recruited monocyte-derived DC (discussed in detail later in this review) and not lung $CD11b^+$ DC are responsible for conidial uptake and antigen presentation in the setting of A. fumigatus induced inflammation.

Intestine

Just like the lung, DC in the intestine are situated on the basolateral side of the epithelial layer largely isolated from the gut microflora. DC in the intestine localize to two major sub-epithelial locations, the lamina propria and the Peyer's patch; both subsets in each region differentially regulate immune responses. The Peyer's patch is a specialized structure that consists of organized T and B cell follicles capped by a unique epithelial cell dome called an M cell. Peyer's patch DC (PP-DC) extend dendrites through M cells to sample antigen from the intestinal lumen. This transcellular method of antigen sampling appears to be distinct from the paracellular sampling that occurs in the lung and outside of the PP in the intestine (Lelouard et al., 2011). Following antigen internalization, PP-DC migrate to the T cell rich zone of the PP to prime naive T cells.

Lamina propria DC (LP-DC) express CD11c, MHCII, and CD103 and can be further divided into $CD11b^+$ and $CD11b^-$ subsets. $CD11b^+$ and $CD11b^-$ LP-DC subsets represent two sides of an equilibrium that maintain the balance between the induction of T_h17 and T_{reg} responses, respectively, in the intestinal wall (Denning et al., 2011). Indeed, $CD11b^+$ LP-DC numbers are elevated in the duodenum and gradually decrease throughout the small intestine and reach their lowest levels in the colon, mirroring the distribution of T_h17 cells. LP-DC play distinct roles in directing $CD4^+$ T cell differentiation in the lamina propria dependent on the local LP-DC to T cell ratio and DC-T cell location along the intestine. Furthermore, the gut microbiota plays a key role in shaping the function of these subsets as LP-DC from mice obtained from separate vendors display strikingly different efficiencies at priming T_h17 cells based in part on the presence or absence of segmented filamentous bacteria (Sczesnak et al., 2011). In addition to their ability to affect T cell responses locally in the intestine, both subsets of LP-DC migrate to draining mesenteric lymph nodes where they can further prime and activate T cells.

The role of PP-DC and LP-DC in generating anti-fungal immunity in the gut is unclear and relatively unstudied. C. albicans, a gut commensal fungus, can cause systemic infection if the gut epithelial/DC barrier is substantially breached and/or in the setting of broad-spectrum antibiotic use leading to Candida overgrowth. Strong induction of T_{reg} cells by LP-DC in the mesenteric lymph node may highlight the critical role of limiting inflammation in the gut in order to maintain the epithelial barrier and prevent disseminated infection. Furthermore, heightened T_h17 responses in the gut impair protective T_h1 responses and worsen Candida infection (Zelante et al., 2007). While bone marrow derived DC produced IL-23 in response to Candida in vitro and IL-23 neutralization promoted fungal clearance in vivo, the identity of the DC subset recognizing and responding to the fungus in this model was not determined. Nevertheless, DC in the gut appear to tightly control tolerance and immunity to fungal

organisms.

Monocytes, monocyte derived DC, and inflammatory DC

Monocytes are derived from the MDP and, in the absence of inflammation, are found in the bone marrow and circulating at low levels in the blood and spleen. Two classes of $CD11b^{+}CD115^{+}$ monocytes arise from the MDP and circulate in the blood, $Ly6C^{+}CCR2^{+}$ and $Ly6C^{-}CX3CR1^{hi}$ monocytes (Geissmann et al., 2003). Monocytes have broad developmental plasticity and can replenish certain subsets of DC and LC in the setting of experimental depletion (Ginhoux et al., 2007) and thus may represent an emergency store of DC precursors that can be rapidly deployed. Under inflammatory conditions $Ly6C^{+}CCR2^{+}$ monocytes migrate to the site of inflammation and acquire surface expression of the DC markers CD11c and MHCII while losing Ly6C (Osterholzer et al., 2009) thus becoming "inflammatory DC". While $Ly6C^{-}CX3CR1^{hi}$ appear not be directly involved in innate immunity to fungi (Dominguez and Ardavin, 2010), $Ly6C^{+}CCR2^{+}$ monocytes play a critical role responding to many medically relevant fungi such as A. fumigatus (Hohl et al., 2009), Cryptococcus neoformans (Osterholzer et al., 2009), and B. dermatitidis (Ersland et al., 2010).

Compared with any other DC subset, monocyte-derived DCs seem to have an outsized role in anti-fungal immunity, particularly through the induction of T_h1 cells. Using $CCR2^{-/-}$ mice (where monocytes are trapped in the bone marrow), inflammatory DC were found to have a critical role in driving a T_h1 response and presenting Histoplasma antigen to $CD4^{+}$ T-cells (Szymczak and Deepe, 2010). $CCR2^{-/-}$ mice also exhibit skewed T_h2 responses in H. capsulatum infection and dramatically greater fungal burden in the lung compared to wild-type (WT) animals (Szymczak and Deepe, 2009). Similar CCR2-dependent phenotypes are found in experimental pulmonary infection with A. fumigatus or C. neoformans: priming of T_h1 cells in response to fungi critically depends on $CCR2^{+}$ monocyte derived inflammatory DC (Osterholzer et al., 2009; Hohl

et al., 2009). To highlight the importance of the tissue environment in DC function, the defect in $CD4^+$ T cell priming by inflammatory DC during respiratory infection with A. fumigatus is restricted to the lung in $CCR2^{-/-}$ mice and not other lymphoid organs such as the spleen (Hohl et al., 2009). Similarly, while $Ly6C^+CCR2^+$ monocytes play a prominent role in delivering B. dermatitidis yeast into skin draining lymph nodes after subcutaneous vaccine delivery, this shuttling function can be compensated in $CCR2^{-/-}$ mice by other skin migratory DC populations (Ersland et al., 2010). Thus, in the setting of the lung, which is the primary route of infection for fungi, but not the skin or the spleen, monocyte-derived DC appear to play a critical role in anti-fungal immunity.

Fungal Recognition by DC

Recognition of fungi by DC is accomplished by a diverse group of PRR that recognize conserved fungal PAMP including proteins, carbohydrates, and nucleic acids (Fig. 2). Anti-fungal immunity depends critically on the recognition of fungi by PRR. Fungal recognition by PPR induces intracellular signaling pathways that lead to DC maturation and secretion of cytokines that instruct the evolving immune response. PRR can also mediate the uptake of fungi by DC and can direct fungi to appropriate intracellular compartments for antigen processing and subsequent presentation. PRR important for the recognition of fungi include Toll-like receptors (TLR) and C-type lectin receptors (CLR), which can respond individually or synergistically to fungi. Other fungal PRR include scavenger receptors such as SCARF1 and CD36 that can mediate binding to C. neoformans (Means et al., 2009) and complement/Fc receptors, which recognize complement factor or antibody coated fungi directly (Taborda and Casadevall, 2002) and mediate phagocytosis.

TLR

Recognition of PAMP by TLR results in engagement of intracellular signaling pathways culminating in the activation of the transcription factors activator protein-1 (AP-1) and

nuclear factor-κB (NF-κB). All TLR transmit their PAMP recognition event via TIR-mediated engagement of myeloid differentiation primary response gene 88 (MyD88) with the exception of TLR3, which recruits the adaptor TIR-domain containing adaptor-inducing IFN-beta (TRIF). A subset of TLR are also able to activate interferon regulatory factor 3 (IRF3) or IRF7 which regulate the expression of type I IFN. Since MyD88 is instrumental in priming T_h1 cells in response to fungi (Rivera et al., 2006), it is generally thought that fungal recognition by TLR induce a T_h1 response. The role of TLR for the induction of anti-fungal T_h17 cells is less clear. By using naive fungus-specific T cell receptor transgenic cells, a recent study demonstrated that TLR-induced MyD88 activity and not dectin-1 or IL-1R signaling, was required for the development of vaccine induced T_h17 cells and resistance to B. dermatitidis infection (Wuthrich et al., 2011). The identity of the TLR driving this response is unknown. TLR are globally expressed on DC although some subsets of DC may express only a subset of TLR. For example, TLR3 is expressed 28-fold higher by $CD8^+$ DC than by $CD4^+CD8^-$ DC in the spleen (Edwards et al., 2003) suggesting that DC subsets are differentially activated by discrete fungal TLR ligands.

TLR2

While TLR-mediated signaling in DC generally favors the development of responses, TLR2 signaling may promote non-protective T_h2 or T_{reg} differentiation. TLR2 mediated recognition of C. albicans results in increased IL-10 production and a concurrent decrease in T_h1 polarization (Netea et al., 2004). As a result, $TLR2^{-/-}$ mice showed increased resistance to disseminated candidiasis that was associated with increased IL-12 and IFN-γ and decreased IL-10 production. Further evidence for the anti-inflammatory role of TLR2 signaling in DC was provided by two additional studies. First, DC recognition of zymosan via TLR2 and dectin-1 promoted T_{reg} cell differentiation via IL-10 and TGF-β secretion (Dillon et al., 2006). Second, live A. fumigatus hyphae

reduced IL-12 and IL-23 production and increased IL-10 production from DC exposed to house dust mite extract in a TLR2 and dectin-1 dependent fashion, suggesting that TLR2 recognition of fungal ligands may promote tolerance rather than protective immunity.

TLR4

Recognition of fungal ligands by TLR4 similarly engenders heterogeneous responses that fail to recapitulate TLR4 mediated responses to the prototypical TLR4 ligand LPS. For example, recognition of C. albicans derived O-linked mannosyl residues by TLR4 promotes proinflammatory cytokines. By contrast, TLR4 binding of the C. neoformans cell wall component glucuronoxylomannan (GXM) does not induce cytokine production despite inducing NF-κB nuclear translocation. As TLR4 signaling in response to LPS requires the assembly of a larger complex consisting of CD14 and MD-2, it is likely that fungal recognition by TLR4 will require accessory signaling molecules that may mediate disparate TLR4 mediated responses to different fungal PAMP.

TLR3 TLR7 TLR9

Multiple studies have demonstrated that fungi are recognized by the endosomal nucleic acid sensing TLR: TLR3, TLR7, and TLR9. For instance, cryptococcal DNA triggered IL-12p40 and CD40 expression in murine DCs and activated NF-κB in TLR9-transfected HEK239 cells (Nakamura et al., 2008). Similarly, A. fumigatus DNA stimulated the production of proinflammatory cytokines in mouse and human DC (Ramirez-Ortiz et al., 2008). Drug-resistant Candida glabrata represents an important emerging opportunistic infection. A recent study demonstrated that C. glabrata induces Type I IFN secretion from DC in a TLR7-dependent but TLR2 and TLR4 independent manner (Bourgeois et al., 2011). TLR9 is often targeted with synthetic oligonucleotides that act as strong adjuvants in new vaccine designs. As more is learned about fungal recognition by these TLR and the responses they engender by DC, fungal ligands may provide additional

tools to promote anti-fungal vaccine immunity.

CLR

Like the TLR, CLR recognize a broad range of PAMP present on fungi. CLR recognize glucan, mannose, or fucose containing structures on fungi and trigger intracellular signaling via ITAM-containing adaptor molecules leading to maturation of DC and the secretion of cytokines. DC express a wide range of CLR, although expression of some CLR are restricted to a particular subset of DC contributing to the functional differences of the DC subsets.

Dectin-1

Prior to the discovery of dectin-1 as the receptor for β-glucan, fungal β-glucans were already in use as powerful immunomodulators and vaccine adjuvants. The discovery of dectin-1 (Brown and Gordon, 2001) has allowed for greater elucidation of the mechanism by which β-glucans exert their effects. Dectin-1 signals via an intracellular domain containing a hemITAM motif that can recruit and activate Syk. Recruitment of Syk by activated dectin-1 results in activation of MAPK, NFAT, and NF-κB via the CARD9 adaptor. Activation of dectin-1 by curdlan, a highly purified β-glucan, elicited IL-6, IL-23, and IL-12 from DC. Curdlan exposed DC loaded with antigen could differentiate naive $CD4^+$ T cells into T_h17 and T_h1 cells, prime protective CTL cells, and promote antibody responses suggesting that dectin-1 links DC-recognition of β-glucans to both T cell and B cell adaptive immunity (Leibundgut-Landmann et al., 2008). While dectin-1 is critical in driving anti-fungal T_h17 cells and resistance to C. albicans, A. fumigatus and Pneumocystis carinii, it was found that vaccine-induced T_h17 cells and immunity to B. dermatitidis are dectin-1 independent (Wuthrich et al., 2011). Dectin-1 can also mediate uptake of fungi by DC via recognition of surface β-glucan. Many fungi, including H. capsulatum, mask β-glucan on their surfaces, highlighting the powerful role of dectin-1 in the recognition and response to fungi.

Dectin-2 and Mincle

While dectin-1 recognizes β-glucan, dectin-2 and Mincle recognize mannose-like structures and require the adaptor FcRγ to signal via Syk. Dectin-2 is most abundantly expressed on inflammatory monocytes and DC. Recognition of α-mannans by dectin-2 induces the secretion of IL-2, IL-10 and TNF-α by DC in vitro (Robinson et al., 2009). Furthermore, in a model of systemic C. albicans infection, dectin-$2^{-/-}$ mice or mice treated with dectin-2 neutralizing mAb failed to develop Candida-specific T_h17 cells. Mincle also induces the production of TNF-α, CXCL1, CXCL2, and IL-10 via Syk and CARD9 upon recognition of C. albicans, Malassezia sp. and Fonsecaea pedrosoi, yet whether Mincle engagement on DC by fungal PAMP promotes anti-fungal immunity remains to be investigated (Sousa Mda et al., 2011). Mincle, which also recognizes a mycobacterial glycolipid, is already the target of novel vaccine designs against mycobacterial pathogens and may prove to be a fruitful target in anti-fungal vaccination efforts.

The mannose receptor (CD206)

CD206 is a transmembrane protein that binds terminal mannose, N-acetyl glucosamine, or fucose sugars and that lacks classical signaling motifs. It can also be cleaved from the cell surface and exists as a soluble receptor in some circumstances. In response to fungal N-linked mannans, CD206 can induce NF-κB activation and the production of IL-12, GM-CSF, IL-8, IL-1β, and IL-6. CD206 also appears to be responsible for the formation of a novel DC phagocytic structure called the "fungipod" which may promote yeast phagocytosis by DC and play an important role in DC-fungi interactions (Neumann and Jacobson, 2010). The role of CD206 in promoting fungal antigen uptake, processing, and presentation by DC remains poorly understood. However due to the wide expression of CD206 on DC subsets, strategies to target vaccine antigen to CD206 could result in broad DC mobilization and potentially robust vaccine immunity.

NLR

Recently, a NOD-like receptor family member was found to play a role in the anti-fungal immunity. Exposure of monocytes to C. albicans germ tubes or A. fumigatus hyphae activated the NLRP3 inflammasome in a Syk-dependent fashion (Hise et al., 2009; Said-Sadier et al., 2010). NLRP3 is activated by a wide range of pathogen- and host-associated stimuli and it is unclear if NLRP3 senses stimuli directly or indirectly. β-glucan also activates the NLRP3 inflammasome in DC although this activation is dispensable for antigen specific T_h1 and T_h17 polarization (Kumar et al., 2009). Fungal structures recognized by NLRP3 may include surface carbohydrates, fungal DNA, or a fungal-induced host factor signifying tissue damage such as ATP. NLRP3 agonists such as aluminum hydroxide have been in use as vaccine adjuvants for decades, thus discerning the mechanism of fungal-induced NLPR3 activation could enhance future vaccine designs against fungi and other pathogens.

Fungal Vaccine strategies targeting DC

Only a single clinical trial evaluating efficacy of a fungal vaccine has been completed in humans (Pappagianis, 1993). A new interest in fungal vaccine development has accompanied the growing knowledge illuminating the critical determinants of host defense against fungal pathogens. More importantly, recent work suggests that it will be possible to create an anti-fungal vaccine that grants protection against multiple fungal pathogens (Wuthrich et al., 2011; Stuehler et al., 2011). At the core of host resistance to fungi, is the induction of strong cellular immunity via appropriate activation of DC. Anti-viral and anti-tumor vaccine strategies have leveraged the central role of DC in priming CTL by first priming autologous monocyte-derived DC with the desired antigen ex vivo before re-administering the loaded DC to the host. In animal models, DC primed with fungi ex vivo promote antifungal immunity in naïve mice. Similarly, DC transfected with fungal RNA ex vivo express fungal proteins on their

surface and promote the development of protective T cell responses (Bozza et al., 2004). These procedures are time-consuming, expensive and for those reasons they are unlikely to be widely adopted in clinical medicine. However, recent technological advances in antigen delivery combined with a greater understanding of DC biology, should allow for effective targeting and loading of DC with immunogenic antigen in vivo.

Because of the dense network of DC in the skin, the lung, and the intestine, vaccine delivery systems that target these DC networks may be more potent (Fig 3). Indeed, when comparing influenza vaccine injection routes, intradermal injection was more than twice as potent at eliciting antibodies than subcutaneous administration in individuals between 18 and 60 years of age (Belshe et al., 2004). A current Phase I clinical trial expected to be completed in early 2012 is evaluating the safety of intravaginal application of a virosome-based recombinant Sap2 therapeutic vaccine against recurrent vulvovaginal candidiasis (VVC) (NCT01067131). Pre-clinical trials in mice demonstrated rapid clearance of Candida and protection from reoccurrence in a murine VVC model following intravaginal administration of the vaccine (Sandini et al., 2011). However, vaccination at these DC rich sites may not represent a universal approach to vaccination against fungi. For example, a live attenuated strain of B. dermatitidis engendered full protection when administered subcutaneously but not when administered intranasally against a lethal pulmonary challenge in mice (Wuthrich et al., 2000). Correspondingly, $CCR2^{-/-}$ mice lacking monocyte-derived inflammatory DC had impaired clearance of A. fumigatus from the lung but not the spleen demonstrating an organ specific role for this DC subset (Hohl et al., 2009). The tissue microenvironment also modulates the function of DC subsets and influences the ability of DC to prime effective T cell responses. DC subsets in the spleen are able to drive T_h17 differentiation in the absence of IL-6 whereas DC from the skin and the gut require IL-6 to drive T_h17 polarization (Hu et al., 2011). This suggests that fungal vaccines will need

to factor in the effect of local cytokine generation when considering a route of vaccination. Thus, the DC subtypes and the tissue microenvironment at the vaccination site may critically modulate vaccine responses to fungal antigens.

A more direct method to target DC is to covalently attach antigen to DC-specific ligands. Fungal pathogens contain substantially mannosylated proteins which are effectively endocytosed by DC via CLR. In fact, mannosylation of the model antigen OVA greatly enhanced its immunogenicity at least in part by increasing its uptake by DC via CLR family members CD206 and DC-SIGN (CD209) (Lam et al., 2007). Other fungal carbohydrates also effectively target antigen to DC. For example, antigen loaded β-glucan particles are actively taken up by DC in a dectin-1 dependent manner. OVA-laden-β-glucan-particle exposed DC were more potent at inducing proliferation of OVA specific $CD4^+$ and $CD8^+$ T cells in vitro compared with soluble OVA (Huang et al., 2010). Furthermore, subcutaneous administration of OVA-laden-β-glucan-particles induced higher OVA-specific T cell polarization toward a T_h1 and T_h17 phenotype than alum-adsorbed OVA and induced the secretion of OVA-specific T_h1 associated IgG2c antibodies. Incredibly, fungi themselves are now being exploited to take advantage of direct targeting and robust activation of DC via the β-glucan/Dectin-1 interaction. In whole recombinant yeast immunization, antigen-expressing S. cerevisiae yeast (which display β-glucan on their surface) are administered to with the goal of eliciting antigen-specific host $CD4^+$ and $CD8^+$ T cell responses (Stubbs et al., 2001). Completed Phase I trials indicate that S. cerevisiae based therapies are safe and well tolerated in humans with Phase II trials currently ongoing (NCT00124215).

A complementary approach to whole recombinant yeast immunization involves the use of nanoparticles in targeting antigen to DC. Nanoparticles are internalized preferentially by DC due to their sub-micron size and can be more specifically targeted to DC through the addition of DC receptor targeting antibodies or DC receptor ligands to

their surface. Nanoparticle mediated targeting of DC enables the bundling of defined antigen or antigens with an adjuvant and a DC receptor targeting molecule allowing for precise delivery to DC. The elegance of this approach was recently demonstrated using a DEC205 F(ab')2 fragment coated nanoparticle containing TLR3, TLR7, & TLR8 ligands and OVA antigen (Tacken et al., 2011). This nanoparticle was designed to target DEC205^{+} DC and to simultaneously deliver the antigen and TLR ligand adjuvant. Targeting of the particles to DC enhanced their immunogenicity, encapsulating the antigen (OVA) increased the potency of the antigen, and co-delivering TLR ligands blocked the development of tolerance and reduced overall toxicity. In total, the study suggests that nanoparticles can deliver vaccine antigen to DC effectively, and that when antigen and adjuvant are delivered together, strong immune responses with limited toxicity can be induced. In a limited way, the targeting nanoparticle loaded with antigen and adjuvant begins to resemble the microbial vaccine target itself.

Since the surfaces of fungi are covered in polysaccharide, carbohydrate or glycoconjugate antigens are attractive targets for anti-fungal vaccine development. Vaccine strategies based on both the glucuronoxylomannan component of the cryptococcal polysaccharide capsule and β-1,3-glucan that is expressed by a broad range of fungi have demonstrated the ability to promote antibody mediated protection against fungal challenge. However, immunogenicity of glycoconjugates is unpredictable and the carbohydrate moiety is thought to be unable to be recognized by T cells directly. Novel findings using a defined glycoconjugate suggest that it is possible to design vaccines where T cells recognize the carbohydrate directly and that such glycoconjugates greatly enhance immunogenicity (Avci et al., 2011). It is tantalizing to speculate that fungal carbohydrates displayed by MHC II could be recognized by T cells in the same way. Immunization with glycosylated peptides was able to generate carbohydrate specific CTL responses (Abdel-Motal et al., 1996) suggesting that

appropriately designed glycoconjugates may be processed and cross-presented to $CD8^+$ T cells. As knowledge of cross-presentation by DC increases, it may be possible to generate fungal carbohydrate specific CTL responses against fungal pathogens. This may be advantageous in immune deficient patients lacking $CD4^+$ T cells, where CD8 T cells compensate and mediate vaccine-induced resistance to pathogenic fungi (Wuthrich et al., 2003).

Conclusions

In this review, we have highlighted the role of diverse DC subsets in anti-fungal immunity and discussed potential strategies to target DC in the generation of novel anti-fungal vaccines. Vaccines may be targeted to DC via interactions with surface receptors or via routes of administration and activate DC through PRR. New vaccine construction technologies expand the available pool of fungal antigens to induce cell-mediated immunity to include carbohydrates and reduce toxicity. Continuing to unearth the central role of DC in anti-fungal immunity will suggest new avenues to develop effective anti-fungal vaccines.

FIGURE LEGENDS

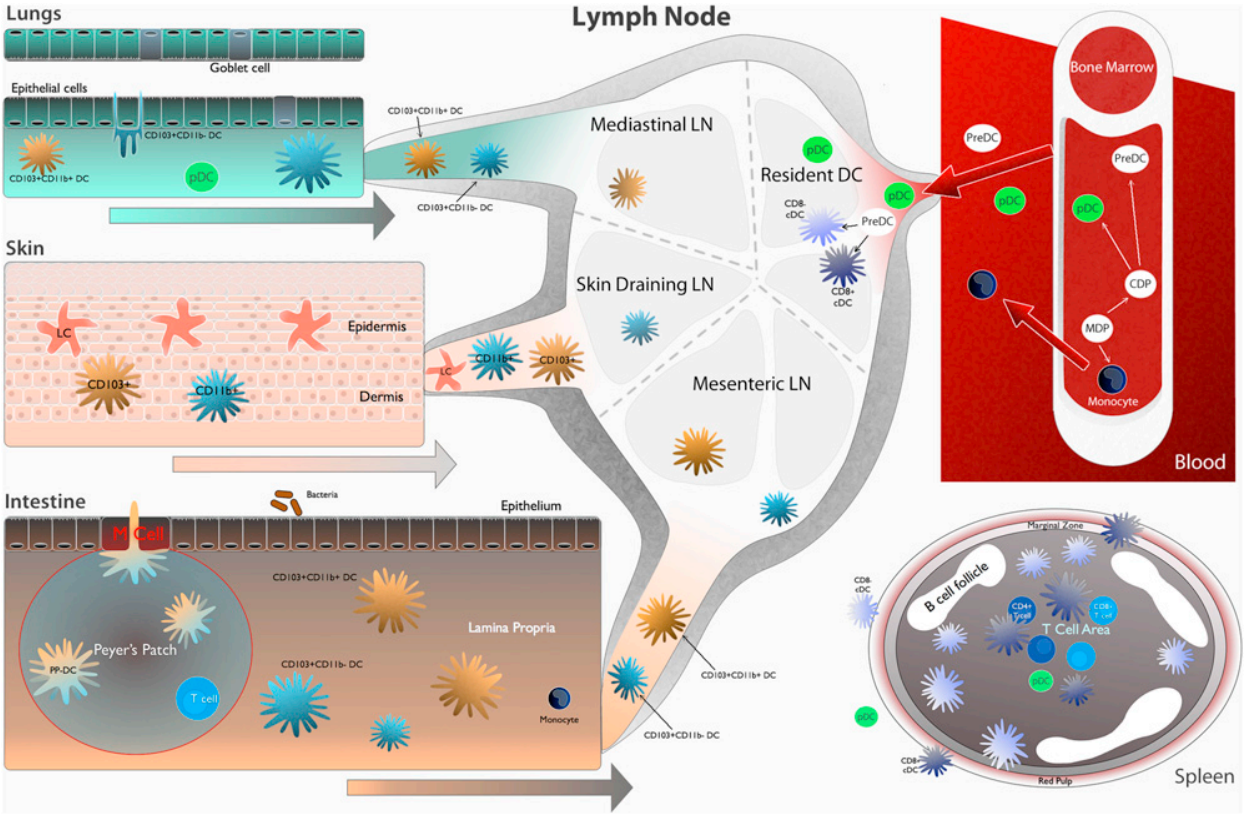

Figure AI-1. Location of DC subsets important in anti-fungal immunity.

DC subsets and monocytes arise from a common precursor in the bone marrow. pDC, monocytes, and PreDC exit the bone marrow and circulate via the blood. Resident CD8+ and CD8- DC exist in the spleen and the lymph node. PreDC seed the lungs, skin, and intestine and give rise to DC subsets in those locations. Migratory DC subsets migrate from peripheral locations to draining lymph nodes where they interact and prime T cells. In the lungs, CD103+ DC sample antigen from the airway lumen via paracellular processes. CD11b+ DC and CD103+ DC migrate to mediastinal lymph nodes. The epidermis of the skin contains a unique DC subset, Langerhans cells (LC) that are seeded in utero and self-renew. LC sample antigen and migrate via the dermis to skin draining lymph nodes. Dermal DC also migrate to skin draining lymph nodes. In the intestine, DC exist in the Peyer's Patch (PP) and the lamina propria (LP). PP-DC

sample antigen using transcellular processes from the intestinal lumen following which they migrate to the T cell rich area of the PP where PP-DC prime T cells. LP-DC subsets migrate to the mesenteric lymph node following antigen sampling. During inflammation, monocytes enter inflamed tissue and differentiate into monocyte-derived DC (Mo-DC) which then carry antigen to draining lymph nodes.

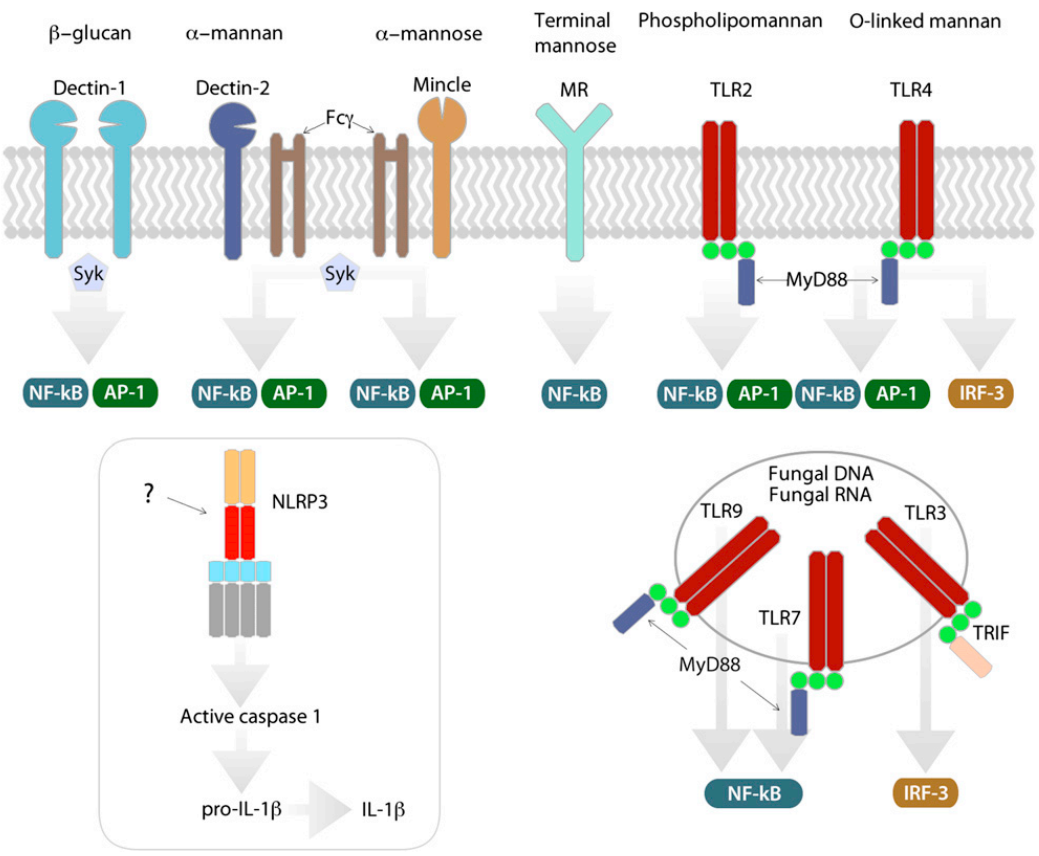

Figure AI-2. Recognition of fungi via DC PRR.

TLR and CLR. Fungal PAMP are recognized by several PRR: Dectin-1 signals via Syk following recognition of β–glucan. Dectin-2 and Mincle, which also signal via Syk following recruitment of Fcγ, recognize alpha-mannan and alpha mannose respectively. Signaling downstream of the mannose receptor (MR) is undefined. TLR and CLR signaling results in downstream activation of NF-κB or AP-1. Some TLR signaling activates IRF3. While fungi activate the NLRP3 inflammasome, the mechanism is undefined. TLR recognize fungal carbohydrates, fungal DNA, and fungal RNA at the DC surface or in endosomal compartments.

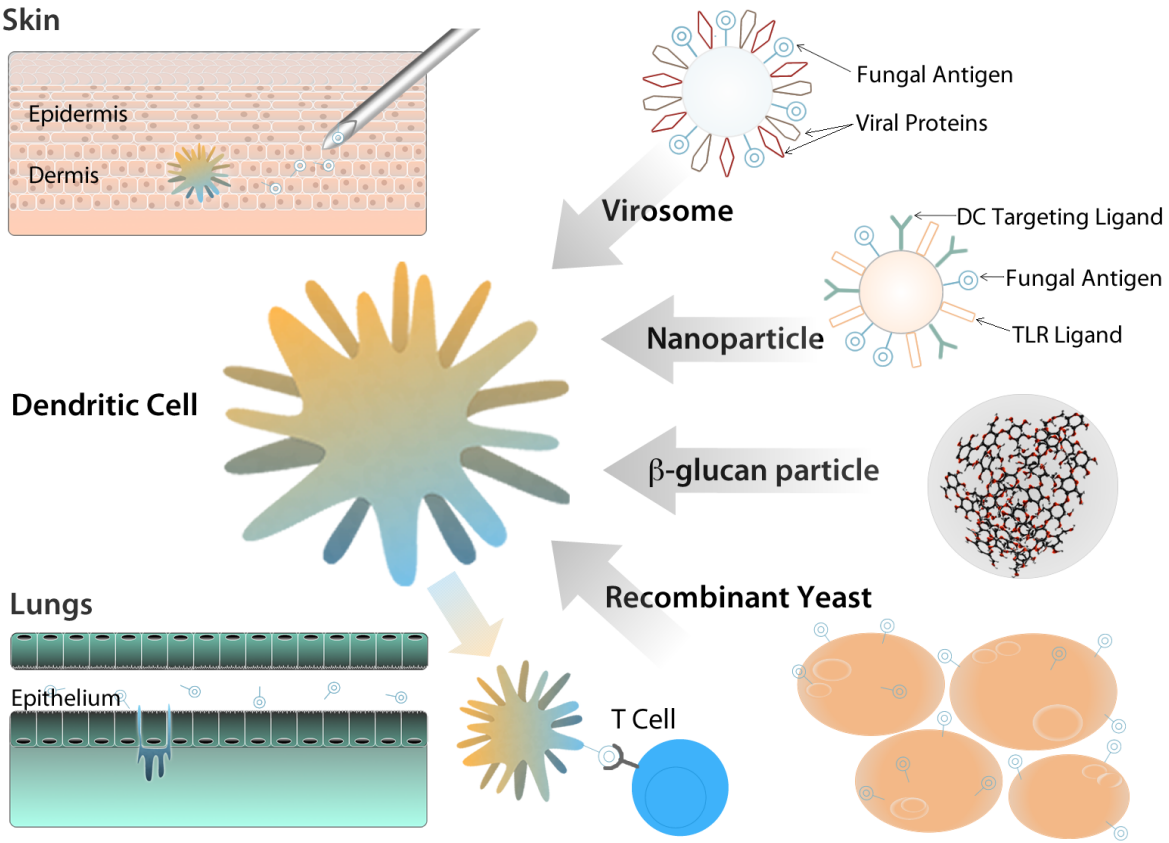

Figure AI-3. DC-based strategies for developing anti-fungal vaccines.

DC subsets may be targeted by varying the route of administration; aerosols target lung DC subsets, intradermal injection targets skin DC. DC can be loaded directly ex vivo before transfer into the host. Recombinant yeast contain ligands recognized by DC and allow for efficient DC uptake of antigen expressing organisms. β–glucan particles robustly activate DC via dectin–1. Virosomes also contain DC targeting ligands and viral PRR ligands that activate DC. Nanoparticles represent a complete engineering solution that incorporate PRR ligands, DC targeting ligands, and vaccine antigens. Following DC targeting, mature DC present antigen and activate naïve T cells.

ACKNOWLEDGEMENTS

Supported by grants from the USPHS to BK and NIEHS to RR. We thank Dr. Carrie Roy for her assistance with graphic design and illustration.

REFERENCES

Abdel-Motal, U. M., Berg, L., Rosen, A., Bengtsson, M., Thorpe, C. J., Kihlberg, J., Dahmen, J., Magnusson, G., Karlsson, K. A., and Jondal, M. (1996). Immunization with glycosylated Kb-binding peptides generates carbohydrate-specific, unrestricted cytotoxic T cells. Eur J Immunol 26, 544-551.

Allan, R. S., Waithman, J., Bedoui, S., Jones, C. M., Villadangos, J. A., Zhan, Y., Lew, A. M., Shortman, K., Heath, W. R., and Carbone, F. R. (2006). Migratory dendritic cells transfer antigen to a lymph node-resident dendritic cell population for efficient CTL priming. Immunity 25, 153-162.

Avci, F. Y., Li, X., Tsuji, M., and Kasper, D. L. (2011). A mechanism for glycoconjugate vaccine activation of the adaptive immune system and its implications for vaccine design. Nat Med 17, 1602-1609.

Backer, R., van Leeuwen, F., Kraal, G., and den Haan, J. M. (2008). CD8- dendritic cells preferentially cross-present Saccharomyces cerevisiae antigens. Eur J Immunol 38, 370-380.

Banchereau, J., and Steinman, R. M. (1998). Dendritic cells and the control of immunity. Nature 392, 245-252.

Beaty, S. R., Rose, C. E. J., and Sung, S. S. (2007). Diverse and potent chemokine production by lung CD11bhigh dendritic cells in homeostasis and in allergic lung inflammation. J Immunol 178, 1882-1895.

Belshe, R. B., Newman, F. K., Cannon, J., Duane, C., Treanor, J., Van Hoecke, C., Howe, B. J., and Dubin, G. (2004). Serum antibody responses after intradermal vaccination against influenza. N Engl J Med 351, 2286-2294.

Benjamin, D. K. J., Stoll, B. J., Gantz, M. G., Walsh, M. C., Sanchez, P. J., Das, A., Shankaran, S., Higgins, R. D., Auten, K. J., Miller, N. A., Walsh, T. J., Laptook, A. R., Carlo, W. A., Kennedy, K. A., Finer, N. N., Duara, S., Schibler, K., Chapman, R. L., Van Meurs, K. P., Frantz, I. D. r., Phelps, D. L., Poindexter, B. B., Bell, E. F., O'Shea, T. M., Watterberg, K. L., and Goldberg, R. N. (2010). Neonatal candidiasis: epidemiology, risk factors, and clinical judgment. Pediatrics 126, e865-73.

Bitar, D., Van Cauteren, D., Lanternier, F., Dannaoui, E., Che, D., Dromer, F., Desenclos, J. C., and Lortholary, O. (2009). Increasing incidence of zygomycosis (mucormycosis), France, 1997-2006. Emerg Infect Dis 15, 1395-1401.

Bozza, S., Montagnoli, C., Gaziano, R., Rossi, G., Nkwanyuo, G., Bellocchio, S., and Romani, L. (2004). Dendritic cell-based vaccination against opportunistic fungi. Vaccine *22*, 857-864.

Bourgeois, C., Majer, O., Frohner, I. E., Lesiak-Markowicz, I., Hildering, K. S., Glaser, W., Stockinger, S., Decker, T., Akira, S., Muller, M., and Kuchler, K. (2011). Conventional dendritic cells mount a type I IFN response against Candida spp. requiring novel phagosomal TLR7-mediated IFN-beta signaling. J Immunol 186, 3104-3112.

Brown, G. D. (2011). Innate antifungal immunity: the key role of phagocytes. Annu. Rev. Immunol. *29*, 1-21.

Brown, G. D., and Gordon, S. (2001). Immune recognition. A new receptor for beta-glucans. Nature 413, 36-37.

Chorro, L., Sarde, A., Li, M., Woollard, K. J., Chambon, P., Malissen, B., Kissenpfennig, A., Barbaroux, J. B., Groves, R., and Geissmann, F. (2009). Langerhans cell (LC) proliferation mediates neonatal development, homeostasis, and inflammation-associated expansion of the epidermal LC network. J Exp Med 206, 3089-3100.

del Rio, M. L., Rodriguez-Barbosa, J. I., Kremmer, E., and Forster, R. (2007). CD103- and CD103+ bronchial lymph node dendritic cells are specialized in presenting and cross-presenting innocuous antigen to CD4+ and CD8+ T cells. J Immunol 178, 6861-6866.

den Haan, J. M., Lehar, S. M., and Bevan, M. J. (2000). CD8(+) but not CD8(-) dendritic cells cross-prime cytotoxic T cells in vivo. J Exp Med 192, 1685-1696.

Denning, T. L., Norris, B. A., Medina-Contreras, O., Manicassamy, S., Geem, D., Madan, R., Karp, C. L., and Pulendran, B. (2011). Functional specializations of intestinal dendritic cell and macrophage subsets that control Th17 and regulatory T cell responses are dependent on the T cell/APC ratio, source of mouse strain, and regional localization. J Immunol 187, 733-747.

Desch, A. N., Randolph, G. J., Murphy, K., Gautier, E. L., Kedl, R. M., Lahoud, M. H., Caminschi, I., Shortman, K., Henson, P. M., and Jakubzick, C. V. (2011). CD103+ pulmonary dendritic cells preferentially acquire and present apoptotic cell-associated antigen. J Exp Med 208, 1789-1797.

Dillon, S., Agrawal, S., Banerjee, K., Letterio, J., Denning, T. L., Oswald-Richter, K., Kasprowicz, D. J., Kellar, K., Pare, J., van Dyke, T., Ziegler, S., Unutmaz, D., and Pulendran, B. (2006). Yeast zymosan, a stimulus for TLR2 and dectin-1, induces regulatory antigen-presenting cells and immunological tolerance. J Clin Invest 116, 916-928.

Dominguez, P. M., and Ardavin, C. (2010). Differentiation and function of mouse monocyte-derived dendritic cells in steady state and inflammation. Immunol Rev 234, 90-104.

Dudziak, D., Kamphorst, A. O., Heidkamp, G. F., Buchholz, V. R., Trumpfheller, C., Yamazaki, S., Cheong, C., Liu, K., Lee, H. W., Park, C. G., Steinman, R. M., and Nussenzweig, M. C. (2007). Differential antigen processing by dendritic cell subsets in vivo. Science 315, 107-111.

Edwards, A. D., Diebold, S. S., Slack, E. M., Tomizawa, H., Hemmi, H., Kaisho, T., Akira, S., and Reis e Sousa, C. (2003). Toll-like receptor expression in murine DC subsets: lack of TLR7 expression by CD8 alpha+ DC correlates with unresponsiveness to imidazoquinolines. Eur J Immunol 33, 827-833.

Ersland, K., Wuthrich, M., and Klein, B. S. (2010). Dynamic interplay among monocyte-derived, dermal, and resident lymph node dendritic cells during the generation of

vaccine immunity to fungi. Cell Host Microbe 7, 474-487.

Fogg, D. K., Sibon, C., Miled, C., Jung, S., Aucouturier, P., Littman, D. R., Cumano, A., and Geissmann, F. (2006). A clonogenic bone marrow progenitor specific for macrophages and dendritic cells. Science 311, 83-87.

Geissmann, F., Jung, S., and Littman, D. R. (2003). Blood monocytes consist of two principal subsets with distinct migratory properties. Immunity 19, 71-82.

Ginhoux, F., Collin, M. P., Bogunovic, M., Abel, M., Leboeuf, M., Helft, J., Ochando, J., Kissenpfennig, A., Malissen, B., Grisotto, M., Snoeck, H., Randolph, G., and Merad, M. (2007). Blood-derived dermal langerin+ dendritic cells survey the skin in the steady state. J Exp Med 204, 3133-3146.

Henri, S., Guilliams, M., Poulin, L. F., Tamoutounour, S., Ardouin, L., Dalod, M., and Malissen, B. (2010a). Disentangling the complexity of the skin dendritic cell network. Immunol Cell Biol 88, 366-375.

Henri, S., Poulin, L. F., Tamoutounour, S., Ardouin, L., Guilliams, M., de Bovis, B., Devilard, E., Viret, C., Azukizawa, H., Kissenpfennig, A., and Malissen, B. (2010b). CD207+ CD103+ dermal dendritic cells cross-present keratinocyte-derived antigens irrespective of the presence of Langerhans cells. J Exp Med 207, 189-206.

Hise, A. G., Tomalka, J., Ganesan, S., Patel, K., Hall, B. A., Brown, G. D., and Fitzgerald, K. A. (2009). An essential role for the NLRP3 inflammasome in host defense against the human fungal pathogen Candida albicans. Cell Host Microbe 5, 487-497.

Hohl, T. M., Rivera, A., Lipuma, L., Gallegos, A., Shi, C., Mack, M., and Pamer, E. G. (2009). Inflammatory monocytes facilitate adaptive CD4 T cell responses during respiratory fungal infection. Cell Host Microbe 6, 470-481.

Hsieh, S. H., Lin, J. S., Huang, J. H., Wu, S. Y., Chu, C. L., Kung, J. T., and Wu-Hsieh, B. A. (2011). Immunization with apoptotic phagocytes containing Histoplasma capsulatum activates functional CD8(+) T cells to protect against histoplasmosis. Infect Immun 79, 4493-4502.

Hu, W., Troutman, T. D., Edukulla, R., and Pasare, C. (2011). Priming microenvironments dictate cytokine requirements for T helper 17 cell lineage commitment. Immunity 35, 1010-1022.

Huang, H., Ostroff, G. R., Lee, C. K., Specht, C. A., and Levitz, S. M. (2010). Robust stimulation of humoral and cellular immune responses following vaccination with antigen-loaded beta-glucan particles. MBio 1 (3), e00164-10.

Idoyaga, J., Suda, N., Suda, K., Park, C. G., and Steinman, R. M. (2009). Antibody to Langerin/CD207 localizes large numbers of CD8alpha+ dendritic cells to the marginal zone of mouse spleen. Proc Natl Acad Sci U S A 106, 1524-1529.

Igyarto, B. Z., Haley, K., Ortner, D., Bobr, A., Gerami-Nejad, M., Edelson, B. T., Zurawski, S. M., Malissen, B., Zurawski, G., Berman, J., and Kaplan, D. H. (2011). Skin-resident murine dendritic cell subsets promote distinct and opposing antigen-specific T helper cell responses. Immunity 35, 260-272.

Jahnsen, F. L., Strickland, D. H., Thomas, J. A., Tobagus, I. T., Napoli, S., Zosky, G. R., Turner, D. J., Sly, P. D., Stumbles, P. A., and Holt, P. G. (2006). Accelerated antigen sampling and transport by airway mucosal dendritic cells following inhalation of a bacterial stimulus. J Immunol 177, 5861-5867.

Kumar, H., Kumagai, Y., Tsuchida, T., Koenig, P. A., Satoh, T., Guo, Z., Jang, M. H., Saitoh, T., Akira, S., and Kawai, T. (2009). Involvement of the NLRP3 inflammasome in innate and humoral adaptive immune responses to fungal beta-glucan. J Immunol 183, 8061-8067.

Lam, J. S., Huang, H., and Levitz, S. M. (2007). Effect of differential N-linked and O-linked mannosylation on recognition of fungal antigens by dendritic cells. PLoS One 2, e1009.

Leibundgut-Landmann, S., Osorio, F., Brown, G. D., and Reis, E. S. C. (2008). Stimulation of dendritic cells via the Dectin-1 / Syk pathway allows priming of cytotoxic T cell responses. Blood 112, 4971-4980.

Lelouard, H., Fallet, M., de Bovis, B., Meresse, S., and Gorvel, J. P. (2011). Peyer's Patch Dendritic Cells Sample Antigens by Extending Dendrites Through M Cell-Specific Transcellular Pores. Gastroenterology, ePub Dec 7 2011.

Li, H. S., Gelbard, A., Martinez, G. J., Esashi, E., Zhang, H., Nguyen-Jackson, H., Liu, Y. J., Overwijk, W. W., and Watowich, S. S. (2011). Cell-intrinsic role for IFN-alpha-STAT1 signals in regulating murine Peyer patch plasmacytoid dendritic cells and conditioning an inflammatory response. Blood 118, 3879-3889.

Lin, J. S., Yang, C. W., Wang, D. W., and Wu-Hsieh, B. A. (2005). Dendritic cells cross-present exogenous fungal antigens to stimulate a protective CD8 T cell response in infection by Histoplasma capsulatum. J Immunol 174, 6282-6291.

Liu, K., and Nussenzweig, M. C. (2010). Origin and development of dendritic cells. Immunol Rev 234, 45-54.

Liu, K., Victora, G. D., Schwickert, T. A., Guermonprez, P., Meredith, M. M., Yao, K., Chu, F. F., Randolph, G. J., Rudensky, A. Y., and Nussenzweig, M. (2009). In vivo analysis of dendritic cell development and homeostasis. Science 324, 392-397.

Luber, C. A., Cox, J., Lauterbach, H., Fancke, B., Selbach, M., Tschopp, J., Akira, S., Wiegand, M., Hochrein, H., O'Keeffe, M., and Mann, M. (2010). Quantitative proteomics reveals subset-specific viral recognition in dendritic cells. Immunity 32, 279-289.

Means, T. K., Mylonakis, E., Tampakakis, E., Colvin, R. A., Seung, E., Puckett, L., Tai, M. F., Stewart, C. R., Pukkila-Worley, R., Hickman, S. E., Moore, K. J., Calderwood, S. B., Hacohen, N., Luster, A. D., and El Khoury, J. (2009). Evolutionarily conserved recognition and innate immunity to fungal pathogens by the scavenger receptors SCARF1 and CD36. J Exp Med 206, 637-653.

Nakamura, K., Miyazato, A., Xiao, G., Hatta, M., Inden, K., Aoyagi, T., Shiratori, K., Takeda, K., Akira, S., Saijo, S., Iwakura, Y., Adachi, Y., Ohno, N., Suzuki, K., Fujita, J., Kaku, M., and Kawakami, K. (2008). Deoxynucleic acids from Cryptococcus

neoformans activate myeloid dendritic cells via a TLR9-dependent pathway. J Immunol 180, 4067-4074.

Netea, M. G., Sutmuller, R., Hermann, C., Van der Graaf, C. A., Van der Meer, J. W., van Krieken, J. H., Hartung, T., Adema, G., and Kullberg, B. J. (2004). Toll-like receptor 2 suppresses immunity against Candida albicans through induction of IL-10 and regulatory T cells. J Immunol 172, 3712-3718.

Neumann, A. K., and Jacobson, K. (2010). A novel pseudopodial component of the dendritic cell anti-fungal response: the fungipod. PLoS Pathog 6, e1000760.

Osterholzer, J. J., Chen, G. H., Olszewski, M. A., Curtis, J. L., Huffnagle, G. B., and Toews, G. B. (2009). Accumulation of CD11b+ lung dendritic cells in response to fungal infection results from the CCR2-mediated recruitment and differentiation of Ly-6Chigh monocytes. J Immunol 183, 8044-8053.

Pappagianis, D. (1993). Evaluation of the protective efficacy of the killed Coccidioides immitis spherule vaccine in humans. The Valley Fever Vaccine Study Group. Am Rev Respir Dis *148*, 656-660.

Pfaller, M. A., and Diekema, D. J. (2007). Epidemiology of invasive candidiasis: a persistent public health problem. Clin Microbiol Rev 20, 133-163.

Ramirez-Ortiz, Z. G., Lee, C. K., Wang, J. P., Boon, L., Specht, C. A., and Levitz, S. M. (2011). A nonredundant role for plasmacytoid dendritic cells in host defense against the human fungal pathogen Aspergillus fumigatus. Cell Host Microbe 9, 415-424.

Ramirez-Ortiz, Z. G., Specht, C. A., Wang, J. P., Lee, C. K., Bartholomeu, D. C., Gazzinelli, R. T., and Levitz, S. M. (2008). Toll-like receptor 9-dependent immune activation by unmethylated CpG motifs in Aspergillus fumigatus DNA. Infect Immun 76, 2123-2129.

Rivera, A., Ro, G., Van Epps, H. L., Simpson, T., Leiner, I., Sant'Angelo, D. B., and Pamer, E. G. (2006). Innate immune activation and CD4+ T cell priming during respiratory fungal infection. Immunity 25, 665-675.

Robinson, M. J., Osorio, F., Rosas, M., Freitas, R. P., Schweighoffer, E., Gross, O., Verbeek, J. S., Ruland, J., Tybulewicz, V., Brown, G. D., Moita, L. F., Taylor, P. R., and Reis e Sousa, C. (2009). Dectin-2 is a Syk-coupled pattern recognition receptor crucial for Th17 responses to fungal infection. J Exp Med 206, 2037-2051.

Said-Sadier, N., Padilla, E., Langsley, G., and Ojcius, D. M. (2010). Aspergillus fumigatus stimulates the NLRP3 inflammasome through a pathway requiring ROS production and the Syk tyrosine kinase. PLoS One 5, e10008.

Sandini, S., La Valle, R., Deaglio, S., Malavasi, F., Cassone, A., and De Bernardis, F. (2011). A highly immunogenic recombinant and truncated protein of the secreted aspartic proteases family (rSap2t) of Candida albicans as a mucosal anticandidal vaccine. FEMS Immunol Med Microbiol 62, 215-224.

Sczesnak, A., Segata, N., Qin, X., Gevers, D., Petrosino, J. F., Huttenhower, C., Littman, D. R., and Ivanov, I. I. (2011). The genome of th17 cell-inducing segmented

filamentous bacteria reveals extensive auxotrophy and adaptations to the intestinal environment. Cell Host Microbe 10, 260-272.

Sousa Mda, G., Reid, D. M., Schweighoffer, E., Tybulewicz, V., Ruland, J., Langhorne, J., Yamasaki, S., Taylor, P. R., Almeida, S. R., and Brown, G. D. (2011). Restoration of pattern recognition receptor costimulation to treat chromoblastomycosis, a chronic fungal infection of the skin. Cell Host Microbe 9, 436-443.

Steinman, R. M., and Cohn, Z. A. (1973). Identification of a novel cell type in peripheral lymphoid organs of mice. I. Morphology, quantitation, tissue distribution. J Exp Med 137, 1142-1162.

Stubbs, A. C., Martin, K. S., Coeshott, C., Skaates, S. V., Kuritzkes, D. R., Bellgrau, D., Franzusoff, A., Duke, R. C., and Wilson, C. C. (2001). Whole recombinant yeast vaccine activates dendritic cells and elicits protective cell-mediated immunity. Nat Med 7, 625-629.

Stuehler, C., Khanna, N., Bozza, S., Zelante, T., Moretti, S., Kruhm, M., Lurati, S., Conrad, B., Worschech, E., Stevanovic, S., Krappmann, S., Einsele, H., Latge, J. P., Loeffler, J., Romani, L., and Topp, M. S. (2011). Cross-protective TH1 immunity against Aspergillus fumigatus and Candida albicans. Blood *117*, 5881-5891.

Sung, S. S., Fu, S. M., Rose, C. E. J., Gaskin, F., Ju, S. T., and Beaty, S. R. (2006). A major lung CD103 (alphaE)-beta7 integrin-positive epithelial dendritic cell population expressing Langerin and tight junction proteins. J Immunol 176, 2161-2172.

Szymczak, W. A., and Deepe, G. S. J. (2009). The CCL7-CCL2-CCR2 axis regulates IL-4 production in lungs and fungal immunity. J Immunol 183, 1964-1974.

Szymczak, W. A., and Deepe, G. S. J. (2010). Antigen-presenting dendritic cells rescue CD4-depleted CCR2-/- mice from lethal Histoplasma capsulatum infection. Infect Immun 78, 2125-2137.

Taborda, C. P., and Casadevall, A. (2002). CR3 (CD11b/CD18) and CR4 (CD11c/CD18) are involved in complement-independent antibody-mediated phagocytosis of Cryptococcus neoformans. Immunity 16, 791-802.

Tacken, P. J., Zeelenberg, I. S., Cruz, L. J., van Hout-Kuijer, M. A., van de Glind, G., Fokkink, R. G., Lambeck, A. J., and Figdor, C. G. (2011). Targeted delivery of Toll-like receptor ligands to human and mouse dendritic cells strongly enhances adjuvanticity. Blood ePub Oct 3 2001.

Takagi, H., Fukaya, T., Eizumi, K., Sato, Y., Sato, K., Shibazaki, A., Otsuka, H., Hijikata, A., Watanabe, T., Ohara, O., Kaisho, T., Malissen, B., and Sato, K. (2011). Plasmacytoid Dendritic Cells Are Crucial for the Initiation of Inflammation and T Cell Immunity In Vivo. Immunity, 35, 958-71.

Wuthrich, M., Filutowicz, H. I., and Klein, B. S. (2000). Mutation of the WI-1 gene yields an attenuated blastomyces dermatitidis strain that induces host resistance. J Clin Invest 106, 1381-1389.

Wuthrich, M., Filutowicz, H. I., Warner, T., and Klein, B. S. (2002). Requisite elements in

vaccine immunity to Blastomyces dermatitidis: plasticity uncovers vaccine potential in immune-deficient hosts. J. Immunol. *169*, 6969-6976.

Wuthrich, M., Filutowicz, H. I., Warner, T., Deepe, G. S. J., and Klein, B. S. (2003). Vaccine immunity to pathogenic fungi overcomes the requirement for CD4 help in exogenous antigen presentation to CD8+ T cells: implications for vaccine development in immune-deficient hosts. J Exp Med 197, 1405-1416.

Wuthrich, M., Gern, B., Hung, C. Y., Ersland, K., Rocco, N., Pick-Jacobs, J., Galles, K., Filutowicz, H., Warner, T., Evans, M., Cole, G., and Klein, B. (2011). Vaccine-induced protection against 3 systemic mycoses endemic to North America requires Th17 cells in mice. J Clin Invest 121, 554-568.

Zelante, T., De Luca, A., Bonifazi, P., Montagnoli, C., Bozza, S., Moretti, S., Belladonna, M. L., Vacca, C., Conte, C., Mosci, P., Bistoni, F., Puccetti, P., Kastelein, R. A., Kopf, M., and Romani, L. (2007). IL-23 and the Th17 pathway promote inflammation and impair antifungal immune resistance. Eur J Immunol 37, 2695-2706.

APPENDIX 2

Structure and function of a fungal adhesin that binds heparin and mimics thrombospondin-1 by blocking T cell activation

T. Tristan Brandhorst[1], René M. Roy[1,4,5], Marcel Wüethrich[1], Som Nanjappa[1], Marco Tonelli[6], Darrell McCaslin[6] and Bruce S. Klein[1,2,3]

[1]The Departments of Pediatrics, [2]Internal Medicine, and [3]Medical Microbiology and Immunology; [4]From the Cell and Molecular Biology Graduate Training Program; [5]the Medical Scientist Training Program, [6]Department of Biochemistry, and the University of Wisconsin-Madison College of Agriculture and Life Science and School of Medicine and Public Health, Madison, WI, 53792

ABSTRACT

Blastomyces adhesin-1 (BAD-1) is a 120-kD surface protein on *Blastomyces dermatitidis* yeast. We show that BAD-1 contains 41 tandem repeats and that deleting even half of them impairs fungal pathogenicity. By NMR, the repeats are tightly folded 17-amino acid loops constrained by a disulfide bond between conserved cysteines. Each loop contains a conserved WxxWxxW motif found in thrombospondin-1 (TSP-1) type 1 heparin-binding repeats. BAD-1 binds heparin specifically and saturably, and is competitively inhibited by soluble heparin, but not by related glycosaminoglycans. By surface plasmon resonance, the affinity of BAD-1 for heparin is 700nM ± 100nM. The putative heparin-biding motif of BAD-1 localizes within the tandem repeat's loop structure. A recombinant protein with 4 folded- and disulfide-constrained repeats bound heparin weakly, but reduction of its disulfide bonds restored binding to heparin. Like TSP-1, BAD-1 blocks T cell activation in a manner requiring the heparan sulfate-modified surface molecule CD47, impairing effector functions. The tandem repeats of BAD-1 thus confer pathogenicity, harbor a tryptophan-rich motif that binds heparin, and suppress T-cell activation via a CD47-dependent mechanism, mimicking TSP-1.

INTRODUCTION

The dimorphic fungus *Blastomyces dermatitidis* is endemic to the Ohio and Mississippi river valleys, where it is the causative agent of blastomycosis. Blastomycosis is one of the principal systemic mycoses of humans and animals worldwide, and results from the inhalation of spores and/or hyphal fragments released into the air by this soil-dwelling fungus. Pulmonary infections that go undiagnosed or untreated may progress and disseminate, leading to substantial morbidity and mortality even in immunocompetent hosts.

Blastomyces adhesin-1 (BAD-1) is a 120-kDa protein of *B. dermatitidis* that mediates multiple functions including adhesion, modulation of pro-inflammatory immune responses and virulence (Brandhorst et al, 2004; Finkel-Jimenez et al, 2001; Newman et al, 1995). A targeted deletion of BAD-1 sharply attenuates pathogenicity in a murine model of lethal pulmonary infection. BAD-1 expression is yeast-phase specific and is induced during the temperature-driven morphological transition of *B. dermatitidis* mold to yeast (Newman et al, 1995; Rooney et al, 2001). Following secretion, BAD-1 coats the yeast surface and mediates binding of yeast to macrophages by CD11b/CD18 (CR3) and CD14 receptors (Newman et al, 1995). This binding fosters entry into phagocytes (Newman et al, 1995), while inhibiting the release of pro-inflammatory cytokines such as TNF-α (Brandhorst et al, 2004; Finkel-Jimenez et al, 2001). Surface bound BAD-1 inhibits TNF-α release in a TGF-β dependent manner, while secreted BAD-1 does so in a manner that is independent of TGF-β (Finkel-Jimenez et al, 2002).

BAD-1 is composed of a short N-terminal region that harbors a secretion signal, an extensive core of tandem repeats that are responsible for adhesion (Hogan et al, 1995), and a C-terminal EGF-like domain that anchors the released protein on the yeast surface by binding chitin (Brandhorst & Klein, 2000). The number of tandem repeats varies between *B. dermatitidis* strains (Klein & Jones, 1990), but they typically comprise

over 80% of the protein's primary sequence. The repeats share 20 strongly conserved amino acids, including two cysteines postulated to define a loop structure via disulfide bonding (Brandhorst et al, 2005). The tandem repeats bind divalent cations including calcium, zinc and copper (Brandhorst et al, 2005) (1:1 stoicheometry) and calcium binding enables the C-terminal EGF domain to fasten itself to exposed yeast cell-wall chitin. The binding of divalent cations and sequence similarities to the EF-hand of thrombospondin-1 (TSP-1), which is a multi-functional extracellular matrix protein (Brandhorst et al, 2005; Frazier, 1987), previously lead us to posit that the BAD-1 tandem repeats might coordinate divalent cations, triggering a conformational shift (Brandhorst et al, 2005). While we observed changes in the peptide mapping patterns of BAD-1 in the presence of calcium, elevated divalent cations unexpectedly failed to impact the secondary structure of the molecule as measured by circular dichroism and tryptophan fluorescence spectroscopy (Brandhorst et al, 2005). These findings prompted questions about the native structure of BAD-1.

In the present study, we sought to elucidate the 3-D structure of BAD-1 by NMR to gain deeper insight into the function of its tandem repeats in the pathogenesis of *B. dermatitidis* infection. By NMR, the repeats adopt a tightly folded 17-amino acid loop conformation, constrained by a disulfide bond between conserved cysteines. We found no evidence for a conformational shift upon interaction of the tandem repeats with divalent cations, nor evidence for an EF-hand structure. Rather, each tandem repeat loop contains the conserved WxxWxxW motif found in TSP-1 type 1 heparin-binding repeats. BAD-1 was found to bind to heparin specifically, saturably and with high affinity. Furthermore, a novel BAD-1 action involved suppression of T lymphocyte activation via interaction with heparan sulfate that decorates CD47 on T cells. Our work sheds new light on the structure and function of BAD-1 in virulence.

RESULTS

Primary structure of BAD-1

Our earlier descriptions of BAD-1 in *B. dermatitidis* ATCC strain 26199 identified 30 tandem repeats based on their adherence to a consensus sequence (Hogan et al, 1995). This criterion may have been unduly stringent. Reanalysis of the conserved residues in BAD-1 shows that the tandem repeat domain extends nearly to the N-terminus of the mature protein (Fig. 1A). This analysis identifies 41 tandem repeats based on conservation of the distance between cysteine pairs and the presence of strictly conserved histidine, tyrosine, and leucine residues (Fig. 1B). This contrasts with prior characterizations of the N-terminus, and highlights the extent to which the tandem repeats dominate the primary structure of the protein. Thus, BAD-1 may be characterized as having two domains: an exceptionally long tandem repeat domain and a chitin-binding, C-terminal EGF-like domain that fixes it to the yeast cell surface.

The tandem repeat mediates virulence

Since BAD-1 is an extended series of 41 tandem repeats with a short EGF-like C-terminal domain (Fig.1), and since the C-terminal domain has proven to be dispensable for pathogenicity (Brandhorst et al, 2003), we formally tested the role of the tandem repeats in virulence. To do so, we engineered a recombinant form of BAD-1 harboring only half the normal complement of tandem repeats and expressed this construct in a strain of *B. dermatitidis* ATCC 26199 from which native BAD-1 had been deleted. Two independently engineered strains (TrepeatΔ20-Y and TrepeatΔ20-AE) were selected for their capacity to display amounts of surface BAD-1 similar to strains expressing either the full-length protein (BAD1-6H-J and -AC) or BAD-1 with a deleted C-terminal region (ΔCterm-BN and -CJ) (Fig. S1). Each of these strains was compared in parallel for pathogenicity in a murine model of lethal pulmonary blastomycosis.

The transformed strains expressing the truncated forms of BAD-1 (TrepeatΔ20) were significantly less virulent than each strain expressing BAD-1 with the full complement of 41 repeats (Fig. 2). In contrast, the presence or absence of the C-terminal region had no significant impact on virulence in this model of infection as previously reported (Brandhorst et al, 2003). Thus, the tandem repeats of BAD-1 are required for pathogenicity in a murine model of lethal pulmonary infection.

Structure of the tandem repeat

Because of the functional significance of the tandem repeats, we sought structural insight into these domains in full length BAD-1 via NMR. The large size of the protein and peak overlap resulting from minor sequence variations between repeats made it difficult to elucidate the 3-D structure of the full-length protein. We therefore expressed a set of representative tandem repeats of identical sequence in *E. coli* (their sequence reflects the most prevalent amino acid in each position). The shortest recombinant protein that we could express in quantity contained four tandem repeats (TR4). Initially, TR4 displayed a random assortment of disulfide linkages, determined by variations in mobility by non-reducing PAGE, (Fig. S2). To correct this, TR4 was reduced, associated with an NiNTA column and then slowly refolded under a glutathione gradient (see Methods). After refolding, variations in mobility resolved into a single, predominant band (Fig. S2). Tryptic digests of TR4 in both refolded and reduced states were examined by LC-MS. Digests of refolded TR4 lacked the reduced versions of cysteine-containing peptides, confirming that the cysteines in TR4 are uniformly disulfide-linked. This was corroborated in NMR studies (below).

^{15}N HSQC NMR analysis of this refolded TR4 molecule produced a pattern of peaks amenable to interpretation, but which otherwise corresponded closely to the pattern of peaks derived from ^{15}N HSQC of full length native BAD-1 (Fig. 3 A-C). This established that the tandem repeats in the TR4 recombinant protein had been refolded

to successfully replicate the conformation of the native repeats, and that these repeats predominantly adopt one single, consistent conformation. Alternative conformations, if present, must be few in number so as to render their NMR signature undetectable.

Many residues of the four identical repeats in TR4 have very similar chemical shifts, resulting in peaks that overlap almost perfectly in the NMR spectra, but unfortunately this was not universally so. Furthermore, no evidence of interaction between repeat domains was found in the NMR spectra and the hinge regions between the tandem repeats were not resolvable via NMR (probably attributable to localized flexibility). These results suggest that TR4 does not adopt a unique tertiary fold in solution and precluded resolution of the molecule as a single homogenous structure. As an alternative, we calculated the 3-dimensional structure for a single, representative BAD-1 repeat. To this aim, the NOESY data derived from the residues of one tandem repeat was identified, compiled separately and submitted for algorithmic derivation of distance constraints and structural calculation. Accommodation of inconsistencies in NOE peak intensities derived from partial peak overlap required relaxation of NOE derived distance restraints (used for automatic calibration by CYANA), marginally increasing average distance limits. Nevertheless, this approach yielded a consistent, tightly folded 17 amino acid loop structure constrained at the base by a disulfide bond between the two conserved cysteines (Fig. 3D). The only reported secondary structure within this loop was in the WxxWxxW motif, which forms a short α-helix. Constraints are reported in Table 1.

The 3-D structure we determined for the tandem repeat is inconsistent with the calcium-binding EF-hand structure previously hypothesized (Brandhorst et al, 2005). Every acidic residue is externalized on the surface of the tandem repeat loop and they are not proximal to one another (Fig. 3E). Furthermore, the interior of the loop is densely occupied by aromatic residue side chains leaving no room for the pentagonal-

bipyramidal calcium-coordination structure typical of an EF-hand. Thus, the high-capacity, low-affinity calcium-binding function of BAD-1 is not derived from an EF-hand-like structure in the tandem repeats. Alternatively, individual repeats could offer bi-dentate interactions with calcium, so that coordination of ions between repeats remains a possibility.

Figure 3F is a composite of the twenty best predictions available from CYANA and illustrates the consistency of this model with regard to the structure of the tandem repeat loop. Variability is predominantly seen in the orientation of surface-exposed side-chains interacting with the solvent environment.

Predicted structure of full length BAD-1

Dynamic light scattering (DLS) data of two independent samples of BAD-1 showed size heterogeneity with polydispersity indices of 0.66 and 0.79, and corresponding hydrodynamic radii of 10±8 and 8±7 nm. The software analyzing size distribution resolves the data into populations of different size particles characterized by mean radii and standard deviations (17 measured correlation functions were individually analyzed; results are the averages of the fitted means and standard deviations). For both sets of data, the software identified a population accounting for ~70% of the scattering intensity with a mean radius of 7.2± 0.5 nm and mean standard deviation for the peak of 1.8± 0.7.

The measured hydrodynamic radius contains contributions from the protein, bound water of hydration, and shape factors (frictional coefficients) (Tanford, 1961). From the partial specific volume of BAD-1, the unhydrated molecule would have a spherical radius of 3.4 nm, which increases to 4.1 nm upon hydration. These computed values are smaller than the value measured by DLS. It would require a sphere containing 6 hydrated BAD-1 polypeptides as the diffusing complex to obtain the smallest, predominant hydrodynamic radius measurement. We attribute the large

measured radius to asymmetry in the shape of the molecule. The ratio of the measured radius to that of the sphere composed of a single hydrated BAD-1 molecule provides a quantitative estimate of this asymmetry, 1.8. The simplest models used to interpret hydrodynamic shapes are based on prolate and oblate ellipsoids of revolution. For an asymmetry of 1.8, a prolate ellipsoid would have semiaxes in the ratio of 15:1:1, (an oblate ellipsoid would have axes in a ratio of 20:20:1). These measurements suggest that the native conformation of the BAD-1 protein is extended, perhaps even rod-like.

NMR modeling depicts a structure for each repeat "loop" that is tightly folded, with 5 amino acids of flexible "hinge" between each one, like beads on a string. Given the results of DLS, it is likely that the hinge regions are afforded only limited flexibility and that the molecule exists in solution in an extended form (Fig. 3G). Energy minimization of the hinge regions of this model, constrained by the stearic limitations of the highly consistent tandem repeat "beads", tends to support the (theoretical) extended, α-helical conformation depicted.

A tryptophan rich motif in the tandem repeat

Each tandem repeat loop of BAD-1 contains a significant number of tryptophans (4 of 24 amino acids - 17%). Because of this, BAD-1 absorbs UV wavelengths exceptionally well and may be detected readily by its characteristic OD280. A 1mg/ml preparation of BAD-1 has an OD280 of over 6.6 absorbance units (Audet et al, 1997). The conserved arrangement of the tryptophans likewise stands out. With rare exception, three of the four tryptophans are arranged in a WxxWxxW motif. This motif is common to a number of glycosaminoglycan (GAG)-binding proteins, and is highly conserved within the type 1 heparin-binding repeats of TSP-1 (Guo et al, 1992).

We initially tested whether BAD-1 might bind GAGs in the extracellular matrix (ECM) by studying the adherence of yeast to Matrigel™, which contains heparan sulfate and other ECM proteins such as laminin, collagen IV and nidogen. *Blastomyces* yeast

bound Matrigel (Fig. 4A). Anti-BAD-1 antiserum blocked yeast binding to Matrigel (Fig. 4B), suggesting that binding is BAD-1 dependent. Yeast did not reproducibly bind highly purified ECM components laminin, collagen IV or nidogen, implying that other Matrigel constituents such as heparan sulfate proteoglycan might be a target of BAD-1.

Heparin binding by BAD-1

We investigated whether native BAD-1 protein could bind heparin. Initially purified BAD-1 was incubated with a heparin-coated agarose resin. Due to the strong UV absorbance of BAD-1, the percentage of BAD-1 that bound to resin could be assayed spectrophotometrically by measuring the OD280 of the aqueous phase before and after incubation. Heparin agarose resin pulled BAD-1 (100µl of 0.1mg/ml) out of solution, with a 20µl volume of resin absorbing nearly 100% of the soluble BAD-1. Binding was dependent upon resin-volume (0.5 - 1.5 µg BAD-1/µl resin) and saturable (Fig. 4C). In subsequent assays, we fluorescently tagged BAD-1 (eFluor605) to quantify binding via fluorescence spectroscopy. Labeling did not alter its binding characteristics since assays with unlabeled protein gave similar results (Fig. S3). Fluorescent BAD-1 bound avidly to heparin-agarose, but not to controls of unmodified agarose resin or resins coated with mannan, BSA or hemoglobin (Fig. 4D). We included the two latter controls since BAD-1 (Brandhorst et al, 2005) and heparin (Grant et al, 1992) both coordinate polyvalent cations and have the potential for non-specific association via polyvalent cation bridging (Uversky et al, 2001). BSA (Bal et al, 1998) and hemoglobin (Amiconi et al, 1981) also coordinate multiple polyvalent cations. Nevertheless, BAD-1 shows little affinity for these control resins, nor to the carbohydrate-rich mannan-agarose resin.

We assessed the specificity of the interaction between BAD-1 and immobilized heparin using soluble competitors (Fig. 4E). Pre-incubation of BAD-1 with soluble heparin diminished its binding to agarose-immobilized heparin in a concentration-dependent manner. Closely related GAGs, including chondroitin sulfate A and

hyaluronan, did not significantly inhibit the binding of BAD-1 to immobilized heparin (Fig. 4F). Dermatan sulfate, also called chondroitin sulfate B, inhibited only at the highest concentrations.

Determination of BAD-1 affinity for heparin by SPR

We measured the affinity of BAD-1 for immobilized heparin by SPR. Biotinylated heparin was affixed to streptavidin-coated SPR chips and the surface was exposed to serial dilutions of BAD-1 (1μM to 31.25nM). The response scaled with the concentration of BAD-1 applied (Fig. 5A). Washing with pH2 buffer + 4M NaCl removed a portion of BAD-1 from the heparin surface. Only during the surface "rebuilding" step, involving re-application of biotinylated heparin, did response levels return to baseline, presumably via soluble heparin inhibition of BAD-1 binding. BAD-1 binding (1μM) could be inhibited by pre-incubation with soluble heparin (100:1). Correcting for the shift in baseline response due to the refractive index of the inhibitor, heparin inhibition neutralizes 96% of the specific binding (Fig. 5A, thick trace).

Association and dissociation kinetics of SPR were modeled in BiaEvaluation 4.1. Analysis of the dissociation curves suggests that they are multiphasic. This complexity could reflect the heterogeneous nature of the surface due to the random nature of heparin biotinylation, or that BAD-1 presents multiple binding sites for heparin. Another possible explanation is that BAD-1 has an affinity not only for immobilized heparin, but also for tandem repeats engaged with heparin surfaces (addressed below).

Binding affinity was quantified by using the last few seconds of each association phase as an estimate of the steady state binding for each injected concentration of BAD-1. The steady state affinity model estimates both the affinity and maximum binding capacity of the surface. Figure 5B was derived from the data in panel A: the maximal binding to the surface was 5400 ± 500 response units. The affinity constant is 700 ± 100 nM. Further studies will allow us to refine the binding model and ascertain

the nature of any multi-valency.

Characterization of the interaction between BAD-1 and heparin

The interaction between heparin and TSP-1 involves an ionic component and may be inhibited by concentrations of NaCl above 350mM (Yabkowitz et al, 1989). We tested whether NaCl could similarly inhibit the binding of BAD-1 to heparin-agarose (Fig. S4A). Binding of BAD-1 to heparin fell sharply at 250mM NaCl and above, suggesting this interaction involves an ionic component. The binding of BAD-1 to heparin is maximal at low pH, it does not fall off substantially until pH 9 (Fig. S4B). and does not require polyvalent cations..

The interaction between TSP-1 and heparin is inhibited by peptides containing a WxxW motif (Guo et al, 1992); for example a peptide with the sequence SHWSPWSS. We used this peptide (and a control, mutant peptide with tryptophan residues replaced by glutamine) to test whether BAD-1 binds to the same site on heparin. The WxxW peptide failed to inhibit, and instead augmented BAD-1 binding to heparin agarose (Fig. 6A). Soluble heparin blocked 65% of BAD-1 binding to heparin agarose and the mutant peptide had no effect.

We next explored using TR4 to block BAD-1 binding to heparin agarose as each repeat bears a WxxWxxW motif. Native TR4, however, bound poorly to immobilized heparin (Fig. 6B) compared to BAD-1. Strong binding to heparin by BAD-1 lacking a C-terminal EGF domain (ΔC-term) confirmed that the domain mediating heparin binding is the tandem repeat. Heparin binding by TR4 could be achieved by reducing its disulfide bonds with DTT, which also enhanced binding by BAD-1 and ΔC-term protein.

Once it was established that reduced TR4 binds heparin agarose, we investigated whether this domain – harboring a WxxWxxW motif – could interfere with BAD-1 binding to heparin. As with the synthetic WxxW peptide, TR4 failed to inhibit binding and instead augmented BAD-1 binding to heparin agarose in a concentration

dependent manner (Fig. 6C). This suggests a process of cooperative binding, with BAD-1 initially binding to heparin and then fostering self-association through the tandem repeats.

BAD-1 inhibits T cell activation via CD47

Molecules with heparin binding motifs can modulate the activation of immune cells such as T cells via interaction with GAG-modified cell surface proteins. The heparin-binding protein, TSP-1, inhibits the activation of T cells via interaction with the surface protein CD47 through a GAG-modified Serine at position 64 (Kaur et al, 2011). We hypothesized that BAD-1 might also block T cell activation in a CD47 dependent manner. Anti-CD3 antibody activation of Jurkat T cells or CD47-deficient JinB8 T cells resulted in a ~25-fold increase in CD69 expression at 2 hours. As reported previously (Kaur et al, 2011), TSP-1 decreased CD69 expression in activated Jurkat T cells by 45% (Fig. 7A), while failing to inhibit the activation of JinB8 T cells (Fig. 7B). BAD-1 likewise sharply reduced CD69 expression in activated Jurkat T cells by 65%, but did not block activation in the JinB8 T cells.

We formally tested the role of GAG modification of CD47 in BAD-1 mediated suppression of T cell activation. We transfected CD47-deficient JinB8 T cells with a plasmid encoding wild-type CD47 or a mutant CD47 containing a serine to alanine substitution that precludes GAG-modification (CD47-S64A). These transfections led to re-expression of CD47 on JinB8 cells. Re-expression of wild-type CD47, but not CD47-S64A, in JinB8 cells permitted TSP-1 to significantly inhibit CD69 induction by 35.1% (Fig 7C). Likewise, BAD-1 significantly inhibited CD69 induction by 34.9% in JinB8 cells transfected with wild-type CD47, but not in JinB8 cell transfected with CD47-S64A. Thus BAD-1, like TSP-1, modulates the activation of T cells via surface protein CD47 and the inhibitory activity of BAD-1 requires CD47 GAG-modification at Serine 64.

We next tested the impact of BAD-1 on the function of primary $CD4^+$ T cells that

respond to *Blastomcyes* in an antigen-specific manner and mediate protective immunity during infection (Wüthrich et al, 2007). We studied naïve $CD4^+$ T cells from the 1807 TCR transgenic mouse (Wuthrich et al, 2011), and analyzed their ability to become activated and differentiate into cytokine producing cells *in vitro* in response to co-culture with *Blastomyces* yeast and dendritic cells (DC). Upon co-culture with yeast, 1807 cells became activated as measured by expression of CD69 in nearly 30% of the cells (Fig. 7D). 1807 cells also responded to the fungus by producing IL-17 and IFN-γ protein (Fig. 7E). The addition of BAD-1 to 1807 cells curtailed their activation and expression of CD69 in response to co-culture with yeast and DC (Fig. 7E). BAD-1 also suppressed 1807 cell production of IL-17 and IFN-γ in a concentration dependent manner. Thus, BAD-1 mimics TSP-1 and is capable of suppressing activation and effector functions of T cells, in this case $CD4^+$ T cells that mediate protective immunity to infection.

DISCUSSION

Herein, we describe novel structural and functional properties of BAD-1, an essential virulence factor of *B. dermatitidis*. We formally establish that the tandem repeats are indispensible for virulence, provide NMR based 3-D structural characterization of the BAD-1 tandem repeats, and identify a tryptophan-rich motif in the tandem repeats that mediates heparin binding and suppression of T cell activation. Though initial analyses of the primary structure of BAD-1 reported 30 highly conserved tandem repeats (Hogan et al, 1995), a more in-depth assessment of stringently conserved elements adds 11 more repeats to this total (Fig. 1A). This new model characterizes BAD-1 as essentially an extended series of tandem repeats (comprising 90% of the protein's length) with a C-terminal, chitin-binding domain to anchor it to the surface of *B. dermatitidis* yeast. Because the C-terminus is dispensable for virulence in a murine model of respiratory infection (Brandhorst et al, 2003), we postulated that virulence must depend upon the tandem repeats. Indeed, we found that partial deletion of the repeats sharply attenuated pathogenicity mediated by BAD-1.

There is precedent for the role of the tandem repeats in the adhesive function of BAD-1 (Hogan et al, 1995; Newman et al, 1995). Pathogens express surface adhesins to invade host tissues and these adhesins often contain tandem repeat domains. In some cases the tandem repeats are themselves responsible for mediating cell surface adhesion (e.g.- *Staphylococcus aureus* MSCRAMM) (Joh et al, 1999). In other cases, the repeats act as "spacer arms" that orient and present a binding domain to host receptors. Some adhesins possess an additional function, unfolding pursuant to ligation and then refolding/contracting to draw the pathogen towards the host cell surface (e.g.- *Candida albicans* Als5p)(Alsteens et al, 2009). By structural analysis, the repeats of BAD-1 are linked together by non-rigid "hinge" regions, like beads on a string. DLS analysis predicts an elongated conformation for BAD-1, arguing for limited flexibility in

these hinge regions. Random orientation of hinge residues would favor an amorphous globular structure, however light scattering supports an elongated non-random structure for full-length BAD-1. Such a structure may be similar to the rod-like adhesins Als5p of *C. albicans* (Verstrepen & Klis, 2006) and invasin of *Yersinia sp.* (Hamburger et al, 1999).

Because the tandem repeats are necessary for virulence, we sought further insight into their structure and function. One notable aspect of their sequence is an exceptionally high tryptophan content. In most proteins perhaps one residue in a hundred will be tryptophan, but BAD-1 surpasses this ratio 17-fold. In nearly every repeat, three tryptophans are arranged in a highly conserved WxxWxxW pattern, a motif proven to mediate heparin binding in TSP-1. Short peptides bearing this motif are capable of binding to GAGs (Yabkowitz et al, 1989), and the presence of adjacent basic residues enhances both affinity and specificity for heparin. In TSP-1, tryptophans are arrayed along a short, α-helical domain, coordinating with basic residues on an adjacent anti-parallel strand to create a surface-exposed recognition groove (Tan et al, 2002). NMR analysis of the BAD-1 tandem repeat model - TR4 - demonstrated that the disulfide bond present within each repeat constrains the 17 residues between them into a consistent, tightly folded loop. While this loop localizes basic residues adjacent to the tryptophans of the WxxWxxW motif, one fold of this loop stretches transversely across these putative active residues in a manner that may interdict surface-exposure. In this way, the 3-D structure of TR4 contrasts with the heparin-binding motif of TSP-1. Nevertheless, strong parallels between BAD-1 and TSP-1 prompted us to explore heparin-binding activity.

Our work discloses a previously undiscovered capacity of BAD-1 to bind heparin. This activity is saturable, specific and high-affinity, and constitutes an advance in our understanding of BAD-1 and *B. dermatitidis* pathogenesis. BAD-1 has been shown to

alter host innate immune responses, suppressing TNF-α (Finkel-Jimenez et al, 2001) and inducing TGF-β production (Finkel-Jimenez et al, 2002) . We now show here that BAD-1 suppresses T lymphocyte receptor signaling in a manner similar to that reported for TSP-1 (Kaur et al, 2011). TSP-1 ligates a heparan sulfate-modified serine residue of CD47, thereby suppressing T cell activation. BAD-1 targets this same T cell co-receptor through the same modified serine and produces similar suppression. This BAD-1 mimicry of TSP-1 resulted in impaired T cell activation and differentiation, with reduced production of effector cytokines including IL-17 and IFN-γ. Since T cell activation is vital to the host's ability to clear yeast via adaptive immunity (Wüthrich et al, 2007), inhibition of T cell function could foster pathogen survival. TSP-1 also regulates immune-tolerance by phagocytic cells (Krispin et al, 2006), nitric oxide signaling (Isenberg et al, 2006), activation of TGF-β (Schultz-Cherry et al, 1994; Young & Murphy-Ullrich, 2004) and the binding and clearance of matrix metalloproteinases involved in the healthy egress of lung inflammatory cells (Bein & Simons, 2000). The ability of BAD-1 to mimic TSP-1 and modulate host immunity to its advantage could hinge on any or all of these activities.

There are additional implications stemming from the finding that BAD-1 binds heparin. Ligation of mammalian cell surface GAGs is a mechanism used by many pathogens. Viruses, bacteria, and parasites exploit host cell-surface GAGs, mediating attachment with adhesins to impede clearance (Rostand & Esko, 1997; Wadstrom & Ljungh, 1999). The BAD-1 adhesin similarly binds yeast to lung epithelial cells (Brandhorst et al, 1999), macrophages (Brandhorst et al, 2003; Hogan et al, 1995; Newman et al, 1995) and ECM. While we do not provide evidence here that the adhesive features of BAD-1 are due to its affinity for heparin, parallels with other pathogens make this idea plausible.

The ability of BAD-1 to bind GAGs may also illuminate the mechanism by which

BAD-1 engages CR3 receptors. We have shown that BAD-1 interactions with heparin are insensitive to heat and do not require divalent cations, however the interaction between BAD-1 and CR3 is sensitive to both heat and [Mg^{2+}] (Newman et al, 1995). It is noteworthy that CR3 binds heparin through a mechanism that is heat sensitive and Mg^{2+} dependent (Diamond et al, 1995). BAD-1 and CR3 could thus interact through a heparin polymer bound in tandem. If heparin enables BAD-1 to ligate heparin-binding receptors, this would increase the number of biologically relevant ligands for BAD-1 mediated adhesion, signal transduction, or signal inhibition.

Our observation that the TR4 repeats did not share the heparin-binding activity of BAD-1 was at first surprising. Heparin binding by Δ-Cterm BAD-1 indicates that BAD-1 engages heparin through its tandem repeats, while NMR analysis showed structural identity between TR4 and the native repeats. Even given the finding that a segment of the repeat loop lies across the putative heparin-binding motif, it was unexpected that our "model" tandem repeat bound heparin poorly. Remarkably, relaxing TR4's structure via disulfide reduction enabled heparin binding up to parity with BAD-1. Unfolding of the loop structure may thus be requisite for heparin binding. While reduction of disulfide bonds in the extra-cellular environment is one means of accomplishing this (e.g.- reduction of plasmin) (Stathakis et al, 1997), the same end could be achieved via proteolysis. As each repeat loop is secured at the base with a disulfide bond, cleavage within the loop(s) would not necessarily divide BAD-1 into fragments - the overall length and possibly even the structure could endure a proteolytic "activation" event.

While TR4 was produced in *E. coli*, and stringently refolded and oxidized with glutathione, native BAD-1 may be subject to modification by endogenous fungal enzymes. BAD-1 can undergo a characteristic, proteolytic degradation during isolation (unpublished observation). Western blots of these preps, probed with anti-BAD-1 reactive to the tandem repeats, display a "ladder" of breakdown products and individual

repeats. It is possible that each repeat harbors a conserved cleavage site for an endogenous fungal protease. Such a proteolytic activation of repeats would not proceed randomly, however, as BAD-1 typically migrates as a single, primary 120 kD band by reducing, denaturing PAGE. The fact that TR4 and peptides that mimic the heparin-binding motif enhance rather than inhibit BAD-1 binding is consistent with the notion that a proteolytic breakdown of BAD-1 might enhance its binding to target GAGs. It seems less likely that the numerous, stringently conserved tandem repeats in BAD-1 exist only to extend the length of the adhesion, while maintaining a conformation that impedes GAG ligation.

Whether the tandem repeats must be modified to bind heparin, and by what means, may become clear once the nature and conformation of the active heparin-binding motif is determined. What is clear at this time is that: 1) NMR analysis indicates that the tandem repeats of BAD-1 tend to adopt the conformation resolved for the repeats in the TR4 model protein, 2) the conformation of the BAD-1 tandem repeats appears to lock the heparin-binding motif into a minimally adhesive state, and 3) despite this, native BAD-1 possesses the capacity to bind heparin with a high affinity. NMR or crystallographic analysis of the structure of the tandem repeat in association with heparin should help resolve this question.

In conclusion, we describe here the NMR based structural features of BAD-1 tandem repeats and a novel heparin-binding function for this essential virulence domain. This activity may govern *B. dermatitidis* yeast adherence to host cells and ECM via ligation of heparan sulfate. In the binding of heparin, BAD-1 mimics TSP-1, similarly down-regulating the activation of T cells through interaction with CD47. These findings shed new light on the structure of BAD-1, its diverse functions, and novel mechanisms through which it may promote fungal pathogenicity.

MATERIALS AND METHODS

Reagents

Complete Mini protease inhibitor tablets (EDTA free) were from Roche (Indianapolis, IN). Unless noted otherwise, chemical reagents were from Sigma.

Fungi

American Type culture Collection (ATCC) strain 26199 of *B. dermatitidis,* a wild-type, virulent isolate originally obtained from a human patient, was used in this study, together with the isogenic non-pathogenic BAD-1 knockout strain (Brandhorst et al, 1999). Truncated chimeras of the BAD-1 gene were used to transform strain #55 to secrete a full length BAD-1 with a 6-his tag (BAD1-6H), BAD-1 lacking the C-terminal region (ΔCterm as previously described) (Brandhorst et al, 2003), and BAD-1 lacking 20 of the tandem repeats (Trepeat20)(described below). All isolates of *B. dermatitidis* were maintained in the yeast form on Middlebrook 7H10 agar slants with oleic acid-albumin complex, grown at 39°C. Liquid cultures of yeast were grown in *Histoplasma* macrophage media (HMM)(Audet et al, 1997).

Expression of a truncated form of BAD-1, Trepeat20

An expression cassette for a truncated form of BAD-1 in which 20 of the tandem repeats were deleted was created by digesting the deletion construct pBAD1-6H (Brandhorst et al, 2003) with BamH1 restriction enzyme (NEB Biolabs, Ipswich, MA) and then re-ligating, removing 1355 bp of the original cDNA. The deletion construct was excised from the pUC18 vector in an EcoR1/Xba1 digest, and then inserted into the EcoR1/ Xba1 sites in the polylinker of plasmid pCB1532 (a vector carrying the Sulphonyl Urea resistance [SUR] gene of *Magneportha grisea*, generously provided by Dr. James Sweigard [Dupont, Wilmington, DE])(Sweigard, 1997). This plasmid was used to transform BAD-1 knockout strain #55 and producing strains were identified by Western

blotting nitrocellulose overlays placed on replica plates of picked transformants, as previously described (Brandhorst et al, 1999). Strains were selected that most closely reconstituted the BAD-1 production seen in the 26199 parental strain. Production levels were estimated by Western blot of surface extracted protein probed with anti-BAD-1 mAb DD5-CB4 (Hogan et al, 1995; Newman et al, 1995) followed by goat anti-mouse (GAM) IgG-alkaline phosphatase (Promega). Production levels were further quantified using a FACscan flow cytometer (Becton Dickenson) using DD5-CB4 and GAM-FITC (Sigma) (Fig. S1).

Murine model of *B. dermatitidis* infection

Male BALB/c mice ~5–6 wk of age (Harlan Sprague Dawley) were infected intra-nasally with *B. dermatitidis* yeasts as previously described (Wüthrich et al, 1998). In brief, mice were anesthetized with inhaled Metafane® (Mallinckrodt Veterinary Inc.). A 25-µl suspension of yeast cells in PBS was then applied drop-wise into their nares. To insure a lethal infection was established, 10^4 yeast were thus administered. Mice were housed according to guidelines of the University of Wisconsin Animal Care Committee, which approved this work.

Expression of recombinant 4-repeat model protein in *E. coli*

Complementary oligos RS33 and RS34 were annealed and ligated into pUC18 digested with BamH1/EcoR1 to make pUC18/33-34.

(RS33-
GATCCGAAGACGACCCTACAACTGTGACTGGGACAAGTCCCATGAGAAGTATGAT
TGGGAGCTCTGGGATAAGTGGTGCAAGGACG,
RS34-
AATTCGTCCTTGCACCACTTATCCCAGAGCTCCCAATCATACTTCTCATGGGACTTG
TCCCAGTCACAGTTGTAGGGTCGTCTTCG)

pUC18/33-34 contains DNA coding for one tandem repeat, with a Bbs I site and a BamHI site just upstream. The annealed complementary oligos RS35 and RS36 were ligated into these sites, creating a new set of BbsI/BamHI sites for the next digestion/ ligation cycle. After each cycle, the newly cloned plasmid was opened by Bbs I/BamHI and purified from an agarose gel (Freeze and Squeeze DNA extraction spin columns, Bio-Rad).

(RS35-

gatccgaagacgaccctacaactgtgactgggacagtcccatgagaagtatgattgggaactctgggataagtggtgca aggac,

RS36-

AGGGGTCCTTGCACCACTTATCCCAGAGTTCCCAATCATACTTCTCATGGGACTTG TCCCAGTCACAGTTGTAGGGTCGTCTTCG)

This process was repeated until the plasmid contained four repeats. The final construct was cut out of pUC18 with BamH1/EcoRI (EcoR1 site blunted) and ligated into pQE32 cut with BamH1/HindIII (HindIII site blunted) creating plasmid pQETR4 for expression of the 4-repeat model protein in *E. coli* with a 6-histidine tag (TR4).

TR4-(Fig. 1C)

MRGSHHHHHHGIRRRPYNCDWDKSHEKYDWELWDKWCKDPYNCDWDKSHEKYDW ELWDKWCKDPYNCDWDKSHEKYDWELWDKWCKDPYNCDWDKSHEKYDWELWDK WCKDELA

TR4 was expressed in *E.coli* by induction with IPTG and isolated from cell lysates using an NiNTA column (Qiagen, Valencia, CA). Protein was refolded while immobilized on NiNTA resin by subjecting it to a gradient from 100% buffer A (6M urea, 10mM hepes, pH8, 300mM NaCl, 10% glycerol, 2mM mercaptoethanol, 1mM $CaCl_2$) to 100% buffer B (10mM hepes, pH8, 300mM NaCl, 10% glycerol, 5mM 4:1 GSH:GSSG, 1mM $CaCl_2$) over the course of three hours. Refolded protein was then eluted with 250mM Imidizole,

which was itself removed by dialysis.

Verification of disulfide linkages in TR4 by mass spectrometry

"In Liquid" digestion and mass spectrometric analysis was done at the Mass Spectrometry Facility (Biotechnology Center, University of Wisconsin-Madison). In short, 5μg of purified protein in 125mM NH_4HCO_3 (pH 8.5) was reduced with DTT (62.5mM final) for 30 minutes at 55°C. Another 5μg sample was left in its native state as a control. Samples were spun through Pierce detergent removal columns (Thermo Scientific) to remove DTT and subsequently digested with trypsin solution (Trypsin Gold from Promega Corp.). Peptides were loaded on LC/MSD TOF (Agilent Technologies) and analyzed by MALDI TOF/TOF (AB SCIEX). (Additional detail available in supplementary data- Materials and Methods)

Estimation of molecular shape by dynamic light scattering

The hydrodynamic radius of BAD-1 was measured by dynamic light scattering (DLS) collected at the 90 degree angle using a Beckman-Coulter N4 Plus instrument with the sampling time and prescaling as optimized by the instrument. Two samples of BAD-1 at 7 μM in 70 mM NaCl, 40 mM Tricine pH 7.0 were measured. For each sample ten autocorrelation functions were recorded and analyzed using both the unimodal and size distribution software supplied with the instrument. The averages reported exclude repetitions with >1% baseline error in unimodal analysis or >5% dust fraction in the size distribution analysis. The refractive index of water at 15°C, 1.333, from instrument's database was used. The contribution of 40 mM tricine to the solvent viscosity was approximated by linear interpolation between increments reported for 20 and 100 mM tricine (Steckel & Eskandar, 2003). This contribution was added to the viscosity computed for 70 mM NaCl at 25°C, and then corrected to 15°C assuming its behavior paralleled that of water (Laue, 1992) for a value of 1.41 cP. For interpretation of the

hydrodynamic results, the partial specific volume of BAD-1 was computed (based on the sequence) to be 0.704 mL/g. Hydration of 0.469 g water/g polypeptide at pH 7 was calculated based on the amino acid composition (Kuntz, 1971). (Additional detail available in supplementary Materials and Methods).

Isolation of BAD-1

BAD-1 was purified as described (Brandhorst et al, 2005) with a modification. Yeasts were grown in liquid HMM in a gyratory shaker at 37°C for 5 days. Yeast were washed once in PBS and BAD-1 was released from cell surfaces with two 1-hour washes in dH_2O and then purified on a metal-chelate resin (NiNTA). Due to its divalent cation-binding property, BAD-1 protein could be purified on NiNTA resin regardless of whether it included a 6-histidine tag. The stringency of the wash buffer was reduced by eliminating imidazole. Homogeneity of purified BAD-1 was analyzed by SDS-PAGE, Sypro Ruby stain (Invitrogen), and Western blot using anti-BAD-1 antibody (DD5-CB4) (Hogan et al, 1995; Klein et al, 1994; Newman et al, 1995).

Binding of yeast to Matrigel

Matrigel (Collaborative Biomedical Products, Bedford, MA) was diluted to 5mg/ml, 0.5mg/ml and 0.05mg/ml in RPMI. 30µl was put into wells of a 96-well plate and allowed to gel at 37YC overnight. *Blastomyces* yeast were labeled with $Na^{51}CrO_4$ for 105 minutes at 37YC, washed and diluted to $2x10^7$/ml in HBSS + 0.1%BSA. 50µl was added to each well and incubated for 60 minutes, then washed with HBSS. Well contents were subjected to scintillation counting (compared to controls with known numbers of labeled yeast) to quantify bound yeast. To block BAD-1-mediated binding, rabbit anti-BAD-1 immune serum (Klein & Jones, 1990) (or control pre-immune serum) was applied to labeled yeast, incubated for 1 hour, and washed with HBSS before binding assays.

Native BAD-1 binding to heparin-agarose

Heparin-agarose resin was obtained from Sigma as were control agarose beads and agarose beads coated with BSA, hemoglobin, and mannan. 100µl of 0.1mg/ml BAD-1 was incubated with agarose resins (5 µl bed volume) in 20mM tricine, pH7, 50mM NaCl for 30min at 25ºC with agitation. Resin beads were pelleted by centrifugation in a microfuge at 7000xG. Concentration of BAD-1 before and after incubation with resin was monitored by A280 via Nanodrop Spectrophotometer (ND1000, Thermo Scientific). Binding was calculated by comparing the A280 of supernates to that of starting material. Binding inhibition studies were done with soluble medical grade heparin purchased from Elkins-Sinn Inc (Cherry Hill, NJ), dermatan sulfate (chondroitin sulfate B)(Sigma), chondroitin sulfate A (chondroitin-4-sulfate, fraction A)(Sigma) and hyaluronan (Sigma). Baseline absorbance was corrected to account for absorbance of added GAG inhibitors. During optimization studies, heparin resin bed volume was varied from 1µl to 20µl, NaCl concentrations were varied from 40mM to 2000mM and alternative buffers were tested (20mM Na-acetate, pH5, 20mM Tricine pH7 and pH8, 20mM Na-carbonate, pH9). Reduction of BAD-1 and TR4 was accomplished with 10mM DTT and heating at 100 ºC for three minutes.

Fluorescent BAD-1 binding to heparin-agarose

BAD-1 binding to heparin and control resins, and binding inhibition studies also were performed using BAD-1 labeled with the eFluor605NC kit from eBioscience (San Diego, CA). BAD-1 was fluorescently labeled following the manufacturer's instructions. BAD-1 (eFluor605) was incubated with heparin-coated agarose beads or control beads in 20mM tricine buffer, pH7, 50mM NaCl and washed three times with the same buffer before quantification. Association of BAD-1 (eFluor605) with resins was verified visually using an Olympus BX60 fluorescent microscope. For binding and inhibition studies, BAD-1 (eFluor605) was quantitated using a FilterMax F5 multi-mode microplate reader

(Molecular Devices, Sunnyvale, CA) and opaque 96 well plates (Costar, Cambridge, MA).

Production of spin-labeled TR4 and native BAD-1 for NMR analysis

E. coli strain XL-1 Blue transformed with pQE-TR4 was grown in defined M9 medium supplemented with ^{15}N ammonium chloride (1g/L) and ^{13}C dextrose (4g/L) (Cambridge Isotope Laboratories Inc., Andover, MA) for 20 hrs at 30^{O}C, under ampicillin selection (100µg/ml) followed by induction with IPTG and 4 hours of further incubation. [^{13}C,^{15}N]-labeled TR4 was purified and refolded as described above. ^{15}N labeled native BAD-1 was produced by growing 26199 *B. dermatitidis* yeast at 37YC for five days in M9 medium supplemented with ^{15}N ammonium chloride (1g/L) and purifying as described above. Purity of isolated proteins was verified by PAGE prior to NMR analysis.

NMR Spectroscopy

All NMR spectra were recorded at the National Magnetic Resonance Facility at Madison (NMRFAM) on Varian VNMRS (600 MHz and 900 MHz) spectrometers equipped with triple-resonance cryogenic probes. The temperature of the sample was regulated at 25YC for experiments. For sequence specific backbone resonance assignments, a series of two-dimensional (2D) and three-dimensional (3D) heteronuclear NMR spectra were collected on a sample containing 0.1 mM of the [^{13}C,^{15}N]-labeled TR4 dissolved in NMR buffer with 10 mM phosphate, pH 8.0, 95% H_2O, 5% D_2O (Sattler M., 1999). Raw NMR data was processed with NMRPipe (Delaglio F., 1995) and analyzed using the program Sparky (Goddard). 2D ^{1}H-^{15}N HSQC and 3D HNCO data sets were used to identify the number of spin systems, and these identifications plus 3D HNCACB and 3D CBCA(CO)NH data sets were used as input to the PINE server to determine sequence specific backbone resonance assignments (Bahrami et al, 2009). Due to the complexity of the system, the automated backbone resonance assignments needed to be refined

manually with the help of a 3D ^{15}N-edited ^{1}H-^{1}H NOESY spectrum. To assign side chain and HB and HA resonances 2D ^{1}H-^{13}C aliphatic HSQC, 3D HBHA(CO)NH, 3D HC(CO)NH, 3D C(CO)NH and 3D H(C)CH TOCSY experiments were used. Furthermore, a 2D ^{1}H-^{13}C aromatic HSQC spectrum together with a 3D ^{13}C aromatic-edited ^{1}H-^{1}H NOESY were used to assign resonances from aromatic side chains. Finally, a 3D ^{15}N-edited ^{1}H-^{1}H NOESY (100 ms mixing time) spectrum, a 3D ^{13}C aliphatic-edited ^{1}H-^{1}H NOESY (100 ms) spectrum and a 3D ^{13}C aromatic-edited ^{1}H-^{1}H NOESY (100 ms) spectrum were acquired and used to derive the distance constraints to determine the three dimensional structure of the protein.

Structure calculation and analysis

^{15}N resolved ^{1}H-^{1}H 3D NOESY and ^{13}C resolved ^{1}H-^{1}H 3D NOESY spectra were used to derive ^{1}H-^{1}H distance restraints. Backbone dihedral angle restraints ϕ and ψ were obtained from ^{1}H, ^{15}N, ^{13}CA, ^{13}CB, ^{13}C′ using TALOS+ software (Shen et al, 2009). CYANA software version 3.0 was used for automated NOESY peaks assignments and structure calculation following the standard simulated annealing protocol (Guntert, 2004). The program PYMOL (Schrödinger sales) was used to calculate the root mean square deviation (rmsd) and for graphical analysis. The PSVS server was used to check the quality of the structures (Bhattacharya et al, 2007).

Surface Plasmon Resonance

Work was done with a Biacore2000 machine (GE Healthcare) at the Biophysics Instrumentation Facility (BIF) at the UW-Madison. To prepare a heparin surface, medical grade heparin was biotinylated with Sulfo-NHS-LC-Biotin (Thermo Scientific) following manufacturer's instructions. Unreacted biotin was removed by ultrafiltration on a Microcon Ultracel YM-3, and then biotinylated heparin (0.1mg/ml) was applied in binding buffer (50mM Hepes, pH 7, 70mM NaCl, 0.1% Tween-20) to a streptavidin-

functionalized Biacore SA chip (GE Healthcare) for 1.5 min at a 20µl/min flow rate. SPR was measured as BAD-1 in binding buffer was circulated over the chip surface at 20 µl/min for 300-600 sec (until equilibrium was reached), followed by a 300 second disassociation phase. BAD-1 was cleansed from the surface between runs with a 1.5 min wash of 10mM Glycine, pH 2.5 containing 4M NaCl. The heparin surface was rebuilt after each wash with a 1.5 min re-application of biotinylated heparin in binding buffer. Background from BAD-1 applied to an uncoated streptavidin surface was subtracted from all readings. Binding inhibition was performed with a 100 fold molar excess of soluble heparin incubated with BAD-1 for 20 min. at room temp prior to circulation over the heparin chip surface. For fitting to the steady state affinity model, the average of the last 2-5 sec of each association phase was used as an estimate of the steady state binding. Data analysis utilized models and software provided in BiaEvaluation 4.1.

Synthesis of Peptide Competitors for Heparin Binding

The UW-biotechnology center synthesized a competitor peptide of SHWSPWSS based on the published sequence known to bind to heparin and inhibit binding by TSP-1 (Guo et al, 1992). This peptide represented a minimalistic version of the WxxWxxW heparin-binding motif. A control peptide SHQSPQSS was synthesized in which the active site tryptophans were replaced with glutamine residues. These peptides were analyzed for purity by HPLC and mass spec and purified/desalted chromatographically.

Pre-treatment of Heparin Resin with Binding Competitors

Heparin resin was washed with binding buffer (20mM tricine buffer, pH7, 50mM NaCl) three times. Binding competitors (WxxW peptide, mutant peptide, TR4 or reduced TR4) were added to 4 cubic mm of resin and incubated with agitation at room temp for 20 min. Resin was washed once with binding buffer before addition of fluorescent BAD-1

(eFluor605) and incubation continued for another 20 min. Resin was washed three times with binding buffer and binding was quantified by fluorescence on a FilterMax F5 multi-mode microplate reader as above.

T-cell Inhibition

T cell inhibition was assessed as described with minor modifications (Kaur et al, 2011). Anti-CD3 antibody (5µg/mL) was immobilized on Nunc Maxisorp 96-well round bottom plates in carbonate buffer (pH 9.5) for 1 hr. Parental Jurkat or related JinB8 (CD47-deficient) T cells were pre-incubated for 10 min at 37YC with 10µg/mL of recombinant TSP-1 (R&D Systems) or native BAD-1 prior to activation with immobilized anti-CD3 antibody for 2 hr. Total RNA was isolated using an RNeasy kit (Qiagen) and RNA was reverse transcribed using iScript cDNA synthesis kit following manufacturer's instructions (Bio-Rad). Real-time PCR primers for human CD69 and human HPRT1 were generated as described (Kaur et al, 2011). Real-time PCR was performed using SsoFast EvaGreen Supermix (Bio-Rad) on a MyIQ real-time PCR detection system (Bio-Rad). Fold change in CD69 mRNA expression was normalized to HRPT1 mRNA levels.

Primary T cells were obtained from 1807 TCR transgenic mice (Wuthrich et al, 2011). $CD4^+$ T cells were purified using magnetic beads (Miltenyi Biotech, Germany) according to the manufacturer's instructions. Purified 1807 cells ($3x10^5$/well) were added to co-cultures of *B. dermatitidis* yeast strain #55 ($3x10^5$/well) and bone-marrow derived DCs ($3x10^5$/well). After 96 hours of co-culture, supernate was harvested and tested for levels of IL-17A or IFN-γ according to manufacturer's instructions (R&D Systems, Minneapolis, MN), and T cells were analyzed by FACscan flow cytometry (Becton Dickenson, Franklin Lakes, NJ) for activation as measured by surface display of CD69 (eBioscience, San Diego, CA). In some experiments, 1807 cells were pre-incubated with BAD-1 in varied amounts for 90 minutes at 37YC, and the cells were

washed free of BAD-1 before addition into the assay. BAD-1 was also tested for suppression of T cell function by adding the protein directly into the co-culture of yeast, DC and T cells.

CD47 Transfection

CD47-deficient JinB8 T cells were transiently transfected with plasmids encoding either CD47 or CD47 with a serine-to-alanine mutation at position 64 (CD47-S64A)(Gift of Dr. David Roberts) using Lipofectamine Plus (Invitrogen). Transfections were performed overnight prior to initiation of experiments. To verify re-expression, untransfected and transfected JinB8 cells were incubated with PE-conjugated anti-CD47 antibody (BD Bioscience) and analyzed by flow cytometry. T cell inhibition experiments were performed, as described above, using these transfected cells.

Statistical Analysis

Kaplan Meier (Fisher & van Belle, 1993) survival curves were generated for mice that received a lethal infection. Survival times of mice that were alive by the end of the study were regarded as censored. Time data were analyzed by the log rank statistic and exact *P* values were computed using the statistical package Stat Xact-3 by CYTEL Software Corporation. Survival of different groups are considered significantly different if the two-sided *P* value is <0.05. When multiple comparisons were made simultaneously, *P* values were adjusted according to Bonferroni's correction to protect the overall significance level of 0.05. All binding data was analyzed by Prism (Graphpad Corp.) with error bars representing simple SEM**.**

Accession number

The coordinates and structure factors have been deposited at the Protein Data Bank (PDB) with the accession code _____.

Supplementary data

Supplementary data follow the figures.

ACKNOWLEDGEMENTS

This work was supported by NIH grants AI35681 (BSK). This study made use of the National Magnetic Resonance Facility at Madison, which is supported by NIH grants P41RR02301 (BRTP/ NCRR) and P41GM66326 (NIGMS). Additional equipment was purchased with funds from the University of Wisconsin, the NIH (RR02781, RR08438), the NSF (DMB-8415048, OIA-9977486, BIR-9214394), and the USDA. We thank Dr. Kenneth Satyshur (Department of Bacteriology) for help with molecular modeling, Grzegorz Sabat (UW-Biotech Center) for performing MS analysis, Milo Westler (Biochemistry) for assistance with NMR work, and Hanna Filutowicz and Kevin Galles for technical assistance. Robert Gordon (Pediatrics) provided assistance with illustrations and Robert Audet performed the matrigel binding analysis and antibody inhibition experiments.

AUTHOR CONTRIBUTIONS

TTB and BK conceived of the experiments. TTB performed the cloning, DNA manipulation, fungal transformation, protein expression and purification, SPR, DLS, and heparin-binding analyses. RR performed the T cell inhibition analysis. MW performed virulence studies in mice. TTB and MT performed the NMR analysis. DM interpreted the SPR and DLS data. Manuscript preparation was done by TTB and BSK with input from RR, MT and DM.

CONFLICT OF INTEREST

The authors declare that they have no conflict of interest.

Table 1. Statistics of NMR Structures of TR4

Conformationally restricting distance constraints	
Intraresidue [i = j]	69
Sequential [(i– j) = 1]	135
Medium Range [1 < (i – j) ≤ 5]	136
Long Range [(i – j) > 5]	57
Total	397
Dihedral angle constraints	
ϕ	13
ψ	13
Number of constraints per residue	21.1
Number of long-range constraints per residue	2.9
CYANA target function [Å]	1.23 $\pm$ 0.05
Average r.m.s.d. to the mean cyana coordinates [Å]	
backbone heavy (N18-C37)	0.40±0.06
all heavy atoms (N18-C37)	0.58±0.05
PROCHECK raw score (ϕ and Ψ/all dihedral angles) (Sippl, 1993)	-0.84/-1.30
PROCHECK Z-scores (ϕ and Ψ/all dihedral angles)	-2.99/-7.69
MOLPROBITY raw score/Z-score (Luthy et al, 1992)	27.35/-3.17
Ramachandran plot summary ordered residue ranges [%]	
most favored regions	85.6
additionally allowed regions	8.9
generously allowed regions	5.6
disallowed regions	0.0
Average number of distance constraints violations per CYANA conformer [Å]	
0.2 – 0.5	1.5
> 0.5	0
Average number of dihedral-angle constraint violations per CYANA conformer [degrees]	
> 10	0

FIGURES

Figure 1

A.

```
MPDIKSVSSILLLVSSSLVAAHPGARYPR-     < Signal sequence, cleaved
DDKYPVNVKYSEHF-                    < Short N-terminal sequence
01)     HHP_KCDW___H______LWDQWC   < 1st six repeats degenerate
02)NGDGHKHFYDCGWGLTHPNYNYRLWKYWC      "
03)   DTKVHYNCELDESHLKYDAGLFKSLC      "
04) TGPGKHLYDCDWPTSHVSYSWYLHDYLC      "
05)  GNGHHPYDCELDSSHEDYSWPLWFKWC      "
06) SGHGRHFYDCKWDNDHEKYDWPLWQYWC   < Beginning of conserved repeats
07) GSHDKDPYNCDWDKFHEKYDWELWNKWC       1
08)     KDPYNCEWDSSHEKYDWELWNKWC       2
09)     KDPYNCEWNSFHEKYDWELWNKWC       3
10)     KDSYNCEWDSSHEKYDWELWNKWC       4
11)     KDPYNCDWDSSHEKFDWGLWSHWC       } four
12) NDYDKYPYNCEWDSSHKKYDLTLWNRWC       } additional
13) SSYDKDPYKCDW__________DLWNQLC      } degenerate
14) SGNGHHFYDCDWDVSYPGYDSHLWDLLC       } repeats
15)    TNNPYNCEWDSSHEKYDWELWDKWC       5
16)     KDPYNCDWDSSHEKYDWDLWNKWC       6
17)     KDPYNCEWDSSHEKYDWELWDKWC       7
18)     KDPYNCDWDSSHEKYDWDLWNKWC       8
19)     KDPYNCEWDSSHEKYDWELWDKWC       9
20)     KDPYNCEWDSSHEKYDWKLWDKWC      10
21)     KDFYNCEWDSSHEKYDWELWDKWC      11
22)     KDSYNCDWDKFHEKYDWELWDKWC      12
23)     KDSYNCDWDKFHEKYDWDLWNKWC      13
24)     KDSYNCDWDKFHEKYDWELWDKWC      14
25)     KDSYNCDWDKFHEKYDWELWDKWC      15
26)     KDFYNCEWDSSHEKYDWELWDKWC      16
27)     KDPYNCEWDSSHEKYDWELWDKWC      17
28)     KDFYNCDWDKFHEKYDWVLWNKWC      18
29)     KDPYNCEWDSSHEKYDWELWDKWC      19
30)     KDPYNCDWDKFHEKYDWDLWNKWC      20
31)     KDPYNCEWDSSHEKYDWELWDKWC      21
32)     KDPYNCEWDSSHEKYDWKLWDKWC      22
33)     KDFYNCEWDSSHEKYDWELWDKWC      23
34)     KDPYNCEWDSSHEKYDWELWDKWC      24
35)     KDPYNCEWDSSHEKYDWELWNKWC      25
36)     KDPYNCEWDSSHEKYDWELWDKWC      26
37)     KDFYNCEWDSSHEKYDWELWDKWC      27
38)     KDPYNCEWDSSHEKYDWELWDKWC      28
39)     KDFYNCEWDSSHEKYDWKLWNKWC      29
40)     KDFYNCEWDSSHEKYDWKLWNKWC      30
41)     KDFYNCEWDSSHEKYDWELWNKWC      31
NKHDEHDKHPWCPVCDPLSGANRCHPTTSCIGTGHSYYCACRAGYKSSHYSHDHKNFRLPFPGYEFLVFTPPGTECDVLCDGY
PHKPAHKLCSEVKVHNYCEP               < C-term. EGF-like domain
```

B.

```
        ---Y-C-W_L---H--Y_F---L---W_LC     -Universally conserved
        KD-YNCE_DWD-F_SHEKYDW-LW-KWC       -Present in highly conserved
```

C.

```
MRGSHHHHHHGIR                      < 6-Histidine tag
1)      RRPYNCDWDKSHEKYDWELWDKWC   < Identical, recombinant repeats
2)      KDPYNCDWDKSHEKYDWELWDKWC
3)      KDPYNCDWDKSHEKYDWELWDKWC
4)      KDPYNCDWDKSHEKYDWELWDKWC
KDELA
```

Figure 1. Primary structure of BAD-1 tandem repeats.

(A) BAD-1 includes 31 highly conserved tandem repeats and 10 degenerate repeats, which make up 90% of the mature protein excepting the C-terminal EGF-like domain (103 amino acids) and 14 amino acids at the N-terminus. Universally conserved amino acids are highlighted. **(B)** Consensus of both universally conserved and highly conserved amino acids. **(C)** Sequence of the recombinant TR4 protein containing 4 identical repeats. Residues at each position represent the residues most commonly found in the corresponding positions of the native repeats.

Figure 2

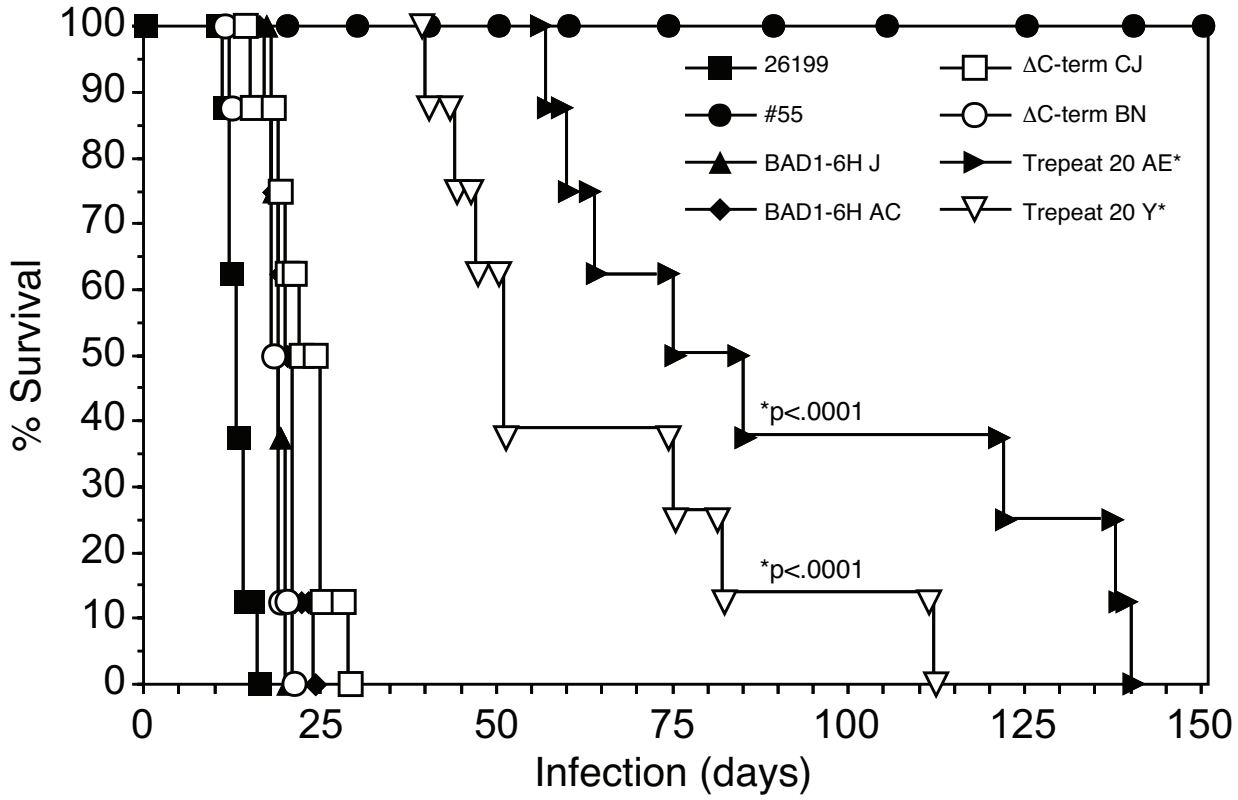

Figure 2. Role of BAD-1 tandem repeats in virulence of *B. dermatitidis in vivo*. Mice received various strains of engineered *B. dermatitidis* yeasts (10^4) intra-nasally in 25-µl PBS. Strains included wild-type, isogenic BAD-1 knockout (#55), strain #55 transformed to re-express BAD-1 (BAD-1-6H) and truncated forms of BAD-1 lacking 20 repeats (Trepeat20) or the C-terminus (ΔC-term). Mice infected with yeast expressing Trepeat20 showed significantly increased survival compared to controls. Mice receiving recombinant strains expressing the full complement of tandem repeats showed no significant alteration in survival compared to mice receiving wild-type 26199 yeast. All mice receiving strain #55 survived until the experiment was terminated five months post-infection.

Figure 3

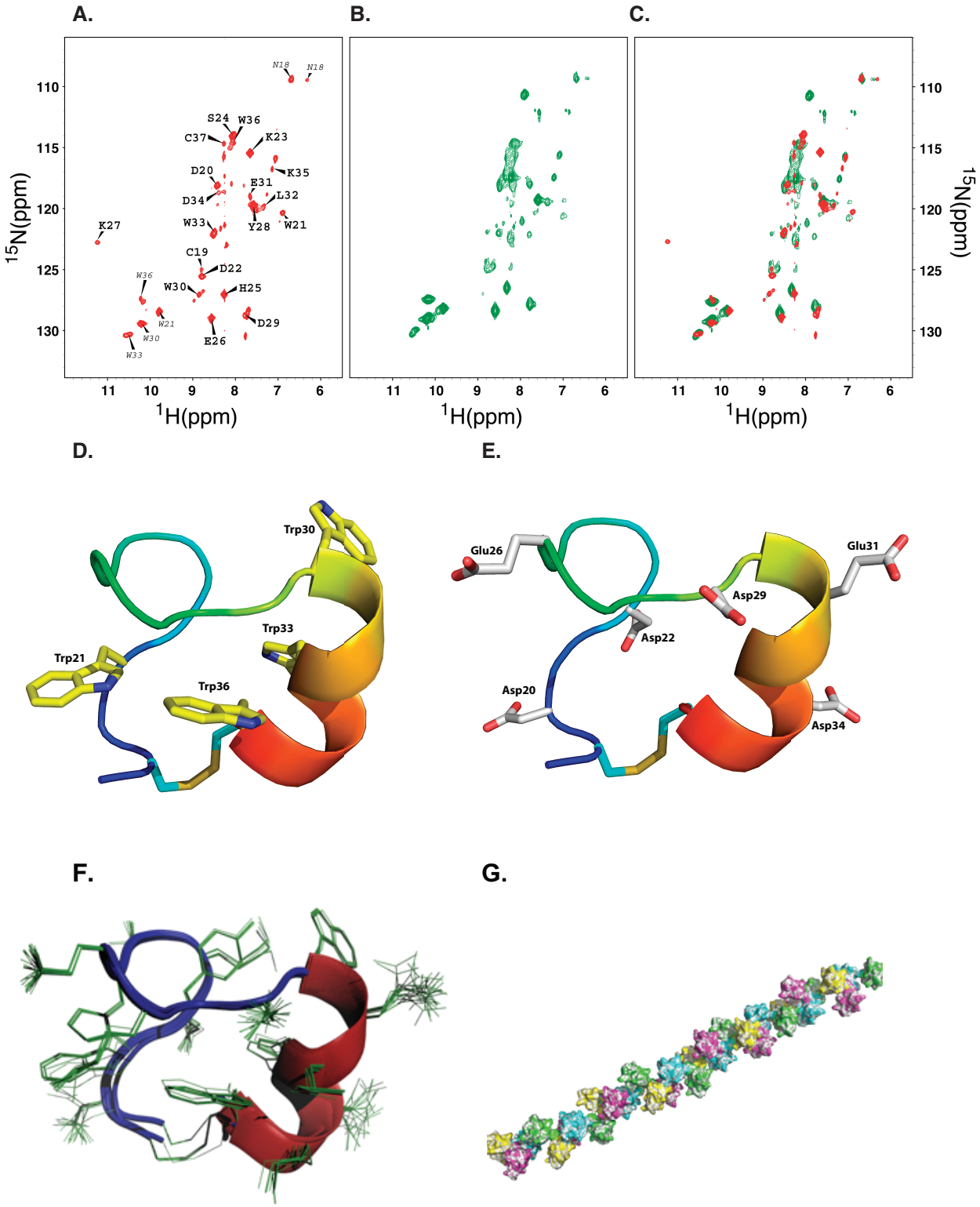
A.
B.
C.
^{15}N(ppm)
^{1}H(ppm)
N18
S24
W36
C37
K23
D20
K35
E31
D34
L32
K27
W33
Y28
W21
C19
D22
W30
H25
D29
E26
D.
E.
Trp30
Trp33
Trp21
Trp36
Glu26
Glu31
Asp29
Asp22
Asp20
Asp34
F.
G.

Figure 3. NMR determination of the structure of the tandem repeats.

(A) ^{1}H-^{15}N HSQC spectrum of TR4. Peaks arising from backbone amides of the representative repeat are labeled, while peaks from side chain N-H groups are indicated with smaller labels. Note that the four tryptophan side chains yield four distinctive peaks indicating distinctive chemical environments. **(B)** ^{1}H-^{15}N HSQC spectrum of full length BAD-1 protein. **(C)** ^{1}H-^{15}N HSQC spectra of TR4 and BAD-1 overlaid to show that the chemical shifts for the amino acids of the TR4 repeats are similar to those of the full length BAD-1 repeats. **(D)** Structure of one tandem repeat loop and its tryptophan residues. We determined the structure of one repeat, focusing upon the loop created by the disulfide bond between the two universally conserved cysteines. The repeat forms two tightly folded turns followed by a short α-helix. All but one of the tryptophan residues are buried in the center of the tandem repeat fold. **(E)** Structure of one tandem repeat loop and its acidic residues. Negatively charged residues are uniformly externalized. **(F)** Overlapping image of the top 20 structural predictions by CYANA. Variability is seen primarily in externalized side-chains (depicted using thin green lines). **(G)** Theoretical structure of the BAD-1 molecule. Model is based on energy minimization of the hinge regions and the fact that extensive stearic hindrance between the tandem-repeat loops further limits flexibility. The overall shape of the tandem repeat favors an extended conformation rather than a random globular conformation. In this model, tandem repeats lie along an alpha helical twist, with roughly 3.2 repeats describing one full turn. Individual tandem repeat structures are sequentially colored: pink, yellow, green, blue (repeated).

Figure 4

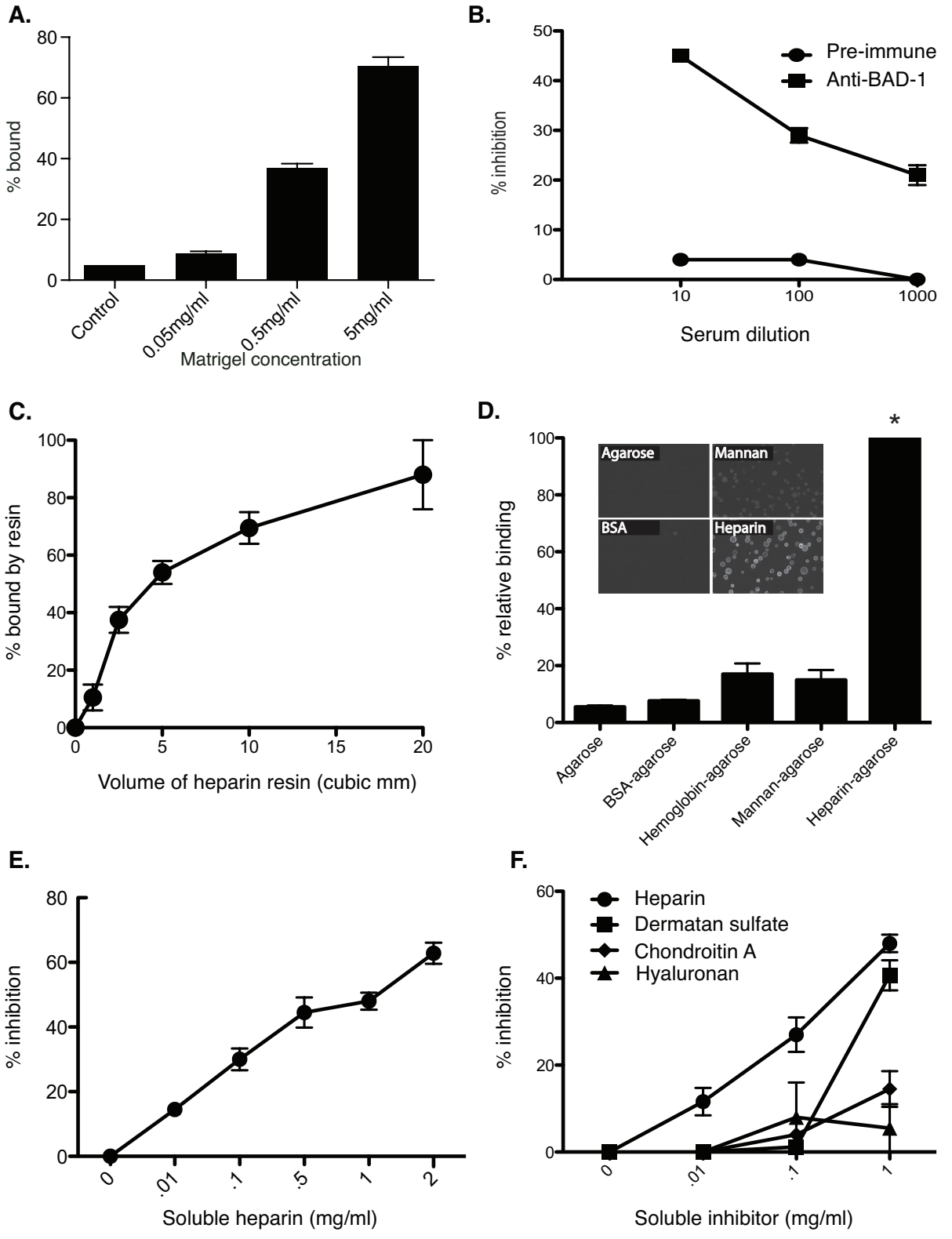
A.
% bound
Control
0.05mg/ml
0.5mg/ml
5mg/ml
Matrigel concentration
B.
% inhibition
Pre-immune
Anti-BAD-1
Serum dilution
C.
% bound by resin
Volume of heparin resin (cubic mm)
D.
% relative binding
Agarose
Mannan
BSA
Heparin
Agarose
BSA-agarose
Hemoglobin-agarose
Mannan-agarose
Heparin-agarose
E.
% inhibition
Soluble heparin (mg/ml)
F.
% inhibition
Heparin
Dermatan sulfate
Chondroitin A
Hyaluronan
Soluble inhibitor (mg/ml)

Figure 4. BAD-1 binding of heparin.

(A) Percentage of $1x10^6$ *B. dermatitidis* yeast that bound to wells coated with increasing concentrations of Matrigel. Control contained no Matrigel. **(B)** Inhibition of yeast binding to Matrigel by different dilutions of anti-BAD-1 antiserum. **(C)** BAD-1 binding of heparin is saturable. 100 µl of 0.1mg/ml BAD-1 was applied to various bed volumes of heparin-agarose resin (400-1500 ng heparin/µl resin). Unound BAD-1 was quantified by A280. **(D)** Binding of BAD-1 to other resins. BAD-1 (eFluor605) pulled down with heparin agarose resin produced a robust fluorescent signal (rightmost column-positive binding control). Binding of BAD-1 (eFluor605) to uncoated agarose resin and resins coated with BSA, hemoglobin or mannan was measured for comparison. Fluorescent BAD-1 bound better to heparin agarose than each control (*, $p<0.05$), and binding to control resins was insignificant ($p>0.05$). Inset: Fluorescent BAD-1 binding to resin surfaces analyzed by fluorescence microscopy. **(E)** Inhibition of BAD-1 binding to heparin resin by soluble heparin. Fluorescent BAD-1 was pre-incubated with increasing concentrations of soluble heparin before exposure to heparin-agarose resin. **(F)** Inhibition of BAD-1 binding to heparin agarose by alternate GAGs. 0.1mg/ml fluorescent BAD-1 was pre-incubated with heparin, dermatan sulfate, chondroitin sulfate A, or hyaluronan for 20 min, followed by incubation with heparin-agarose for 30 min. Inhibition by heparin is significant vs. controls and other GAGs. *, $p<0.05$. Chondroitin sulfate A and hyaluronan are not significantly different from each other or controls. Dermatan sulfate inhibits BAD-1 binding only at 1mg/ml, but not at lower concentrations. Results are the mean ± SEM of two to five experiments/panel.

Figure 5

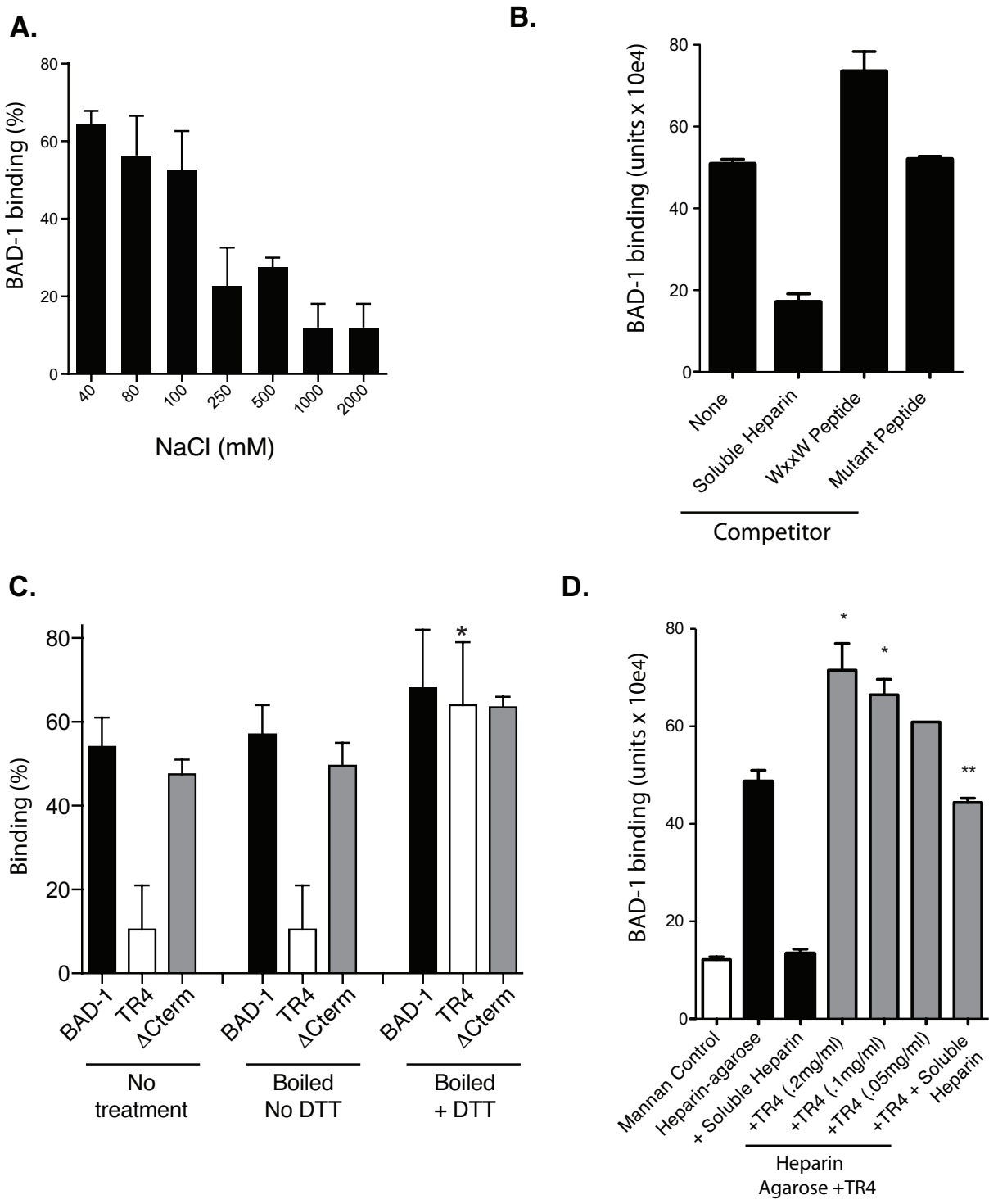
A.
BAD-1 binding (%)
0
20
40
60
80
40
80
100
250
500
1000
2000
NaCl (mM)
B.
BAD-1 binding (units x 10e4)
0
20
40
60
80
None
Soluble Heparin
WxxW Peptide
Mutant Peptide
Competitor
C.
Binding (%)
0
20
40
60
80
*
BAD-1
TR4
ΔCterm
No treatment
Boiled No DTT
Boiled + DTT
D.
BAD-1 binding (units x 10e4)
0
20
40
60
80
*
*
**
Mannan Control
Heparin-agarose + Soluble Heparin
+TR4 (.2mg/ml)
+TR4 (.1mg/ml)
+TR4 (.05mg/ml)
+TR4 + Soluble Heparin
Heparin Agarose +TR4

Figure 5. Affinity of BAD-1 for heparin measured by SPR.

(A) Biotinylated heparin was applied to a streptavidin Biacore-SA chip to create an immobilized heparin surface. 1 μM BAD-1 was applied to the surface until it reached equilibrium, and then sequential 1:2 dilutions were applied until equilibrium was reached. Heparin inhibition of 1μM BAD-1 binding was done at a 100:1 molar ratio of inhibitor to ligand; the resultant response is depicted as a darker line. **(B)** Kd of 700 ± 100nM was calculated using the BIAevaluation software, extrapolating a theoretical Rmax of 5400 ± 500. Results are representative of three independent experiments.

Figure 6

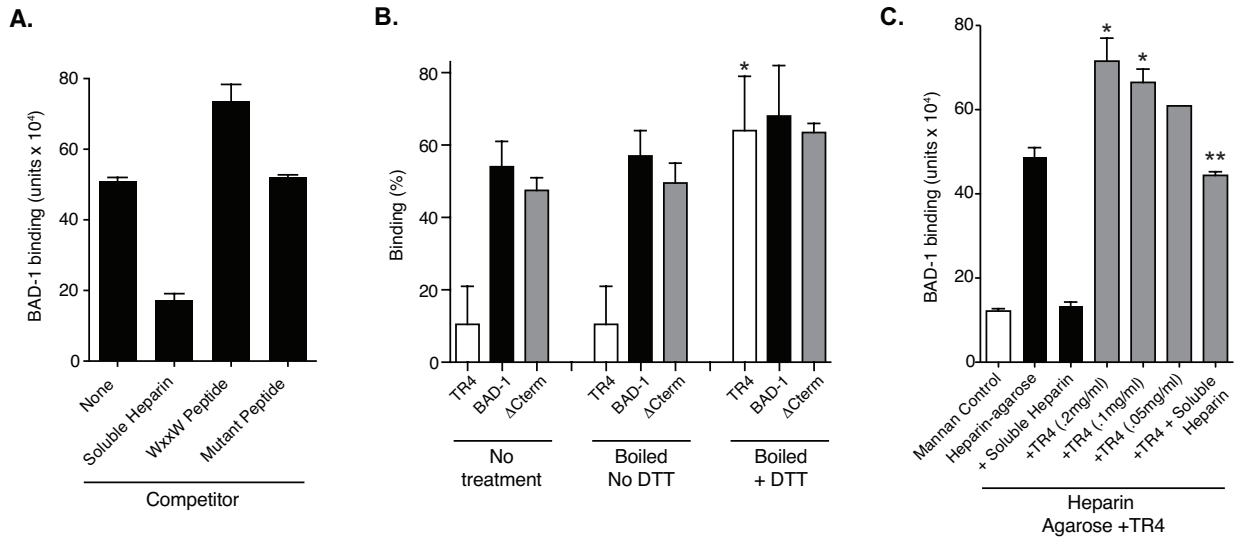

Figure 6. Influence of competitors on BAD-1 binding to heparin.

(A) Effect of a WxxW motif heparin-binding peptide on binding of BAD-1 (eFluor605) to immobilized heparin. "None" denotes BAD-1 binding to heparin agarose with no competitor. The WxxW peptide, or a mutant control peptide, was incubated with heparin resin at 1mg/ml before addition of fluorescent BAD-1. Binding was quantitated by fluorescence units detected in a Filtermax F5 plate reader. Results are the mean ± SEM two experiments. **(B)** Effect of TR4 reduction on binding to heparin. Samples were incubated with resin directly or first boiled for 3 min in buffer alone or buffer with 5mM DTT. TR4 has four copies of the BAD-1 tandem repeat. ΔCterm has all 41 repeats, but no C-terminal EGF-like domain. Binding was quantified by A280 measurement. Reduced TR4 bound significantly better than untreated TR4 or TR4 boiled without DTT (*, $p<0.05$). Results are the mean ± SEM of two experiments. **(C)** Effect of reduced TR4 on binding of BAD-1 (eFluor605) to immobilized heparin. BAD-1 binding to heparin agarose was quantified with or without pretreatment of resin with

reduced TR4 as in panel C. BAD-1 binding was quantified by fluorescence units as above. Mannan resin is a background control. Heparin resin pre-treated with reduced TR4 at 0.2 and 0.1mg/ml bound BAD-1 significantly better than untreated heparin resin **(***, $p<0.05$). Soluble heparin significantly blocked binding of BAD-1 to both of these pre-treated resins (**, $p<0.05$).

Figure 7

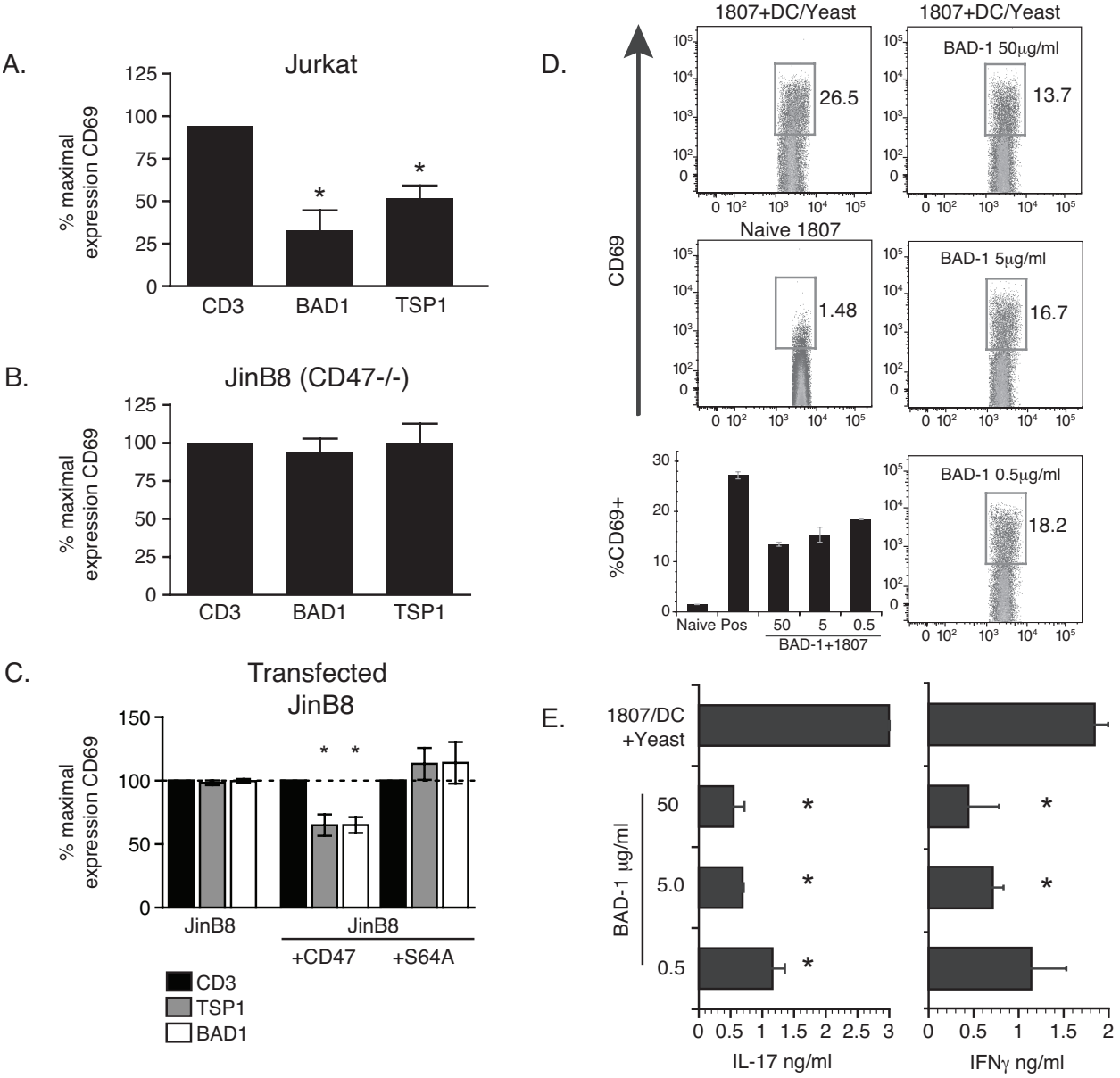

Figure 7. Suppression of T cell activation mediated by BAD-1 binding of CD47. **(A)** BAD-1 inhibition of CD69 expression is dependent on CD47. Jurkat T cells were activated by anti-CD3 antibody alone (5μg/ml) or in the presence of BAD-1 or TSP1 (10μg/ml) for 2 hours *in vitro*. RNA was isolated and relative CD69 mRNA expression determined by real-time PCR. **(B)** JinB8 T cells lacking CD47 were activated by anti-CD3 antibody alone or in the presence of BAD-1 or TSP1 for 2 hours *in vitro*. RNA was

isolated and relative CD69 mRNA expression determined as above. **(C)** Un-transfected JinB8 cells and cells transfected with CD47 and CD47-S64A were activated by anti-CD3 antibody alone or in the presence of BAD-1 or TSP-1 for 2 hours *in* vitro. RNA was isolated and relative CD69 mRNA expression determined as above. Values are percent activation relative to stimulated cells ± SD of 4 experiments for data in panels A-C; *, $p<0.05$. **(D)** $CD4^+$ T cells from 1807 TCR Tg mice were exposed to increasing amounts of BAD-1 for 90 minutes, washed and added to co-culture of *B. dermatitidis* yeast and DC for 96 hours. After incubation, the T cells were analyzed by flow cytometry for expression of CD69. **(E)** Supernates were collected from co-cultures in panel D and assayed by ELISA for IL-17A and IFN-γ content. *, $p<0.05$. vs. control. Results are representative of 2-4 independent experiments for panels D and E.

SUPPLEMENTARY MATERIAL

Materials and Methods

Analysis of disulfide binding in TR4

"In Liquid" digestion and mass spectrometric analysis was done at the Mass Spectrometry Facility [Biotechnology Center, University of Wisconsin-Madison]. In short, 5μg [15μl] of purified protein in 125mM NH_4HCO_3 [pH 8.5] was reduced with 5ul of 250mM DTT [62.5mM final] for 30 minutes at 55^0C, and another 5μg sample was left on ice in its native state as a control. Post reduction, both treated and control samples were spun through Pierce detergent removal columns [Thermo Scientific] to remove the majority of DTT from the reduced sample. Samples were subsequently denatured with 10µl of 8M Urea and diluted to 50µl for tryptic digestion with: 2.5µl ACN, 7.5µl of 0.2% ProteaseMAX™ (Promega Corp.), 5µl 25mM NH_4HCO_3 (pH 8.5) and 5µl trypsin solution (10ng/µl *Trypsin Gold* from PROMEGA Corp. in 25mM NH_4HCO_3). Digestion was conducted for 60 minutes at 40°C, then an additional 2.5μl of trypsin solution was added (final enzyme:substrate 1:67) and digestion proceeded overnight at 37°C. The reaction was terminated by acidification with 2.5% TFA (Trifluoroacetic Acid) to 0.3% final. Degraded ProteaseMAX™ was removed via centrifugation (max speed, 10minutes) and the peptides loaded directly on LC/MSD TOF (Agilent Technologies) or solid phase extracted (*ZipTip® C18* pipette tips, Millipore) and analyzed on MALDI TOF/TOF (AB SCIEX).

MALDI TOF/TOF Analysis

Peptides were eluted off the C18 column with 1ul of acetonitrile/H_2O/TFA (60%:40%:0.1%) into 0.5ml Protein LoBind tube (Eppendorf), and 0.5ul was deposited onto the Opti-TOF™ 384 Well plate (AB SCIEX) and re-crystalized with 0.5μl of matrix

(10mg/ml α-Cyano-4hydroxycinnamic acid in acetonitrile/H_2O/TFA [75%:25%:0.1%]). Peptide Map Fingerprint result-dependent MS/MS analysis was performed on a 4800 Matrix-Assisted Laser Desorption/Ionization-Time of Flight-Time of Flight (MALDI TOF-TOF) mass spectrometer (AB SCIEX). In short, peptide fingerprint was generated scanning 700-4,000 Da mass range using 1000 shots acquired from 20 randomized regions of the sample spot at 4000 intensity of OptiBeam™ on-axis Nd:YAG laser with 200Hz firing rate and 3 to 7ns pulse width in positive reflectron mode. Fifteen most abundant precursors, excluding trypsin autolysis peptides and sodium/potassium adducts, were selected for subsequent tandem MS analysis where 1200 total shots were taken with 4400 laser intensity and 1.5 kV collision induced dissociation (CID) using air. Post-source decay (PSD) fragments from the precursors of interest were isolated by timed-ion selection and reaccelerated into the reflectron to generate the MS/MS spectrum. Raw data was deconvoluted using GPS Explorer™ software and submitted for peptide mapping and MS/MS ion search analysis against user defined *Blastomyces dermatitidis* database (19,127 protein entries) with an in-house licensed Mascot search engine (Matrix Science, London, UK) with Methionine oxidation and Lysine carbamylation as variable modifications.

LC-MS analysis

Peptides and intact protein species were chromatographically resolved with Phenomenex Jupiter 5μm C4 300A 2.0x50mm column, equipped with guard column containing the same resolving media, on an Agilent 1200 HPLC with an autosampler held at 5^0C, using linear gradient of 98% Water: 2% acetonitrile 0.1% Formic acid to 90% Acetonitrile 10% water 0.1% Formic acid over 25 minutes. The flow rate was .25 ml/min. The gradient was as follows:

Time (min)	%B

0	2
1	2
25	90
26	95
27	2
42	2

The mass spectrometer used in conjunction with chromatographic separation was an Agilent LC/MSD TOF with electrospray ionization used in positive ion mode (http://www.biotech.wisc.edu/facilities/massspec/instrumentationoverview/LCMSDTOF) Lists of peptide masses were generated in Agilent MassHunter Qualitative Analysis using the Find Compound by Molecular Feature. To deconvolute intact MW of protein species Agilent BioConfirm Software version A.02.00 was used. The following instrumental parameters were used to generate the most optimum protonated ions [M+H$^{\oplus}$] in Positive Mode: Capillary voltage 3600 V; Drying Gas 6.0 l/min; Nebulizer 30 psig; Gas temperature 350°C; Oct DC1 39.5 V; Fragmentor 130 V; Oct RF 250 V; Skimmer 60V. Internal calibration was achieved with assisted spray of two reference masses, 922.0098 m/z and 121.0509 m/z.

DLS analysis of BAD-1

For both sets of data, the software identified a population accounting for ~70% of the scattering intensity with a mean radius of 7.2 ± 0.5 nm and mean standard deviation for the peak of 1.8± 0.7. The remaining scattering intensity was attributed to a population with a much broader size range. The mean radius among all repetitions was 111± 89 nm with a mean peak standard deviation of 16±16 nm. Interestingly the first peak was the same in the two protein samples, but the second peaks mean radius was very different 160 ± 22 and 68 ± 10. This analysis makes it clear that the BAD-1 preparations have some heterogeneity in size, possibly due to some aggregation or perhaps other

contaminant, but has a dominant fraction of a fairly homogeneous size of 7.2 nm, which is taken to be the monomer.

Figure S1

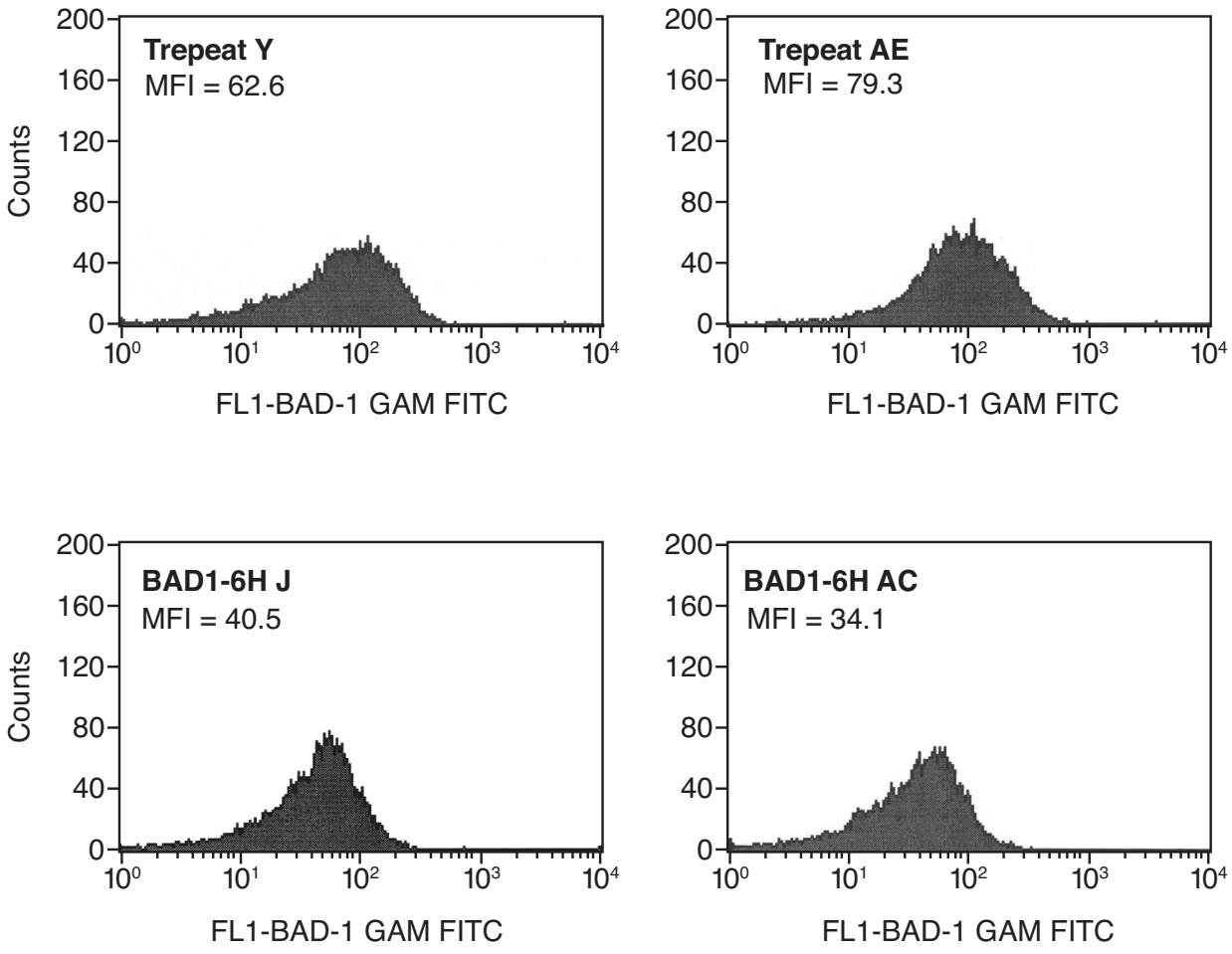

Figure A2-S1. Recombinant *B. dermatitidis* yeast displaying BAD-1 derivatives. Yeast were probed with primary anti-BAD-1 monocolonal antibody DD5-CB4 and a secondary GAM-FITC antibody (Sigma) to quantify surface BAD-1 using a FACscan flow cytometer (Becton Dickenson). *B. dermatitidis* yeast transformed to produce truncated forms of BAD-1 (Trepeat Y and –AE, bearing half the normal number of tandem repeats) displayed as much or more BAD-1 on their surfaces as yeast transformed to produce full-length BAD-1 (BAD1-6H J and –AC). Truncated and full-length forms both included a 6-histidine tag for purification. MFI = mean fluorescence intensity.

Figure S2

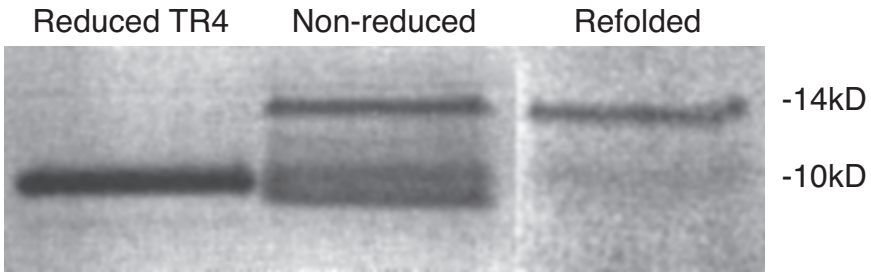

Figure A2-S2. Refolding and analysis of TR4 expressed and purified from *E.coli.* TR4 migrated at varied *Mr* under non-reducing conditions (Non-reduced), and chiefly at 10kD under reducing conditions (Reduced TR4). Refolding conditions and glutathione gradient parameters were adjusted until TR4 eluted from the NiNTA column as a single predominant band (Refolded). This band migrated at 14kD and was subjected to NMR analysis to confirm that the residues in refolded TR4 and the residues of native BAD-1 existed in identical environments.

Figure S3

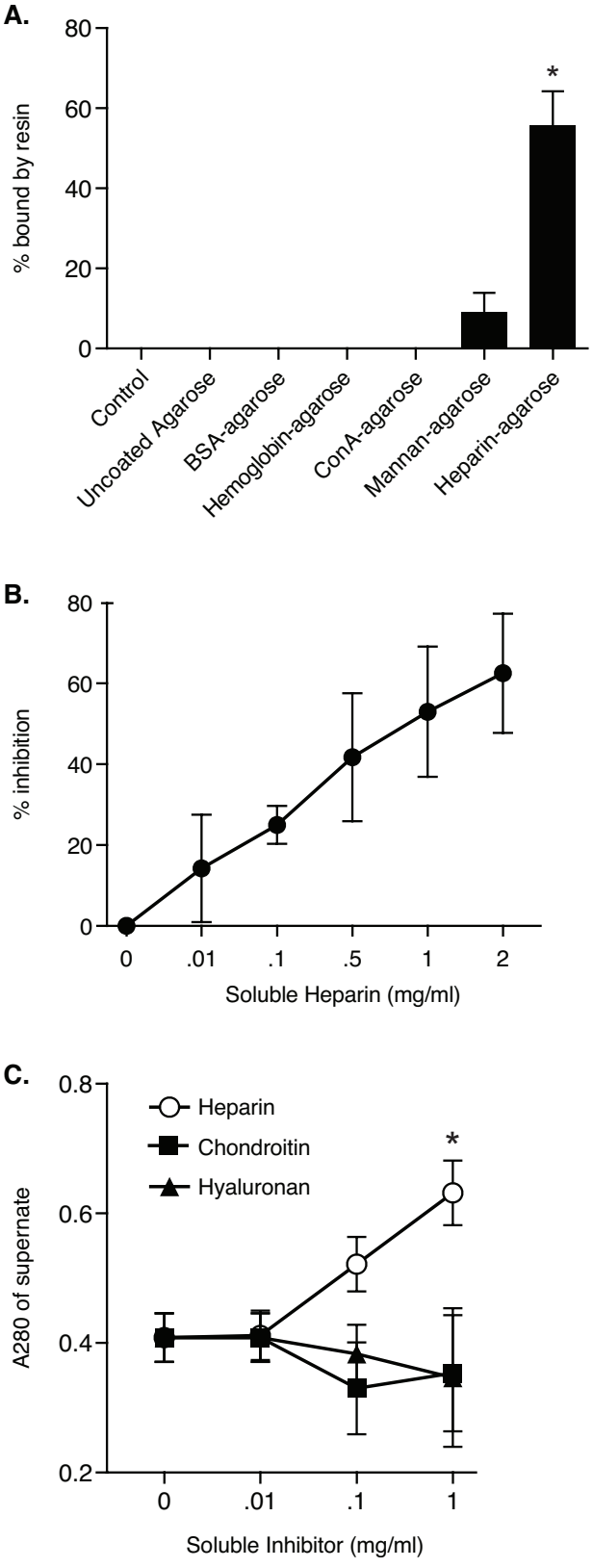
A.
% bound by resin
80
60
40
20
0
*
Control
Uncoated Agarose
BSA-agarose
Hemoglobin-agarose
ConA-agarose
Manman-agarose
Heparin-agarose
B.
% inhibition
80
60
40
20
0
0
.01
.1
.5
1
2
Soluble Heparin (mg/ml)
C.
A280 of supernate
0.8
0.6
0.4
0.2
Heparin
Chondroitin
Hyaluronan
*
0
.01
.1
1
Soluble Inhibitor (mg/ml)

Figure A2-S3. BAD-1 binding to heparin agarose.

BAD-1 heparin binding was quantified by comparing the initial A280 of the purified, soluble BAD-1 to the A280 of BAD-1 in the unbound aqueous phase. **(A)** Binding of BAD-1 to heparin and alternative resins. Heparin agarose resin pulled down the majority of BAD-1 in this assay (right column). The relative binding of BAD-1 to no-agarose control, uncoated agarose resin and resins coated with BSA, hemoglobin, ConA and mannan was measured for comparison. BAD-1 bound better to heparin agarose than control resins (*, $p<0.05$), while binding to control resins was insignificant ($p>0.05$). **(B)** Inhibition of BAD-1 binding to heparin resin by soluble heparin. BAD-1 was pre-incubated with increasing amounts of soluble heparin prior to exposure to heparin-agarose resin. **(C)** Inhibition of BAD-1 binding to heparin agarose by alternate GAGs. 0.1mg/ml BAD-1was pre-incubated with heparin, chondroitin sulfate A, or hyaluronan for 20 min, followed by exposure to heparin-agarose for an additional 30 min. The A280 of the starting BAD-1 solution was 0.8 ± 0.04 and the A280 of the positive binding control was 0.4 ± 0.04 (~50% binding). Heparin inhibited binding significantly better than controls (*, $p<0.05$), while inhibition by chondroitin and hyaluronan were not significant ($p>0.05$).

Figure S4

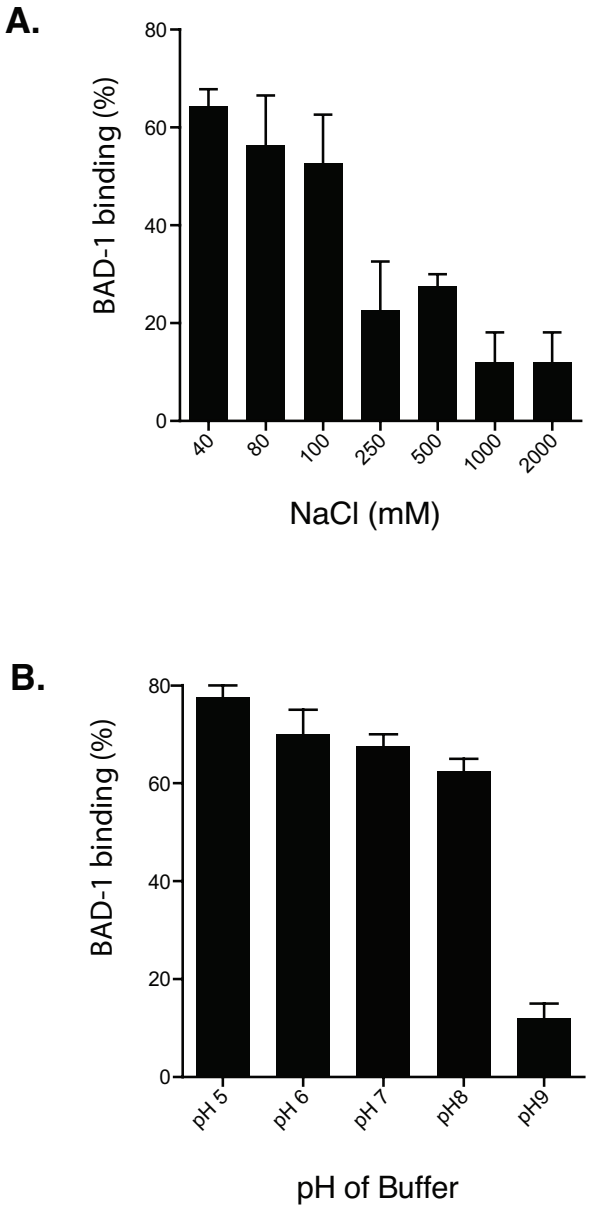

Figure A2-S4. Effect of salt and pH on binding of BAD-1 to heparin.

Effect of NaCl **(A)** and pH **(B)** on binding of BAD-1 to immobilized heparin. A known concentration of BAD-1 was incubated with heparin agarose. The percentage of BAD-1 bound was quantified by measuring A280 of supernate after incubation, compared to that of the starting material. Results are the mean ± SEM of two independent experiments.

REFERENCES

Blastomyces dermatitidis Sequencing Project. Broad Institute of Harvard and MIT.

Alsteens D, Dupres V, Klotz SA, Gaur NK, Lipke PN, Dufrene YF (2009) Unfolding Individual Als5p Adhesion Proteins on Live Cells. *ACS Nano* **3:** 1677-1682

Amiconi G, Civalleri L, Condo SG, Ascoli F, Santucci R, Antonini E (1981) Evidence for multiple differing cation binding sites on hemoglobin A and S. *Hemoglobin* **5:** 231-240

Audet R, Brandhorst TT, Klein B (1997) Purification in quantity of the secreted form of WI-1: a major adhesin on Blastomyces dermatitidis yeasts. *Protein Expr Purif* **11:** 219-226

Bahrami A, Assadi AH, Markley JL, Eghbalnia HR (2009) Probabilistic interaction network of evidence algorithm and its application to complete labeling of peak lists from protein NMR spectroscopy. *PLoS Comput Biol* **5:** e1000307

Bal W, Christodoulou J, Sadler PJ, Tucker A (1998) Multi-metal binding site of serum albumin. *J Inorg Biochem* **70:** 33-39

Bein K, Simons M (2000) Thrombospondin type 1 repeats interact with matrix metalloproteinase 2. Regulation of metalloproteinase activity. *The Journal of biological chemistry* **275:** 32167-32173

Bhattacharya A, Tejero R, Montelione GT (2007) Evaluating protein structures determined by structural genomics consortia. *Proteins* **66:** 778-795

Brandhorst T, Klein B (2000) Cell wall biogenesis of Blastomyces dermatitidis. Evidence for a novel mechanism of cell surface localization of a virulence-associated adhesin via extracellular release and reassociation with cell wall chitin. *J Biol Chem* **275:** 7925-7934

Brandhorst T, Wüthrich M, Finkel-Jimenez B, Klein B (2003) A C-terminal EGF-like domain governs BAD1 localization to the yeast surface and fungal adherence to phagocytes, but is dispensable in immune modulation and pathogenicity of Blastomyces dermatitidis. *Mol Microbiol* **48:** 53-65

Brandhorst TT, Gauthier GM, Stein RA, Klein BS (2005) Calcium binding by the essential virulence factor BAD-1 of Blastomyces dermatitidis. *J Biol Chem* **280:** 42156-42163

Brandhorst TT, Wüthrich M, Finkel-Jimenez B, Warner T, Klein BS (2004) Exploiting type 3 complement receptor for TNF-alpha suppression, immune evasion, and progressive pulmonary fungal infection. *J Immunol* **173:** 7444-7453

Brandhorst TT, Wüthrich M, Warner T, Klein B (1999) Targeted gene disruption reveals an adhesin indispensable for pathogenicity of Blastomyces dermatitidis. *J Exp Med* **189:** 1207-1216

Delaglio F. GS, Vuister G. W., Zhu G., Pfeifer J., Bax, A. (1995) NMRPipe: a multidimensional spectral processing system based on UNIX pipes. *J Biomol NMR* **6:** 277-293

Diamond MS, Alon R, Parkos CA, Quinn MT, Springer TA (1995) Heparin is an adhesive ligand for the leukocyte integrin Mac-1 (CD11b/CD1). *J Cell Biol* **130:** 1473-1482

Finkel-Jimenez B, Wüthrich M, Brandhorst T, Klein BS (2001) The WI-1 adhesin blocks phagocyte TNF-alpha production, imparting pathogenicity on Blastomyces dermatitidis. *J Immunol* **166:** 2665-2673

Finkel-Jimenez B, Wuthrich M, Klein BS (2002) BAD1, an essential virulence factor of Blastomyces dermatitidis, suppresses host TNF-alpha production through TGF-beta-dependent and -independent mechanisms. *Journal of immunology* **168:** 5746-5755

Fisher LD, van Belle G (1993) Biostatistics: A Methodology for the Health Sciences. *John Wiley & Sons, New York***:** 611-613

Frazier WA (1987) Thrombospondin: a modular adhesive glycoprotein of platelets and nucleated cells. *J Cell Biol* **105:** 625-632

Goddard TDaK, D.G. Sparky 3. University of California, San Francisco.

Grant D, Long WF, Williamson FB (1992) A potentiometric titration study of the interaction of heparin with metal cations. *Biochem J* **285 (Pt 2):** 477-480

Guntert P (2004) Automated NMR structure calculation with CYANA. *Methods Mol Biol* **278:** 353-378

Guo NH, Krutzsch HC, Negre E, Zabrenetzky VS, Roberts DD (1992) Heparin-binding peptides from the type I repeats of thrombospondin. Structural requirements for heparin binding and promotion of melanoma cell adhesion and chemotaxis. *The Journal of biological chemistry* **267:** 19349-19355

Hamburger ZA, Brown MS, Isberg RR, Bjorkman PJ (1999) Crystal structure of invasin: a bacterial integrin-binding protein. *Science* **286:** 291-295

Hogan LH, Josvai S, Klein BS (1995) Genomic cloning, characterization, and functional analysis of the major surface adhesin WI-1 on Blastomyces dermatitidis yeasts. *J Biol Chem* **270:** 30725-30732

Isenberg JS, Ridnour LA, Dimitry J, Frazier WA, Wink DA, Roberts DD (2006) CD47 is necessary for inhibition of nitric oxide-stimulated vascular cell responses by thrombospondin-1. *The Journal of biological chemistry* **281:** 26069-26080

Joh D, Wann ER, Kreikemeyer B, Speziale P, Hook M (1999) Role of fibronectin-binding MSCRAMMs in bacterial adherence and entry into mammalian cells. *Matrix Biol* **18:** 211-223

Kaur S, Kuznetsova SA, Pendrak ML, Sipes JM, Romeo MJ, Li Z, Zhang L, Roberts DD (2011) Heparan sulfate modification of the transmembrane receptor CD47 is necessary for inhibition of T cell receptor signaling by thrombospondin-1. *The Journal of biological chemistry* **286:** 14991-15002

Klein BS, Chaturvedi S, Hogan LH, Jones JM, Newman SL (1994) Altered expression of

surface protein WI-1 in genetically related strains of Blastomyces dermatitidis that differ in virulence regulates recognition of yeasts by human macrophages. *Infect Immun* **62:** 3536-3542

Klein BS, Jones JM (1990) Isolation, purification, and radiolabeling of a novel 120-kD surface protein on Blastomyces dermatitidis yeasts to detect antibody in infected patients. *J Clin Invest* **85:** 152-161

Krispin A, Bledi Y, Atallah M, Trahtemberg U, Verbovetski I, Nahari E, Zelig O, Linial M, Mevorach D (2006) Apoptotic cell thrombospondin-1 and heparin-binding domain lead to dendritic-cell phagocytic and tolerizing states. *Blood* **108:** 3580-3589

Kuntz ID (1971) Hydration of Macromolecules. III. Hydration of Polypeptides. *J Am Chem Soc* **93:** 514-516

Laue TMS, B. D.; Ridgeway, T. M.; Pelletier, S. L. (1992) *Computer-aided interpretation of analytical sedimentation data for proteins.* , Cambridge, United Kingdom: Royal Society of Chemistry.

Luthy R, Bowie JU, Eisenberg D (1992) Assessment of protein models with three-dimensional profiles. *Nature* **356:** 83-85

Newman SL, Chaturvedi S, Klein BS (1995) The WI-1 antigen of Blastomyces dermatitidis yeasts mediates binding to human macrophage CD11b/CD18 (CR3) and CD14. *J Immunol* **154:** 753-761

Rooney PJ, Sullivan TD, Klein BS (2001) Selective expression of the virulence factor BAD1 upon morphogenesis to the pathogenic yeast form of Blastomyces dermatitidis: evidence for transcriptional regulation by a conserved mechanism. *Mol Microbiol* **39:** 875-889

Rostand KS, Esko JD (1997) Microbial adherence to and invasion through proteoglycans. *Infection and immunity* **65:** 1-8

Sattler M. SJ, Griesinger C. (1999) Heteronuclear multidimensional NMR experiments for the structure determination of proteins in solution employing pulsed field gradients. *Prog NMR Spectr* **34:** 93-158

Schultz-Cherry S, Lawler J, Murphy-Ullrich JE (1994) The type 1 repeats of thrombospondin 1 activate latent transforming growth factor-beta. *The Journal of biological chemistry* **269:** 26783-26788

Shen Y, Delaglio F, Cornilescu G, Bax A (2009) TALOS+: a hybrid method for predicting protein backbone torsion angles from NMR chemical shifts. *J Biomol NMR* **44:** 213-223

Sippl MJ (1993) Recognition of errors in three-dimensional structures of proteins. *Proteins* **17:** 355-362

Stathakis P, Fitzgerald M, Matthias LJ, Chesterman CN, Hogg PJ (1997) Generation of angiostatin by reduction and proteolysis of plasmin. Catalysis by a plasmin reductase secreted by cultured cells. *The Journal of biological chemistry* **272:** 20641-20645

Steckel H, Eskandar F (2003) Factors affecting aerosol performance during nebulization with jet and ultrasonic nebulizers. *Eur J Pharm Sci* **19:** 443-455

Sweigard J (1997) A series of vectors for fungal transformation. *Fungal Gentetics Newsletter* **44:** 52-53

Tan K, Duquette M, Liu JH, Dong Y, Zhang R, Joachimiak A, Lawler J, Wang JH (2002) Crystal structure of the TSP-1 type 1 repeats: a novel layered fold and its biological implication. *J Cell Biol* **159:** 373-382

Tanford C (1961) *Phyical Chemistry of Macromolecules*, New York: John Wiley & Sons, Inc.

Uversky VN, Li J, Fink AL (2001) Metal-triggered structural transformations, aggregation, and fibrillation of human alpha-synuclein. A possible molecular NK between Parkinson's disease and heavy metal exposure. *The Journal of biological chemistry* **276:** 44284-44296

Verstrepen KJ, Klis FM (2006) Flocculation, adhesion and biofilm formation in yeasts. *Molecular microbiology* **60:** 5-15

Wadstrom T, Ljungh A (1999) Glycosaminoglycan-binding microbial proteins in tissue adhesion and invasion: key events in microbial pathogenicity. *J Med Microbiol* **48:** 223-233

Wüthrich M, Chang WL, Klein BS (1998) Immunogenicity and protective efficacy of the WI-1 adhesin of Blastomyces dermatitidis. *Infect Immun* **66:** 5443-5449

Wüthrich M, Filutowicz HI, Allen HL, Deepe GS, Klein BS (2007) V{beta}1+ J{beta}1.1+/ V{alpha}2+ J{alpha}49+ CD4+ T Cells Mediate Resistance against Infection with Blastomyces dermatitidis. *Infect Immun* **75:** 193-200

Wuthrich M, Hung CY, Gern BH, Pick-Jacobs JC, Galles KJ, Filutowicz HI, Cole GT, Klein BS (2011) A TCR transgenic mouse reactive with multiple systemic dimorphic fungi. *Journal of immunology* **187:** 1421-1431

Yabkowitz R, Lowe JB, Dixit VM (1989) Expression and initial characterization of a recombinant human thrombospondin heparin binding domain. *The Journal of biological chemistry* **264:** 10888-10896

Young GD, Murphy-Ullrich JE (2004) The tryptophan-rich motifs of the thrombospondin type 1 repeats bind VLAL motifs in the latent transforming growth factor-beta complex. *The Journal of biological chemistry* **279:** 47633-47642

APPENDIX 3

The Quest for the Chitin Receptor

René M. Roy, Tristan Brandhorst, Scott Berry, and Bruce S. Klein

INTRODUCTION

The rising incidence of fungal infections is a serious emerging infectious disease threat that is linked to the increase in immunocompromised individuals. Carbohydrates of the fungal cell wall trigger inflammatory responses from immune cells via ligation of specific pattern recognition receptors. For example, beta-glucan is recognized by dectin-1 [1] and mannans are recognized by dectin-2 [2] and DC-SIGN and the mannose receptor [3]. Another fungal cell wall carbohydrate, chitin, was recently shown to induce innate allergic inflammation characterized by eosinophilia and alternatively activated macrophages. Chitin, a linear polysaccharide of beta-1,4 N-acetyl-D-glucosamine, also comprises the exoskeleton of insects, the shell of crustaceans, and the cuticle and egg shell of helminths, which, along with fungi represent environmental compounds whose exposure is associated with the development of allergy and asthma [4]. Several proteins are known to interact with chitin or acetylated structures [5-8], however, to date no protein that mediates the biological inflammatory effects of chitin have been found.

We decided to take advantage of a novel purification technology: Immiscible Filtration Assisted by Surface Tension (IFAST), to seek potential receptors for chitin. We hypothesized that chitin protein complexes from lysates would be isolated more effectively using this protocol than with traditional bead bound immunoprecipitation protocols. We have developed a method to coat magnetic particles with fungal carbohydrates and have demonstrated proof-of-concept using the beta-glucan interaction with dectin-1. Thus we anticipate being able to isolate and charaterize novel chitin receptors using this technique.

RESULTS

Dectin-1 binding to beta-glucan by IFAST

To demonstrate proof-of-concept, we coated magnetic polystyrene beads with curdlan, a highly pure beta glucan polymer. We then co-incubated beta-glucan coated or uncoated beads with a lysate of RAW macrophages that had been transfected with dectin-1 linked to an HA-tag. We also incubated beta glucan coated and uncoated beads with untransfected RAW macrophage lysate. The beads were then passed through the IFAST device and collected. Beads were then incubated with an anti-HA antibody conjugated to HRP. The beads were washed by centrifugation and resuspended in TMB and the color monitored. Beads coated with curdlan and incubated with lysate from dectin-1 transfected RAW macrophages demonstrated were able to transform the substrate to its colored form indicating the presence of HRP, and indirectly the presence of dectin-1, whereas uncoated beads and coated beads not incubated with transfected RAW cells failed to induce a color change. This suggests that the IFAST system can reliably detect protein carbohydrate interactions.

Production of soluble chitin oligomers

In order to coat magnetic beads with chitin, we first need to generate soluble chitin oligomers. Polymers of N-acetyl glucosamine are quite insoluble above 6 sugar residues and commercial sources are lacking. To prepare chitin oligomers, we solubilized chitin particles (Sigma) for 30 minutes in concentrated HCl to begin a slow hydrolysis of the polysaccharide bonds followed by slow neutralization on ice with NaOH. Large chitin polysaccharides precipitate as the solution returns to neutral pH and chitooligomers remain in solution. The solution is dialyzed against water to remove salt and N-acetyl glucosamine monomers, dimers and trimers, in order to obtain pure chitin oligosaccharide. Using this process yielded pure chito-oligomers primarily of 4, 5, and, 6 residues with trace amounts of 7 and 8 residue oligomers as determined by HPLC

analysis.

Binding of chitin to macrophage is mediated by chitin oligosaccharides

To determine if chito-oligosaccharides mediated the binding of chitin rather than N-acetyl glucosamine monomers, we FITC labelled chitin particles for use in binding assays with macrophages. Chitin particles bind to macrophage and airway epithelial cells in a dose-depedent and time dependent manner [9]. To test if chitin oligo-saccharides mediate the binding of chitin particles to macrophages, I pre-incubated the cells with soluble oligo-saccharides or N-acetyl glucosamine for 30 minutes (to compete for binding) prior to adding FITC-labeled chitin particles. Pre-incubation of cells with soluble oligo-saccharides but not N-acetyl glucosamine (1 unit length) sharply reduced chitin particle binding to macrophages (Figure 1). To further establish that chitin oligo-saccharides mediate binding to macrophages, I surface-coated fluorescent silica beads with chitin oligo-saccharides; I verified coating by detection of oligoGlcNAc with wheat germ agglutinin. In a binding assay, oligoGlcNAc-coated beads bound to macrophages and epithelial cells 2 to 3 fold better than did control beads (Figure 2), providing additional evidence that short oligo-saccharides mediate attachment of chitin particles to cells in the airway.

The FInal Steps

Using chitin oligosaccharide coated magnetic beads we plan to isolate potential chitin receptors from macrophage and airway epithelial cells. Early attempts using the IFAST system have yielded a marked decrease in the number of proteins bound to the magnetics beads as determined by SDS-PAGE analysis

. Preliminary identification of proteins isolated by the IFAST system by mass spectrometry have not yielded any surface expressed molecules to date. However, we remain confident that the long elusive chitin receptor may be at hand.

FIGURES

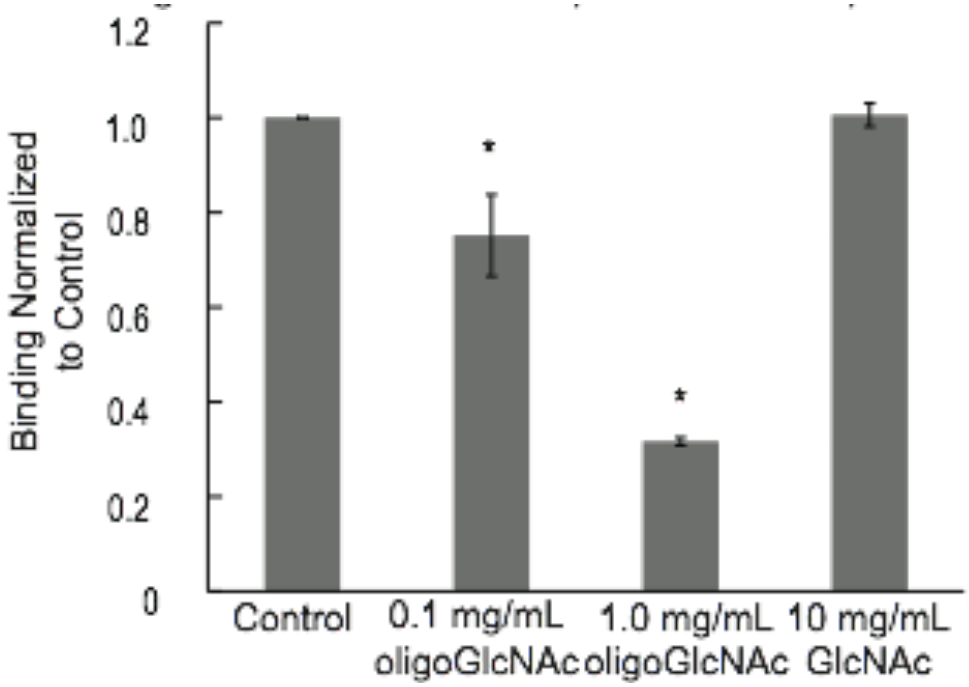

Figure A3-1. Chitin oligosaccharides block binding of chitin particles to macrophages. Chitin oligosaccharides (oilgoGlcNAc) or N-acetyl glucosamine (GlcNAc) were incubated with macrophages for 30 minutes. Then FITC-labeled chitin particles were added for 1 hour at 4°C. Cells were washed, fixed, and mounted for analysis by fluorescent microscopy. Results are the mean of three experiments +/- SEM. Binding was normalized to maximal binding which was set equal to 1. * = $P<0.05$.

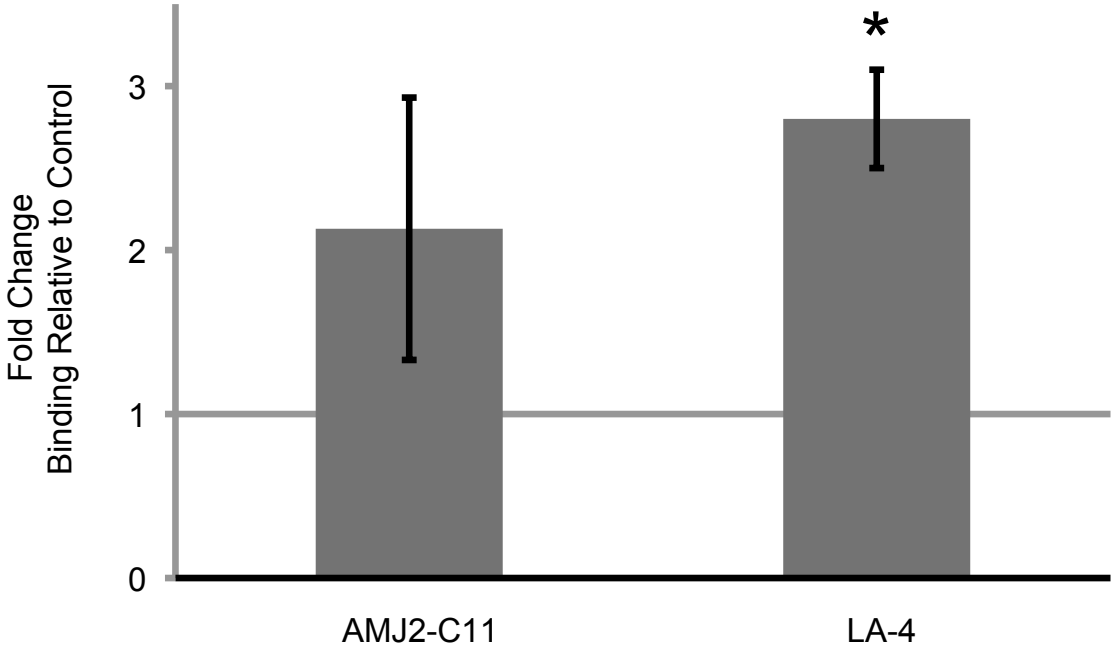

Figure A3-2. Chitin oligosaccharides mediate binding to macrophages and epithelial cells. Chitin oligosaccharide coated red fluorescent beads or uncoated green fluorescent control beads were incubated with AMJ2-C11 macrophages or LA-4 airway epithelial cells at 4°C. Samples were washed, fixed, and analyzed by fluorescent microscopy. Data is expressed as fold-increase of coated beads vs uncoated beads +/- SEM (red vs green). * = $p<0.05$

REFERENCES

1. Brown GD, Gordon S (2001) Immune recognition. A new receptor for beta-glucans. Nature 413: 36-37.

2. Saijo S, Ikeda S, Yamabe K, Kakuta S, Ishigame H et al. (2010) Dectin-2 recognition of alpha-mannans and induction of Th17 cell differentiation is essential for host defense against Candida albicans. Immunity 32: 681-691.

3. Cambi A, Netea MG, Mora-Montes HM, Gow NA, Hato SV et al. (2008) Dendritic cell interaction with Candida albicans critically depends on N-linked mannan. J Biol Chem 283: 20590-20599.

4. Gern JE, Lemanske RFJ, Busse WW (1999) Early life origins of asthma. J Clin Invest 104: 837-843.

5. Chang YY, Chen SJ, Liang HC, Sung HW, Lin CC et al. (2004) The effect of galectin 1 on 3T3 cell proliferation on chitosan membranes. Biomaterials 25: 3603-3611.

6. Krzeslak A, Lipinska A (2004) Galectin-3 as a multifunctional protein. Cell Mol Biol Lett 9: 305-328.

7. McGreal EP, Miller JL, Gordon S (2005) Ligand recognition by antigen-presenting cell C-type lectin receptors. Curr Opin Immunol 17: 18-24.

8. Schlosser A, Thomsen T, Moeller JB, Nielsen O, Tornoe I et al. (2009) Characterization of FIBCD1 as an acetyl group-binding receptor that binds chitin. J Immunol 183: 3800-3809.

9. Roy RM, Wuthrich M, Klein BS (2012) Chitin elicites CCL2 from airway epithelial cells and induces CCR2-dependent innate allergic inflammation in the lung. J Immunol 189: In Press.